Aalto University
School of Science

Timo Voipio

Polarization of pulsed random beams

Master's thesis submitted in partial fulfillment of the requirements for the degree of Master of Science in Technology in the Degree Programme in Engineering Physics and Mathematics.

Espoo 28.11.2011

Thesis supervisor:

Prof. Ari T. Friberg

Thesis instructor:

D.Sc. (Tech.) Tero Setälä

AALTO UNIVERSITY
SCHOOL OF SCIENCE

ABSTRACT OF THE
MASTER'S THESIS

Author: Timo Voipio

Title: Polarization of pulsed random beams

Date: 28.11.2011 Language: English Number of pages: 6+71

Department of Applied Physics

Professorship: Optics Code: Tfy-125

Supervisor: Prof. Ari T. Friberg

Instructor: D.Sc. (Tech.) Tero Setälä

Polarization of light beams exhibits rich mathematical structure and great variety of applications in diverse areas, such as near-field optics, light–matter-interaction and optical communications. The polarization of light beams has been studied extensively for random, statistically stationary beams, but so far no consistent formalism has been introduced for characterizing partial polarization of pulsed beams.

The polarization formalism for stationary fields is presented in time and frequency domains in terms of the temporal polarization matrix and the cross-spectral density matrix, including some recent developments on the connection between temporal and spectral polarization. After recalling the theory for stationary fields, the main part of the thesis develops the polarization matrix formalism for non-stationary fields in both time and frequency domains. The connection between temporal and spectral polarization is derived and analyzed in terms of the measurable polarization quantities, the temporal and spectral degrees of polarization and the temporal and spectral Stokes parameters. Examples are used to illustrate how the degree and state of polarization of a pulse may change with time or frequency. One of the examples describes a pulse whose temporal degree of polarization and polarization state may be tailored while keeping the pulse spectrally fully polarized.

The last part of the thesis presents an optical arrangement for modifying the temporal profile of pulses by using a cascade of dispersive optical elements and time-dependent phase filters, which forms the temporal analogy of a spatial imaging system. The polarization properties of a pulse may be adjusted in versatile ways by applying different temporal magnification to the pulse's orthogonal polarization components.

Keywords: Polarization, coherence, electromagnetic theory, pulsed light

AALTO-YLIOPISTO
PERUSTIETEIDEN KORKEAKOULU

DIPLOMITYÖN
TIIVISTELMÄ

Tekijä: Timo Voipio

Työn nimi: Pulssitettujen satunnaisten säteiden polarisaatio

Päivämäärä: 28.11.2011 Kieli: Englanti Sivumäärä: 6+71

Teknillisen fysiikan laitos

Professuuri: Optiikka Koodi: Tfy-125

Valvoja: Prof. Ari T. Friberg

Ohjaaja: TkT Tero Setälä

Valon polarisaatiolla on monitahoinen matemaattinen rakenne sekä suuri määrä hyödyntämiskohteita eri tieteen ja tekniikan alueilla, kuten lähikenttäoptiikassa, valon ja aineen vuorovaikutuksessa sekä optisessa tiedonsiirrossa. Valonsäteiden polarisaatiota on tutkittu laajasti satunnaisten, tilastollisesti stationaaristen säteiden osalta, mutta tähän mennessä pulssitettujen säteiden osittaisen polarisaation kuvaamiseen ei ole kehitetty johdonmukaista, kattavaa teoriaa.

Työn aluksi esitellään stationaaristen kenttien kuvaamiseen käytetty polarisaatioformalismi aikatasossa polarisaatiomatriisin ja taajuustasossa ristispektrimatriisin (cross-spectral density matrix, CSD) avulla. Stationaaristen kenttien polarisaatioteorian kertaamisen jälkeen työn pääasiallisessa osuudessa kehitetään polarisaatiomatriisiformalismi ei-stationaarisille kentille aika- ja taajuustasoissa. Aika- ja taajuustason polarisaation välille johdetaan yhteys, jota analysoidaan mitattavissa olevien aika- ja taajuustasojen suureiden, polarisaatioasteen ja Stokesin parametrien, avulla. Valopulssin polarisaatioasteen ja -tilan muuttumista ajan ja taajuuden funktiona havainnollistetaan esimerkein. Yksi esimerkeistä kuvaa pulssia, jonka aikatason polarisaatioastetta ja -tilaa voidaan muokata halutulla tavalla pulssin pysyessä kuitenkin taajuustasossa täysin polaroituna.

Työn viimeinen osuus esittelee optisen laitteiston, jolla voidaan muokata pulssien aikaprofiilia. Laitteisto perustuu peräjälkeen aseteltuihin dispersiivisiin optisiin elementteihin ja aikariippuviin vaihesuotimiin, jotka yhdessä muodostavat aika-avaruuden analogian paikka-avaruudessa toimivasta optisesta kuvantamisjärjestelmästä. Pulssin polarisaatioominaisuuksia voidaan muokata moninaisilla tavoilla kohdistamalla pulssin keskenään kohtisuoriin polarisaatiokomponentteihin toisistaan eroavat aikasuurennokset.

Avainsanat: Polarisaatio, koherenssi, sähkömagneettinen teoria, pulssitettu valo

Preface

This Master's Thesis has been prepared while working at the Optics and Photonics research group in the Department of Applied Physics at Aalto University.

First and foremost I sincerely want to thank my supervisor, Professor Ari T. Friberg, and my instructor, Docent, D.Sc. (Tech.) Tero Setälä, for the opportunity and privilege of doing this work under their expert tutelage. Their insight and ideas have been invaluable during the preparation of this thesis, and their prompt and thorough feedback has been deeply appreciated when I have been writing this work. I would also like to acknowledge my collagues in the Optics group, MSc. Timo Hakkarainen, MSc. Henri Kellock, and MSc. Andreas Norrman, for providing a stimulating and open working environment.

I would like to thank, and will indeed thank, my fellow singers in the Polytech Choir for their support, and for providing ample diversions — sometimes maybe even too ample, but no less was expected.

Above all, I want to express my thanks to my parents Marja and Tauno, my sister Mari, and my brother Ville for their example and support during this quarter century we have been here together. And, finally, thank you, Ainu, for keeping my feet solidly grounded and for being patient with me at the times when I was preoccupied with this thesis. どうも有り難うございました！

Otaniemi, November 28, 2011

Timo Voipio

Contents

Chapter 1

Introduction

Polarization of light is a topic that has intrigued scientists and engineers for centuries [1]. Its appearance is usually associated with the observation of double refraction of light in calcite crystal in 1600s [2]. A significant advance took place in early 1800s, when it was shown that light is fundamentally a propagating wave, whose oscillations are orthogonal to the direction of propagation, and it is this transverse nature of light which is the origin of the polarization phenomena [3, 4]. At the end of the 19^{th} century, wave and polarization phenomena of light were united by the formulation of Maxwell's equations, connecting optics with electromagnetism and indicating that light consists of transversally vibrating electric and magnetic fields [5]. At present polarization of light is an extensively studied topic with an extraordinarily rich mathematical structure and a diversity of applications, e.g., in near-field optics, light–matter interaction, biophysics, and nanophotonics [6–9].

All light, whether generated naturally or in laboratory, exhibits some random fluctuations due to the statistical nature of the emission processes, mechanical vibrations of laser cavities, turbulence in the propagation medium, etc. This implies that an accurate description of the polarization of light fields necessarily requires a statistical treatment. The theoretical foundation for characterizing polarization and coherence of fluctuating light was established by the coherence-matrix formalism, developed in the 1950s [10–12]. The formalism was constructed for beam-like electromagnetic fields in the time domain, and it holds for light in which the character of the field's fluctuations does not vary in time, i.e., stationary light. In particular, the degree of polarization was introduced to characterize the partial polarization of a random field, and the Stokes parameters, originally developed to quantify the polarization state of light, were extended to partially polarized cases [12]. A significant extension of the theory emerged a quarter of a century later, when polarization of stationary light was considered in the frequency (spectral) domain and the spectral

degree of polarization was put forward [13, 14]. The spectral theory is more general than the previous time-domain formulation as it provides insight into the spectral structure of the field's polarization. Today, the statistical treatment of polarization has established its status as a standard tool for characterizing random electromagnetic fields [15–18]. Besides these important developments, the degree of polarization has also turned up in recent results on the polarization dynamics of stationary fields, both in beam-like, two-dimensional, fields [19, 20] and in general, three-dimensional fields [21, 22]. In particular, it has been demonstrated that information can be encoded in the polarization dynamics of a field and transmitted through an optical communications system [23].

A general feature common to almost all previously conducted research on partial polarization is the assumption of a stationary field. However, every light field is, to some extent, pulsed. The importance and relevance of pulsed, non-stationary, fields has grown after the advent of pulsed lasers, optical modulators, ultrafast optics, and the entire field of optical communications. Until now, the study of the coherence properties of pulses has been mostly limited to the scalar picture, where polarization phenomena play no role [24, 25]. An exception is provided by the analysis of the polarization properties of a particular Gaussian Schell-model (GSM) pulse [26], but no general treatment of pulsed random electromagnetic beams has been presented thus far.

In this work, a thorough and consistent formalism is constructed for characterizing partial polarization of non-stationary electromagnetic beams, both in time domain and in frequency domain. It is shown that, unlike in the stationary case, the quantities used for characterizing temporal polarization are time dependent, indicating that both the degree and the state of polarization may vary within a pulse. In addition, the connection between temporal and spectral polarizations is considered, and it is pointed out that temporal polarization depends, in general, on spectral coherence. Also an equivalence theorem is established under which fields of different temporal coherence have identical spectral polarization properties. The theory is illustrated by analyzing an electromagnetic GSM beam, showing that polarization state can be different at different points in the pulse, and that it can be modified by altering the beam parameters. Moreover, the polarization properties in the time and frequency domains can be completely different. The polarization formalism of pulsed random light is applied to the physically interesting example of imaging with a time lens. With this method, the polarization state within the pulse can be tailored in diverse ways. In particular, it is shown that a very narrow time window of full polarization can be introduced in the midst of an otherwise weakly polarized pulse. This result is expected to find use in applications involving light–matter interaction.

This thesis is organized as follows: Chapter 2 reviews the fundamentals of electromag-

netic optical beams and outlines the mathematical tools for treating statistical quantities. Chapters 3 and 4 recall the previously established theory used for treating partial polarization of stationary electromagnetic beams in time and frequency domains, respectively. Chapter 5 introduces a consistent formalism for describing partial polarization of pulsed, non-stationary electromagnetic beams in time domain. Chapter 6 presents the treatment of partially polarized pulsed beams in frequency domain, shows the connection between temporal and spectral polarization, and illustrates the polarization formalism using several examples. In Chap. 7 the polarization theory is applied to study the effect of a time lens on the partial polarization of light pulses. Chapter 8 presents the main conclusions of this work.

Chapter 2

Electromagnetic random beams

This chapter reviews the fundamentals of electromagnetic beams starting from the Maxwell equations and proceeding to show how electromagnetic beams can be approximated as plane-wave like fields propagating in a single direction. In order to have tools for characterizing random electromagnetic fields, theory of random processes and their second-order correlation functions is also recalled.

2.1 Basics of electromagnetic fields

The behavior of an electromagnetic field is characterized by the Maxwell equations, which in SI units are [27]

$$\nabla \cdot \mathbf{D}(\mathbf{r}, t) = \rho(\mathbf{r}, t), \tag{2.1a}$$

$$\nabla \cdot \mathbf{B}(\mathbf{r}, t) = 0, \tag{2.1b}$$

$$\nabla \times \mathbf{E}(\mathbf{r}, t) = -\frac{\partial \mathbf{B}(\mathbf{r}, t)}{\partial t}, \tag{2.1c}$$

$$\nabla \times \mathbf{H}(\mathbf{r}, t) = \mathbf{j}(\mathbf{r}, t) + \frac{\partial \mathbf{D}(\mathbf{r}, t)}{\partial t}, \tag{2.1d}$$

where $\mathbf{E}$ is electric field, $\mathbf{H}$ is magnetic field, $\mathbf{D}$ is electric flux density, and $\mathbf{B}$ is magnetic flux density. The source terms in the equations are free charge density ρ and free current density $\mathbf{j}$. For dielectric materials, the densities of free charges and currents are negligible, and thus ρ and $\mathbf{j}$ are both 0. The first equation, (2.1a), is Gauss's law, and it states that electric charge density is the source of the electric field. The second equation, (2.1b), states that magnetic field is sourceless, i.e., no magnetic monopoles exist. Equation (2.1c), Faraday's law, expresses that a time-varying magnetic field induces an electric field.

Ampère's law (including Maxwell's modification), Eq. (2.1d), states that a magnetic field is induced by both electric current and a time-varying electric field. Equations (2.1), with the exception of the displacement current term $\partial\mathbf{D}/\partial t$ in Eq. (2.1d), were discovered by others, but the equations were made consistent by the addition of the displacement current term by J. C. Maxwell.

The interaction of electromagnetic field and matter is described by the constitutive relations

$$\mathbf{D}(\mathbf{r}, t) = \epsilon_0 \mathbf{E}(\mathbf{r}, t) + \mathbf{P}(\mathbf{r}, t), \tag{2.2a}$$

$$\mathbf{B}(\mathbf{r}, t) = \mu_0 \left[\mathbf{H}(\mathbf{r}, t) + \mathbf{M}(\mathbf{r}, t)\right], \tag{2.2b}$$

where $\mathbf{P}$ is polarization, $\mathbf{M}$ is magnetization, ϵ_0 is permittivity of free space, and μ_0 is permeability of free space.

In an isotropic, linearly polarizable and homogeneous medium the polarization and magnetization depend only on the history of the electric field and magnetic field, respectively, via the equations

$$\mathbf{P}(\mathbf{r}, t) = \epsilon_0 \int_{-\infty}^{t} \chi(t - t')\mathbf{E}(\mathbf{r}, t')\mathrm{d}t', \tag{2.3a}$$

$$\mathbf{M}(\mathbf{r}, t) = \int_{-\infty}^{t} \eta(t - t')\mathbf{H}(\mathbf{r}, t')\mathrm{d}t', \tag{2.3b}$$

where respectively $\chi(\tau)$ is electric susceptibility and $\eta(\tau)$ is magnetic susceptibility. Equations (2.3) are consistent with the causality principle as the integrations extend only to the time at which the polarization and magnetization are evaluated.

As evident from Eqs. (2.3), the interaction between electromagnetic field and a material medium is not straightforward to handle in time domain. A more convenient description is obtained by moving from the space–time domain to the space–frequency domain. The time and frequency domains are connected by the Fourier transform and its inverse as

$$\tilde{\mathbf{f}}(\omega) = \frac{1}{2\pi} \int_{-\infty}^{\infty} \mathbf{f}(t) e^{i\omega t} \mathrm{d}t, \tag{2.4}$$

$$\mathbf{f}(t) = \int_{-\infty}^{\infty} \tilde{\mathbf{f}}(\omega) e^{-i\omega t} \mathrm{d}\omega, \tag{2.5}$$

where $\mathbf{f}(t)$ is a function in time domain and $\tilde{\mathbf{f}}(\omega)$ is its frequency domain counterpart. The Fourier expansion effectively represents a time-domain function as a sum of monochromatic components, weighted by $\tilde{\mathbf{f}}(\omega)$.

The Maxwell equations in the frequency domain for a dielectric medium with no

electric charge ($\rho = \mathbf{j} = 0$) are given by the Fourier transforms of Eqs. (2.1):

$$\nabla \cdot \mathbf{D}(\mathbf{r}, \omega) = 0, \tag{2.6a}$$

$$\nabla \cdot \mathbf{B}(\mathbf{r}, \omega) = 0, \tag{2.6b}$$

$$\nabla \times \mathbf{E}(\mathbf{r}, \omega) = i\omega \mathbf{B}(\mathbf{r}, \omega), \tag{2.6c}$$

$$\nabla \times \mathbf{H}(\mathbf{r}, \omega) = -i\omega \mathbf{D}(\mathbf{r}, \omega). \tag{2.6d}$$

The constitutive relations in frequency domain are, in principle, obtained similarly by taking the Fourier transform of the time-domain constitutive relations. The integrals in Eqs. (2.3) closely resemble convolution integrals, however, the upper bounds are some finite t instead of infinity, and indeed the susceptibilities are not physically defined for arguments $t - t' = \tau \leq 0$, i.e., the future values of the electric and magnetic fields do not affect the present polarization and magnetization. The susceptibility functions may be mathematically continued to all values of τ by defining $\chi(\tau) = \eta(\tau) = 0$ for $\tau < 0$. The upper integration limit may then be replaced with positive infinity without affecting the value of the integral, and the integrals in Eqs. (2.3) are then formally convolution integrals. The convolution theorem states that the Fourier transform of a convolution is the product of the Fourier transforms of the convolved functions.

Using Eqs. (2.2) and (2.3), the constitutive relations in the frequency domain take the form

$$\mathbf{D}(\mathbf{r}, \omega) = \epsilon(\omega) \mathbf{E}(\mathbf{r}, \omega), \tag{2.7a}$$

$$\mathbf{B}(\mathbf{r}, \omega) = \mu(\omega) \mathbf{H}(\mathbf{r}, \omega). \tag{2.7b}$$

where $\epsilon(\omega) = \epsilon_0 [1 + \tilde{\chi}(\omega)]$ and $\mu(\omega) = \mu_0 [1 + \tilde{\eta}(\omega)]$, respectively, where $\tilde{\chi}(\omega)$ is the Fourier transform of the continued $\chi(\tau)$ and $\tilde{\eta}(\omega)$ is the Fourier transform of the continued $\eta(\tau)$. The continuation of the susceptibility functions $\chi(\tau)$ and $\eta(\tau)$ has certain consequences that warrant attention. Since the susceptibilities are non-zero only for positive values of the argument τ, their Fourier transforms are analytic functions in the upper half-space [27]. Therefore, the real and imaginary parts of the frequency domain functions are Hilbert transforms of each other. This shows that dispersion and absorption are connected, known as the Kramers–Kronig relations or dispersion relations.

Combining Eqs. (2.6) and (2.7) yields the Hemholtz equations

$$\nabla^2 \mathbf{E}(\mathbf{r}, \omega) - \omega^2 \epsilon(\omega) \mu(\omega) \mathbf{E}(\mathbf{r}, \omega) = 0, \tag{2.8}$$

$$\nabla^2 \mathbf{H}(\mathbf{r}, \omega) - \omega^2 \epsilon(\omega) \mu(\omega) \mathbf{H}(\mathbf{r}, \omega) = 0. \tag{2.9}$$

The partial differential equations for electric and magnetic fields are now uncoupled and mathematically similar in form, which makes finding the solution easier. However, in addition to the Hemholtz equations, the electric and magnetic fields are coupled via the Maxwell equations, and thus the electric and magnetic fields depend on each other.

A set of solutions to the Hemholtz equation for the electric field is the set of functions of the form

$$\mathbf{E}(\mathbf{r}, \omega) = \mathbf{E}(\mathbf{k}, \omega) e^{i\mathbf{k}\cdot\mathbf{r}}. \tag{2.10}$$

Each $\mathbf{E}(\mathbf{r}, \omega)$ corresponds to a monochromatic plane wave. The quantity $\mathbf{k}$ is the (frequency-dependent) wave vector, and it fulfills

$$k^2 = \mathbf{k}\cdot\mathbf{k} = \omega^2\epsilon(\omega)\mu(\omega) = \frac{\omega^2 n^2(\omega)}{c^2}, \tag{2.11}$$

where c is the speed of light in vacuum, $c = (\epsilon_0\mu_0)^{-1/2}$, and $n(\omega)$ is the refractive index of the propagation medium, $n^2(\omega) = \epsilon(\omega)\mu(\omega)/\epsilon_0\mu_0$. This equality is also called the *dispersion relation*. The plane wave is also the solution to the Hemholtz equation for the magnetic field, since the equations are mathematically identical. Inserting the plane-wave solution to the constitutive relations (2.7) and to the Maxwell equations (2.6) yields

$$\mathbf{k}\cdot\mathbf{E}(\mathbf{r}, \omega) = 0, \tag{2.12a}$$

$$\mathbf{k}\cdot\mathbf{H}(\mathbf{r}, \omega) = 0, \tag{2.12b}$$

$$\mathbf{k}\times\mathbf{E}(\mathbf{r}, \omega) = \omega\mu(\omega)\mathbf{H}(\mathbf{r}, \omega), \tag{2.12c}$$

$$\mathbf{k}\times\mathbf{H}(\mathbf{r}, \omega) = -\omega\epsilon(\omega)\mathbf{E}(\mathbf{r}, \omega). \tag{2.12d}$$

Equations (2.12a) and (2.12b) indicate that, if $\mathbf{k}$ is real, both the electric and magnetic fields are perpendicular to $\mathbf{k}$. From this follows that, even though the electric and magnetic field vectors have three orthogonal components, the components are not independent of each other. Equations (2.12c) and (2.12d) both indicate that, again assuming real $\mathbf{k}$, the electric and magnetic fields are perpendicular to each other.

A monochromatic wave propagating to the half-space $z > 0$ with arbitrary spatial dependency may be expressed as a sum of monochromatic plane waves. The wave vector of each component is $\mathbf{k} = k_x\hat{u}_x + k_y\hat{u}_y + k_z\hat{u}_z$. In order to fulfill the dispersion relation (2.11), the wave vector must obey $k^2 = k_x^2 + k_y^2 + k_z^2 = \omega^2 n^2(\omega)/c^2$. Therefore, given the frequency, two of the three components of the wave vector may be choosen freely, and the third is then dictated by the dispersion relation: $\mathbf{k} = k_x\hat{u}_x + k_y\hat{u}_y + \sqrt{\omega^2 n^2/c^2 - k_x^2 - k_y^2}\,\hat{u}_z$. This

leads to the angular spectrum representation

$$\widetilde{\mathbf{E}}(\mathbf{r},\omega) = \int \widetilde{\mathbf{E}}(k_x,k_y,\omega)e^{i\left(k_x x+k_y y+\sqrt{\omega^2 n^2/c^2-k_x^2-k_y^2}\,z\right)}\mathrm{d}k_x\,\mathrm{d}k_y. \tag{2.13}$$

A number of monochromatic fields of different frequencies may be combined to form a polychromatic wave:

$$\mathbf{E}(\mathbf{r},t) = \iint \widetilde{\mathbf{E}}(k_x,k_y,\omega)e^{i(\mathbf{k}\cdot\mathbf{r}-\omega t)}\mathrm{d}k_x\,\mathrm{d}k_y\,\mathrm{d}\omega, \tag{2.14}$$

where again $\mathbf{k}$ must satisfy $k^2 = k_x^2 + k_y^2 + k_z^2 = \omega^2 n^2/c^2$. If all components of $\mathbf{k}$ are real, then values of k_x, k_y over which the integration is done are limited inside a circle of radius k. However, if k_z is allowed to be imaginary with $k_z = ik_z''$, then $k^2 = k_x^2+k_y^2-k_z''^2$, i.e., allowed values of (k_x, k_y) lie outside a circle of radius k. When the wave vector with imaginary z component is inserted into (2.14), it is seen that the spatial part of the exponential term is

$$e^{i(\mathbf{k}\cdot\mathbf{r})} = e^{i(k_x x+k_y y)}e^{-k_z'' z}, \tag{2.15}$$

which varies with unit amplitude in the transverse plane and decays exponentially (assuming positive k_z'') along the z axis. These decaying components are called evanescent waves. They carry high-frequency spatial information, but due to the exponential term they do not propagate very far, even in vacuum.

If all significant contributions to the field arise from components with k_x and k_y much smaller in magnitude than k_z, then a first-order approximation may be used remove the square root in the calculation of k_z:

$$\sqrt{k^2-(k_x^2+k_y^2)} = k\left[1-(k_x^2+k_y^2)/k^2\right]^{1/2} \approx k\left[1-(k_x^2+k_y^2)/2k^2\right]. \tag{2.16}$$

This is called the paraxial approximation. In the paraxial approximation the field may be written

$$\mathbf{E}(\mathbf{r},t) = \iiint \widetilde{\mathbf{E}}(k_x,k_y,\omega)e^{i\{k_x x+k_y y+[k-(k_x^2+k_y^2)/2k]z-\omega t\}}\mathrm{d}k_x\,\mathrm{d}k_y\,\mathrm{d}\omega. \tag{2.17}$$

It is of interest to note that Eq. (2.17) is the general solution to the so-called parabolic Hemholtz equation, which is obtained from the Hemholtz equation in Eq. (2.8) under paraxial conditions.

An axial polychromatic plane wave consists of different frequency components all propagating in the same direction, i.e., $k_x = k_y = 0$. This may be thought of as the limiting case of the paraxial approximation. Formally, $\widetilde{\mathbf{E}}(k_x,k_y,\omega) = \widetilde{\mathbf{E}}(\omega)\delta(k_x)\delta(k_y)$, and thus after the integration over k_x and k_y and adding the time dependence explicitly the field is given

by

$$\mathbf{E}(\mathbf{r}, t) = \int \widetilde{\mathbf{E}}(\omega) e^{i(kz-\omega t)} \mathrm{d}\omega. \tag{2.18}$$

The parameter $k = k_0 n(\omega) = \omega n(\omega)/c$ may be identified as the propagation constant $\beta = n\omega/c$, which tells how much the phase of the component at frequency ω changes on propagation over a unit distance. The expression for the electric field, written in terms of the propagation constant, is

$$\mathbf{E}(\mathbf{r}, t) = \int \widetilde{\mathbf{E}}(\omega) e^{i[\beta(\omega)z-\omega t]} \, \mathrm{d}\omega. \tag{2.19}$$

If the propagation constant is known as a function of frequency, the expression for the electric field can be given more explicit forms, as shown in Chap. 7.

2.2 Random processes

All existing electric fields are, at least up to some degree, non-deterministic or random functions of time. Thus a formalism is required for the characterization of the properties of the non-deterministic behavior of the electric fields. The formalism of random processes offers just this.

A complex function $Z(t)$ is called a *random process* (or a stochastic process) if the value of $Z(t)$ depends on time t, but not deterministically. The behavior of a random process is characterized by the probability distribution $p(z; t)$. The probability that at time t_1, the random variable $Z = Z(t_1)$ has its value in the $\mathrm{d}^2 z$-sized region around z is given by $p(z; t_1)\, \mathrm{d}^2 z$. The probability distribution may be used to calculate the average, or mean, of the process $Z(t)$ by

$$\langle Z(t) \rangle = \int z p(z; t) \, \mathrm{d}^2 z, \tag{2.20}$$

where the integration is over all the possible values of $Z(t)$. The expectation value of any function of $Z(t)$ is calculated by

$$\langle f[Z(t)] \rangle = \int f(z) p(z; t) \, \mathrm{d}^2 z. \tag{2.21}$$

The correlation between the values $Z(t_1)$ and $Z(t_2)$ of the process at times t_1, t_2 is measured by the autocorrelation function $\Gamma(t_1, t_2)$:

$$\Gamma(t_1, t_2) = \langle Z^*(t_1) Z(t_2) \rangle = \iint z_1^* z_2 p_2(z_1, z_2; t_1, t_2) \, \mathrm{d}^2 z_1 \mathrm{d}^2 z_2, \tag{2.22}$$

where $p_2(z_1, z_2; t_1, t_2)$ is the joint, or two-fold, probability density of z at times t_1 and t_2, i.e., the probability that $Z(t_1)$ has the outcome z_1 and $Z(t_2)$ has the outcome z_2. More generally, the expectation value of any function which depends on $Z(t)$ at two instants of time is given by

$$\langle f[Z(t_1), Z(t_2)]\rangle = \iint f(z_1, z_2) p_2(z_1, z_2; t_1, t_2)\, \mathrm{d}^2 z_1 \mathrm{d}^2 z_2. \tag{2.23}$$

Higher-order correlations are calculated accordingly:

$$\langle f[Z(t_1), \ldots, Z(t_n)]\rangle = \int f(z_1, \ldots, z_n) p_n(z_1, \ldots, z_n; t_1, \ldots, t_n)\, \mathrm{d}^2 z_1 \cdots \mathrm{d}^2 z_n, \tag{2.24}$$

where $p_n(z_1, \ldots, z_n; t_1, \ldots, t_n)$ is the n-fold probability density of $Z(t)$ [18].

The (second-order) cross-correlation function of two random processes $Z_1(t)$ and $Z_2(t)$ is

$$\Gamma_{12}(t_1, t_2) = \langle Z_1^*(t_1) Z_2(t_2)\rangle = \iint z_1^* z_2 p_{12}(z_1, z_2; t_1, t_2)\, \mathrm{d}^2 z_1 \mathrm{d}^2 z_2, \tag{2.25}$$

where $p_{12}(z_1, z_2; t_1, t_2)$ is the joint probability distribution of $Z_1(t)$ and $Z_2(t)$. If the correlation function has the value 0, the processes $Z_1(t)$ and $Z_2(t)$ are *uncorrelated*. If the processes $Z_1(t)$ and $Z_2(t)$ are statistically *independent*, then $p_{12}(z_1, z_2; t_1, t_2) = p_1(z_1; t_1) p_2(z_2; t_2)$, where $p_1(z_1; t_1)$ and $p_2(z_2; t_2)$ are the probability distributions of $Z_1(t)$ and $Z_2(t)$, respectively. An equivalent way of expressing this is that their mutual correlation function factorizes: $\langle Z_1^*(t_1) Z_2(t_2)\rangle = \langle Z_1^*(t_1)\rangle \langle Z_2(t_2)\rangle$.

A process is called *stationary* in the strict sense if its statistical properties do not depend on the origin of time [18], i.e., all its n-fold probability densities are invariant under the translation of all time coordinates by a common time delay T. A less strict property is wide sense stationarity, which requires that only the 1- and 2-fold probability densities are invariant in time, i.e., the expectation values that depend only on a single time variable become independent of time, and the expectation values involving two time variables t_1, t_2 only depend on their difference $\tau = t_2 - t_1$. The auto- and cross-correlation functions (2.22) and (2.25) become

$$\Gamma(\tau) = \langle Z^*(t_1) Z(t_1 + \tau)\rangle = \int z_1^* z_2 p_2(z_1, z_2; \tau)\, \mathrm{d}^2 z_1 \mathrm{d}^2 z_2, \tag{2.26}$$

and

$$\Gamma_{12}(\tau) = \langle Z_1^*(t_1) Z_2(t_1 + \tau)\rangle = \iint z_1^* z_2 p_{12}(z_1, z_2; \tau)\, \mathrm{d}^2 z_1 \mathrm{d}^2 z_2. \tag{2.27}$$

If $Z(t)$ is a stationary process and if its every realization ${}^{(k)}Z(t)$ carries all the statistical information related to the process, the process is called *ergodic*. Thus in the case of an

ergodic process, the time averages of all realizations ${}^{(k)}Z(t)$

$$\langle Z(t)\rangle_t = \lim_{T\to\infty} \frac{1}{T} \int_{t-T/2}^{t+T/2} {}^{(k)}Z(t')\,\mathrm{d}t', \tag{2.28}$$

and the ensemble average

$$\langle Z(t)\rangle_e = \lim_{N\to\infty} \frac{1}{N} \sum_{k=1}^{N} {}^{(k)}Z(t), \tag{2.29}$$

are equal and independent of time t. Similar relation holds for higher-order correlations. In this chapter, stationarity and ergodicity are assumed, and thus the time and ensemble averages are equal and independent of time t, and so the choice of the average and the time dependency are not shown.

The cross-correlation of two processes may be normalized using the mean-square averages of the processes. The normalized cross-correlation coefficient $\gamma_{12}(t_1, t_2)$ is defined via

$$\Gamma_{12}(t_1, t_2) = \sqrt{\langle |Z_1(t_1)|^2\rangle \langle |Z_2(t_2)|^2\rangle}\, \gamma_{12}(t_1, t_2). \tag{2.30}$$

The coefficient $\gamma_{12}(t_1, t_2)$ is bounded in absolute value by $|\gamma_{12}(t_1, t_2)| \leq 1$, which can be shown both for ensemble average and for time average with the Cauchy-Schwarz inequality for sums and integrals, respectively. Similar relation holds for autocorrelation functions, with

$$\Gamma(t_1, t_2) = \sqrt{\langle |Z(t_1)|^2\rangle \langle |Z(t_2)|^2\rangle}\, \gamma(t_1, t_2). \tag{2.31}$$

The normalized autocorrelation function $\gamma(t_1, t_2)$ is bounded with $|\gamma(t_1, t_2)| \leq 1$. Due to the properties of the autocorrelation function, the equal-time value is $\gamma(t, t) = 1$.

In this section the random processes have been presented as only having time dependency. However, the processes may also depend on other variables besides or instead of time, e.g., position $\mathbf{r}$ or frequency ω. The calculation of the correlations with respect to frequency or position are fully analogous to the time-dependent correlations.

2.3 Complex analytic signal

This thesis examines the characteristics of a fluctuating electric field, i.e., the electric field is described by a random process $\mathbf{E}^{(\mathrm{r})}(\mathbf{r}, t)$, where each component of the electric field vector has zero mean. The superscript (r) indicates that the process is real-valued, to differentiate it from the complex analytic process corresponding to the electric field.

The physical electric field itself is a real quantity, and the field vector at a single point in time does not carry any information on the time evolution of the field. A convenient way

of representing a time-varying real quantity is the *complex analytic signal*, defined by [18]

$$\mathbf{E}(\mathbf{r},t) = \int_0^\infty \widetilde{\mathbf{E}}(\mathbf{r},\omega)e^{-i\omega t}\mathrm{d}\omega, \tag{2.32}$$

where $\widetilde{\mathbf{E}}(\mathbf{r},\omega)$ is the frequency-domain representation of the signal, given by

$$\widetilde{\mathbf{E}}(\mathbf{r},\omega) = \frac{1}{2\pi}\int_{-\infty}^\infty \mathbf{E}^{(\mathrm{r})}(\mathbf{r},t)e^{i\omega t}\mathrm{d}t. \tag{2.33}$$

The properties of the frequency-domain representation are presented in more detail in Chap. 4. At this point it is important to note that since $\mathbf{E}^{(\mathrm{r})}(\mathbf{r},t)$ is real, the frequency-domain signal is symmetric in the sense that $\widetilde{\mathbf{E}}(\mathbf{r},\omega) = \widetilde{\mathbf{E}}^*(\mathbf{r},-\omega)$, where the asterisk denotes complex conjugate. Hence, the negative-frequency components carry the same information as the positive-frequency components, and integrating only over the positive-frequency components in Eq. (2.32) leads to no information loss. The complex analytic signal $\mathbf{E}(\mathbf{r},t)$ is analytic in the lower half-plane of complex time t, which implies that its real and imaginary parts form a Hilbert transform pair [18].

The complex analytic signal representation is advantageous due to its mathematical simplicity. Especially useful is the fact that the complex analytic signal of a quasi-monochromatic field, a field which only consists of components with frequencies very near to the field's central frequency, closely resembles that of a completely monochromatic field, and, e.g., the instantaneous intensity of a quasi-monochromatic signal is obtained simply as the square of the absolute value of the signal at that instant. The complex analytic signal is also important in the field of quantum optics.

Chapter 3

Stationary electromagnetic beams in time domain

This chapter recalls the formalism used to characterize statistically stationary electromagnetic beams in time domain, starting from the coherence and polarization matrices and then introducing the quantities used for characterizing partial polarization, the degree of polarization and the Stokes parameters.

3.1 Coherence matrix

The statistical properties of a stationary beam may be represented using the *electric mutual coherence matrix* or coherence matrix $\mathbf{\Gamma}(\mathbf{r}_1, \mathbf{r}_2, \tau)$, a 2×2 matrix which is defined by [18]

$$\begin{aligned}\mathbf{\Gamma}(\mathbf{r}_1, \mathbf{r}_2, \tau) &= \langle \mathbf{E}^*(\mathbf{r}_1, t)\mathbf{E}^T(\mathbf{r}_2, t+\tau)\rangle \\ &= \begin{bmatrix} \langle E_x^*(\mathbf{r}_1, t)E_x(\mathbf{r}_2, t+\tau)\rangle & \langle E_x^*(\mathbf{r}_1, t)E_y(\mathbf{r}_2, t+\tau)\rangle \\ \langle E_y^*(\mathbf{r}_1, t)E_x(\mathbf{r}_2, t+\tau)\rangle & \langle E_y^*(\mathbf{r}_1, t)E_y(\mathbf{r}_2, t+\tau)\rangle \end{bmatrix},\end{aligned} \tag{3.1}$$

where $\mathbf{E}$ is the electric field (zero-mean complex analytic signal) column vector, T denotes the matrix transpose, τ is the time delay, and the angle brackets denote time average as defined in Eq. (2.28) or ensemble average as defined in Eq. (2.29). The above mutual coherence matrix describes the correlations between the different field components at two points in space and time. The coherence matrix can be shown to be Hermitian and non-negative definite in the sense that [18]

$$\mathbf{\Gamma}(\mathbf{r}_1, \mathbf{r}_2, \tau) = \mathbf{\Gamma}^\dagger(\mathbf{r}_2, \mathbf{r}_1, -\tau), \tag{3.2}$$

and

$$\sum_{n,m=1,2} \mathbf{a}^{\dagger}(\mathbf{r}_m, t_m)\mathbf{\Gamma}(\mathbf{r}_m, \mathbf{r}_n, t_m - t_n)\mathbf{a}(\mathbf{r}_n, t_n) \geq 0, \tag{3.3}$$

where the dagger denotes the Hermitian adjoint. The quantity $\mathbf{a}(\mathbf{r}, t)$ is an arbitrary well-behaved complex-valued vector function.

The coherence matrix may be decomposed using the identity matrix $\mathbf{I} = \boldsymbol{\sigma}_0$ and the three Pauli matrices $\boldsymbol{\sigma}_1, \boldsymbol{\sigma}_2, \boldsymbol{\sigma}_3$ [6]

$$\boldsymbol{\sigma}_1 = \begin{bmatrix} 1 & 0 \\ 0 & -1 \end{bmatrix} \quad \boldsymbol{\sigma}_2 = \begin{bmatrix} 0 & 1 \\ 1 & 0 \end{bmatrix} \quad \boldsymbol{\sigma}_3 = \begin{bmatrix} 0 & -i \\ i & 0 \end{bmatrix}, \tag{3.4}$$

as the basis matrices. This basis is trace-orthonormal, i.e., $\mathrm{tr}\,[\boldsymbol{\sigma}_i\boldsymbol{\sigma}_j] = 2\delta_{ij}$, where tr is the trace operator and δ_{ij} is the Kronecker delta symbol. The coherence matrix, or any 2×2 matrix, may be decomposed as

$$\mathbf{\Gamma}(\mathbf{r}_1, \mathbf{r}_2, \tau) = \frac{1}{2}\sum_{i=0}^{3} S_{\mathrm{t}i}^{(2)}(\mathbf{r}_1, \mathbf{r}_2, \tau)\boldsymbol{\sigma}_i, \tag{3.5}$$

where the expansion coefficients $S_{\mathrm{t}i}^{(2)}$ may be obtained by

$$S_{\mathrm{t}i}^{(2)}(\mathbf{r}_1, \mathbf{r}_2, \tau) = \mathrm{tr}\,\left[\mathbf{\Gamma}(\mathbf{r}_1, \mathbf{r}_2, \tau)\boldsymbol{\sigma}_i\right], \tag{3.6}$$

due to the trace-orthonormality of $\boldsymbol{\sigma}_i$. The expansion coefficients $S_{\mathrm{t}i}^{(2)}(\mathbf{r}_1, \mathbf{r}_2, \tau)$ of the coherence matrix are called the *2-point Stokes parameters* or generalized Stokes parameters. Explicitly, they are given by [28]

$$S_{\mathrm{t}0}^{(2)}(\mathbf{r}_1, \mathbf{r}_2, \tau) = \Gamma_{xx}(\mathbf{r}_1, \mathbf{r}_2, \tau) + \Gamma_{yy}(\mathbf{r}_1, \mathbf{r}_2, \tau), \tag{3.7a}$$

$$S_{\mathrm{t}1}^{(2)}(\mathbf{r}_1, \mathbf{r}_2, \tau) = \Gamma_{xx}(\mathbf{r}_1, \mathbf{r}_2, \tau) - \Gamma_{yy}(\mathbf{r}_1, \mathbf{r}_2, \tau), \tag{3.7b}$$

$$S_{\mathrm{t}2}^{(2)}(\mathbf{r}_1, \mathbf{r}_2, \tau) = \Gamma_{xy}(\mathbf{r}_1, \mathbf{r}_2, \tau) + \Gamma_{yx}(\mathbf{r}_1, \mathbf{r}_2, \tau), \tag{3.7c}$$

$$S_{\mathrm{t}3}^{(2)}(\mathbf{r}_1, \mathbf{r}_2, \tau) = i\left[\Gamma_{yx}(\mathbf{r}_1, \mathbf{r}_2, \tau) - \Gamma_{xy}(\mathbf{r}_1, \mathbf{r}_2, \tau)\right]. \tag{3.7d}$$

The 2-point parameters are, in general, complex-valued. The parameters may be expressed using the correlation coefficient $\gamma_{ij}(\mathbf{r}_1, \mathbf{r}_2, \tau)$, defined as

$$\Gamma_{ij}(\mathbf{r}_1, \mathbf{r}_2, \tau) = \sqrt{I_i(\mathbf{r}_1)I_j(\mathbf{r}_2)}\,\gamma_{ij}(\mathbf{r}_1, \mathbf{r}_2, \tau), \tag{3.8}$$

where $I_i(\mathbf{r}_1) = \langle |E_i(\mathbf{r}_1, t)|^2 \rangle$ and $I_j(\mathbf{r}_2) = \langle |E_j(\mathbf{r}_2, t)|^2 \rangle$ are the intensities of the polarization components i and j of the beam at points $\mathbf{r}_1$ and $\mathbf{r}_2$, respectively. The correlation coefficient

is normalized such that its absolute value is bounded as $0 \leq |\gamma_{ij}(\mathbf{r}_1, \mathbf{r}_2, \tau)| \leq 1$, which follows from the general properties of second-order correlation functions in Eq. (2.30).

3.1.1 Degree of coherence

The ability of a field to interfere with itself is characterized by the degree of coherence $\gamma_{\mathrm{EM}}(\mathbf{r}_1, \mathbf{r}_2, \tau)$. The degree of coherence measures how strongly the field interferes with itself in a Young's two-pinhole interference experiment [29]. The interference may equally well be seen in the modulation of the intensity as well as the modulation of the polarization state. Quantitatively the visibility of modulation, and thus the degree of coherence, is expressed by the normalized mutual coherence function [30]

$$\gamma^2_{\mathrm{EM}}(\mathbf{r}_1, \mathbf{r}_2, \tau) = \frac{\mathrm{tr}\ [\mathbf{\Gamma}(\mathbf{r}_1, \mathbf{r}_2, \tau) \cdot \mathbf{\Gamma}(\mathbf{r}_2, \mathbf{r}_1, -\tau)]}{I(\mathbf{r}_1) I(\mathbf{r}_2)}. \tag{3.9}$$

The mutual coherence function is bounded as $0 \leq \gamma_{\mathrm{EM}}(\mathbf{r}_1, \mathbf{r}_2, \tau) \leq 1$, where the lower bound corresponds to complete incoherence and the upper bound to complete coherence. The degree of coherence is invariant under (different) unitary transformations at the two points. If the field is completely coherent in a finite volume for all time delays τ, the field is monochromatic and the coherence matrix factorizes as

$$\mathbf{\Gamma}(\mathbf{r}_1, \mathbf{r}_2, \tau) = \mathbf{E}^*(\mathbf{r}_1)\mathbf{E}^T(\mathbf{r}_2)e^{-i\omega\tau}, \tag{3.10}$$

and also vice versa [31].

3.1.2 Polarization matrix

The matrix

$$\mathbf{J}(\mathbf{r}) = \mathbf{\Gamma}(\mathbf{r}, \mathbf{r}, 0), \tag{3.11}$$

is called the *single-point equal-time coherence matrix* or *polarization matrix* and is elemental in the analysis of polarization, as seen in the next section. The polarization matrix is purely Hermitian, i.e.,

$$\mathbf{J}(\mathbf{r}) = \mathbf{J}^\dagger(\mathbf{r}), \tag{3.12}$$

which follows directly from Eq. (3.2), and non-negative definite in the usual sense, i.e.,

$$\mathbf{a}^\dagger \mathbf{J}(\mathbf{r}) \mathbf{a} \geq 0, \tag{3.13}$$

where $\mathbf{a}$ is an arbitrary complex vector. The non-negative definity follows directly from that of the coherence matrix in Eq. (3.3) by setting $t_1 = t_2$ and $\mathbf{r}_1 = \mathbf{r}_2 = \mathbf{r}$. Since the polarization matrix is Hermitian and non-negative definite, its eigenvalues are real and non-negative, and thus $\det \mathbf{J} \geq 0$, where det denotes determinant, and $\operatorname{tr} \mathbf{J}(\mathbf{r}) \geq 0$. The diagonal elements $J_{xx}(\mathbf{r})$ and $J_{yy}(\mathbf{r})$ are the intensities $I_x(\mathbf{r})$ and $I_y(\mathbf{r})$ of the x and y components of the beam, respectively, and thus the trace of the polarization matrix is the total intensity $\operatorname{tr} \mathbf{J}(\mathbf{r}) = I(\mathbf{r}) = I_x(\mathbf{r}) + I_y(\mathbf{r})$. The off-diagonal element $J_{xy}(\mathbf{r})$ characterizes the correlations between the orthogonal field components. Its absolute value is bounded from above by $|J_{xy}(\mathbf{r})| \leq \sqrt{J_{xx}(\mathbf{r}) J_{yy}(\mathbf{r})}$ due to the non-negativity of the determinant. The correlation between the orthogonal field components may then be described with the normalized correlation coefficient

$$\gamma_{xy}(\mathbf{r}) = J_{xy}(\mathbf{r}) / \sqrt{J_{xx}(\mathbf{r}) J_{yy}(\mathbf{r})}, \tag{3.14}$$

which is bounded as $0 \leq |\gamma_{xy}(\mathbf{r})| \leq 1$. The lower bound corresponds to no correlation between the x and y components of the field and the upper bound to full correlation.

3.2 Polarization of an electromagnetic field

The polarization of an electromagnetic field is a description of how the electric field vector evolves in time. The field may be unpolarized, partially polarized, or fully polarized, depending on the degree of correlation between the two electric components and their intensities. Complete polarization is characterized by the correlation between the field components attaining its maximum value, that is, $|\gamma_{xy}(\mathbf{r})| = 1$, and thus equivalently $\det \mathbf{J}(\mathbf{r}) = 0$. Complete unpolarization is characterized by no correlation between the field components, i.e., $|\gamma_{xy}(\mathbf{r})| = 0$, and equal intensities in both field components, i.e., $J_{xx}(\mathbf{r}) = J_{yy}(\mathbf{r})$. The latter condition ensures that there is no preferred direction of polarization. Intermediate cases correspond to partially polarized fields.

3.2.1 Degree of polarization

The polarization matrix of any beam may be uniquely decomposed into a sum of two polarization matrices, one of which represents a fully unpolarized beam and the other a fully polarized beam, i.e.,

$$\mathbf{J}(\mathbf{r}) = \mathbf{J}^{(\mathrm{unpol})}(\mathbf{r}) + \mathbf{J}^{(\mathrm{pol})}(\mathbf{r}), \tag{3.15}$$

with

$$\mathbf{J}^{(\mathrm{unpol})}(\mathbf{r}) = A(\mathbf{r}) \begin{bmatrix} 1 & 0 \\ 0 & 1 \end{bmatrix}, \qquad \mathbf{J}^{(\mathrm{pol})}(\mathbf{r}) = \begin{bmatrix} B(\mathbf{r}) & D(\mathbf{r}) \\ D^*(\mathbf{r}) & C(\mathbf{r}) \end{bmatrix}, \tag{3.16}$$

where $A(\mathbf{r}), B(\mathbf{r}), C(\mathbf{r}) \geq 0$ and $B(\mathbf{r})C(\mathbf{r}) - |D(\mathbf{r})|^2 = 0$. These matrices fulfill the conditions given for fully unpolarized and fully polarized fields stated above. The existence and uniqueness of this decomposition for any polarization matrix is known as Stokes's theorem [32]. The theorem has also been extended to the propagation of the cross-spectral density matrix (frequency domain equivalent of the coherence matrix), but then the decomposition does not exist for all beams [32–34].

The traces of $\mathbf{J}^{(\mathrm{unpol})}(\mathbf{r})$ and $\mathbf{J}^{(\mathrm{pol})}(\mathbf{r})$ give the energy carried by the unpolarized and polarized components of the beam. The fraction of the beam energy in the fully polarized component, called the *degree of polarization*, is

$$P_{\mathrm{t}}(\mathbf{r}) = \frac{\operatorname{tr}\mathbf{J}^{(\mathrm{pol})}(\mathbf{r})}{\operatorname{tr}\mathbf{J}(\mathbf{r})} = \sqrt{1 - 4\frac{\det\mathbf{J}(\mathbf{r})}{\operatorname{tr}^2\mathbf{J}(\mathbf{r})}} = \sqrt{2\frac{\operatorname{tr}\mathbf{J}^2(\mathbf{r})}{\operatorname{tr}^2\mathbf{J}(\mathbf{r})} - 1}, \tag{3.17}$$

which may take values in the interval $0 \leq P_{\mathrm{t}}(\mathbf{r}) \leq 1$. The value $P_{\mathrm{t}}(\mathbf{r}) = 0$ corresponds to unpolarized field and $P_{\mathrm{t}}(\mathbf{r}) = 1$ to fully polarized field at point $\mathbf{r}$. Other values correspond to a partially polarized field.

3.2.2 Stokes parameters and Poincaré sphere

The polarization matrix $\mathbf{J}(\mathbf{r})$ may be expressed using the Pauli decomposition, similarly to that of the coherence matrix in Eq. (3.5):

$$\mathbf{J}(\mathbf{r}) = \frac{1}{2}\sum_{i=0}^{3} S_{\mathrm{t}i}(\mathbf{r})\boldsymbol{\sigma}_i, \tag{3.18}$$

with

$$S_{\mathrm{t}i}(\mathbf{r}) = \operatorname{tr}\left[\mathbf{J}(\mathbf{r})\boldsymbol{\sigma}_i\right]. \tag{3.19}$$

The expansion coefficients, or *Stokes parameters* are real due to the Hermiticity of the Pauli matrices and the polarization matrix. Written out explicity, the Stokes parameters are [6, 18, 35]

$$S_{\mathrm{t}0}(\mathbf{r}) = J_{xx}(\mathbf{r}) + J_{yy}(\mathbf{r}), \tag{3.20a}$$

$$S_{\mathrm{t}1}(\mathbf{r}) = J_{xx}(\mathbf{r}) - J_{yy}(\mathbf{r}), \tag{3.20b}$$

$$S_{\mathrm{t}2}(\mathbf{r}) = J_{xy}(\mathbf{r}) + J_{yx}(\mathbf{r}), \tag{3.20c}$$

$$S_{\mathrm{t}3}(\mathbf{r}) = i\left[J_{yx}(\mathbf{r}) - J_{xy}(\mathbf{r})\right]. \tag{3.20d}$$

A more intuitive interpretation is obtained when the matrix $\mathbf{J}(\mathbf{r})$ is transformed to different coordinate systems. The coordinate system (α, β) is defined by the basis vectors $\hat{u}_\alpha = \left(\hat{u}_x + \hat{u}_y\right)/\sqrt{2}$ and $\hat{u}_\beta = \left(-\hat{u}_x + \hat{u}_y\right)/\sqrt{2}$. The (r, l) coordinate system is defined using the right- and left-circularly polarized states as basis vectors, i.e., $\hat{u}_r = \left(\hat{u}_x - i\hat{u}_y\right)/\sqrt{2}$ and $\hat{u}_l = \left(\hat{u}_x + i\hat{u}_y\right)/\sqrt{2}$. Expressing each Stokes parameter using a convenient basis gives

$$S_{\mathrm{t}0}(\mathbf{r}) = I_x(\mathbf{r}) + I_y(\mathbf{r}), \tag{3.21a}$$

$$S_{\mathrm{t}1}(\mathbf{r}) = I_x(\mathbf{r}) - I_y(\mathbf{r}), \tag{3.21b}$$

$$S_{\mathrm{t}2}(\mathbf{r}) = I_\alpha(\mathbf{r}) - I_\beta(\mathbf{r}), \tag{3.21c}$$

$$S_{\mathrm{t}3}(\mathbf{r}) = I_r(\mathbf{r}) - I_l(\mathbf{r}), \tag{3.21d}$$

where the shorthand $I_i(\mathbf{r}) = J_{ii}(\mathbf{r})$ has been used. It is evident that $S_{\mathrm{t}0}(\mathbf{r})$ gives the total intensity of the field, $S_{\mathrm{t}1}(\mathbf{r})$ gives the excess of x-polarized component over the y-polarized component, $S_{\mathrm{t}2}(\mathbf{r})$ gives the excess of the component along the $+45^\circ$ direction over the component along the $+135^\circ$ direction, and $S_{\mathrm{t}3}(\mathbf{r})$ gives the excess of right circular polarized component over the left circular polarized component.

One can show that $S_{\mathrm{t}1}^2(\mathbf{r}) + S_{\mathrm{t}2}^2(\mathbf{r}) + S_{\mathrm{t}3}^2(\mathbf{r}) \leq S_{\mathrm{t}0}^2(\mathbf{r})$. The normalized Stokes parameters are then defined as

$$s_{\mathrm{t}i}(\mathbf{r}) = \frac{S_{\mathrm{t}i}(\mathbf{r})}{S_{\mathrm{t}0}(\mathbf{r})}, \tag{3.22}$$

where $i = 1, 2, 3$, each $s_{\mathrm{t}i}(\mathbf{r})$ is bounded as $|s_{\mathrm{t}i}(\mathbf{r})| \leq 1$, and the square sum of the normalized parameters is $s_{\mathrm{t}1}^2(\mathbf{r}) + s_{\mathrm{t}2}^2(\mathbf{r}) + s_{\mathrm{t}3}^2(\mathbf{r}) \leq 1$.

Expressing the elements of $\mathbf{J}(\mathbf{r})$ in Eq. (3.17) in terms of the Stokes parameters shows that

$$P_{\mathrm{t}}^2(\mathbf{r}) = \frac{S_{\mathrm{t}1}^2(\mathbf{r}) + S_{\mathrm{t}2}^2(\mathbf{r}) + S_{\mathrm{t}3}^2(\mathbf{r})}{S_{\mathrm{t}0}^2(\mathbf{r})} = s_{\mathrm{t}1}^2(\mathbf{r}) + s_{\mathrm{t}2}^2(\mathbf{r}) + s_{\mathrm{t}3}^2(\mathbf{r}). \tag{3.23}$$

The parameter triplet $S_{\mathrm{t}1}(\mathbf{r}), S_{\mathrm{t}2}(\mathbf{r}), S_{\mathrm{t}3}(\mathbf{r})$ may be interpreted to represent a point in a three-dimensional space, and so the polarization state of a field may be stated using the Poincaré vector, defined as [35]

$$\mathbf{S}_{\mathrm{t}}(\mathbf{r}) = S_{\mathrm{t}1}(\mathbf{r})\hat{u}_1 + S_{\mathrm{t}2}(\mathbf{r})\hat{u}_2 + S_{\mathrm{t}3}(\mathbf{r})\hat{u}_3, \tag{3.24}$$

where $\hat{u}_1, \hat{u}_2, \hat{u}_3$ are mutually orthogonal unit vectors. It is then seen that

$$P_{\mathrm{t}}(\mathbf{r}) = \frac{|\mathbf{S}_{\mathrm{t}}(\mathbf{r})|}{S_{\mathrm{t}0}(\mathbf{r})}. \tag{3.25}$$

The length of the normalized Poincaré vector $\mathbf{S}_{\mathrm{t}}(\mathbf{r})/S_{\mathrm{t}0}(\mathbf{r})$ therefore gives the degree of

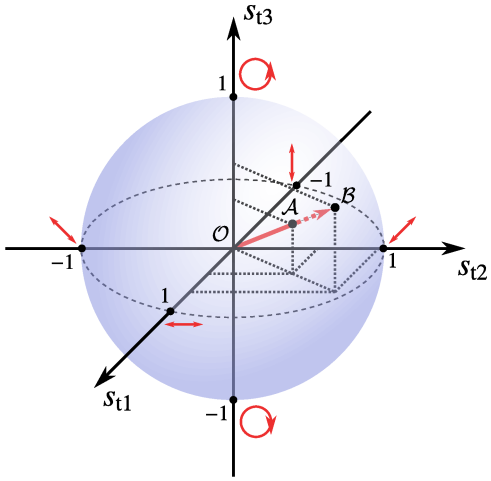

Figure 3.1: The Poincaré sphere. The red markings denote the polarization state at the points where the axes pierce the sphere surface. The points on the equator of the sphere, shown by the dashed circle, correspond to fully linearly polarized states. The poles of the sphere correspond to circularly polarized states. Other points on the sphere surface correspond to elliptically fully polarized states, and points inside the sphere correspond to partially polarized states. Point $\mathcal{A}$ represents the polarization state of a partially elliptically polarized beam. The length of the segment $\mathcal{OA}$ is the degree of polarization of the beam, and the polarization state of the fully polarized part of the beam is obtained by continuing the line segment $\mathcal{OA}$ to the surface of the sphere (point $\mathcal{B}$).

polarization, as seen from Eq. (3.25). The normalized Poincaré vector may be understood to represent a point inside or on a unit sphere, the Poincaré sphere, as illustrated in Fig. 3.1. Points on the surface of the sphere represent fully polarized states, points inside the sphere represent partially polarized states, and the center of the sphere represents the fully unpolarized state.

The points on the equator plane of the sphere correspond to linear polarization states [$s_{t3}(\mathbf{r}) = 0$], the poles of the sphere correspond to circular polarization states, and other points correspond to elliptical polarization states. The sense of rotation of the circular and elliptical polarization states is given by the hemisphere in which the point is: points on the 'northern' hemisphere [$s_{t3}(\mathbf{r}) > 0$] represent right-handed polarization states, and points on the 'southern' hemisphere correspond to left-handed polarization states.

As mentioned in connection with Eq. (3.15), a partially polarized field may be divided into fully polarized and fully unpolarized parts. The normalized Stokes parameters of the polarized part of the beam turn out, after a brief calculation, to be

$$s_{ti}^{(\mathrm{pol})}(\mathbf{r}) = \frac{S_{ti}(\mathbf{r})}{P_{\mathrm{t}}(\mathbf{r})S_{\mathrm{t}0}(\mathbf{r})} = \frac{s_{ti}(\mathbf{r})}{P_{\mathrm{t}}(\mathbf{r})}, \tag{3.26}$$

which is consistent with Eq. (3.23). The result can be interpreted in terms of the Poincaré sphere by noting that if point $\mathcal{A}$ inside the sphere corresponds to the polarization state of a certain field, then the polarization state of the fully polarized part of the field is obtained by dividing the normalized Stokes parameters of the field by the degree of polarization, giving the coordinates of point $\mathcal{B}$. Point $\mathcal{B}$ is obtained geometrically by continuing the line segment $\mathcal{OA}$, where $\mathcal{O}$ is the center of the sphere, to the sphere's surface.

Chapter 4

Stationary electromagnetic beams in frequency domain

A time-varying signal may be expressed as a sum of single-frequency components via the Fourier transform of the signal, as shown in the previous chapter. This frequency representation is more convenient than the time representation when dealing with problems involving, e.g., interaction with matter, as evident from Eq. (2.7). The results from the frequency domain representation are also more general than the ones from the time domain representation: in the time domain, the signal is often assumed to be quasimonochromatic, but in frequency domain this assumption is not necessary. This chapter presents the polarization and coherence properties of frequency domain fields.

4.1 Cross-spectral density matrix

The coherence properties of a stationary random beam in the frequency domain are encoded in the (electric) *cross-spectral density matrix* $\mathbf{W}(\mathbf{r}_1, \mathbf{r}_2, \omega)$ defined by [18, 36]

$$\langle \widetilde{\mathbf{E}}^*(\mathbf{r}_1, \omega) \widetilde{\mathbf{E}}^T(\mathbf{r}_2, \omega') \rangle = \mathbf{W}(\mathbf{r}_1, \mathbf{r}_2, \omega) \delta(\omega - \omega'), \tag{4.1}$$

where $\widetilde{\mathbf{E}}(\mathbf{r}_1, \omega)$ is the Fourier component of the electric field at frequency ω as defined in Eq. (2.33) and the angle brackets denote ensemble average over all the realizations of the field. The Dirac delta, which arises from the stationarity of the beam, indicates that the different spectral components are uncorrelated. The cross-spectral density matrix is Hermitian in the sense that

$$\mathbf{W}(\mathbf{r}_1, \mathbf{r}_2, \omega) = \mathbf{W}^\dagger(\mathbf{r}_2, \mathbf{r}_1, \omega), \tag{4.2}$$

and is related to the (time domain) mutual coherence matrix in Eq. (3.1) via the Fourier transform as

$$\mathbf{W}(\mathbf{r}_1, \mathbf{r}_2, \omega) = \frac{1}{2\pi} \int_{-\infty}^{\infty} \mathbf{\Gamma}(\mathbf{r}_1, \mathbf{r}_2, \tau) e^{i\omega\tau} \mathrm{d}\tau, \tag{4.3}$$

$$\mathbf{\Gamma}(\mathbf{r}_1, \mathbf{r}_2, \tau) = \int_{0}^{\infty} \mathbf{W}(\mathbf{r}_1, \mathbf{r}_2, \omega) e^{-i\omega\tau} \mathrm{d}\omega, \tag{4.4}$$

which is a special case of the generalized Wiener-Khintchine theorem [18]. The cross-spectral density matrix is also non-negative definite in the sense that

$$\sum_{m,n=1,2} \mathbf{a}^{\dagger}(\mathbf{r}_m) \mathbf{W}(\mathbf{r}_m, \mathbf{r}_n, \omega) \mathbf{a}(\mathbf{r}_n) \geq 0, \tag{4.5}$$

where $\mathbf{a}(\mathbf{r})$ is an arbitrary complex vector function.

The cross-spectral density matrix can be expressed using the Pauli decomposition similar to Eq. (3.5), with the coherence matrix replaced by the cross-spectral density matrix. The expansion coefficients are the 2-point (or generalized) spectral Stokes parameters [37]:

$$S_{\mathrm{s}0}^{(2)}(\mathbf{r}_1, \mathbf{r}_2, \omega) = W_{xx}(\mathbf{r}_1, \mathbf{r}_2, \omega) + W_{yy}(\mathbf{r}_1, \mathbf{r}_2, \omega), \tag{4.6a}$$

$$S_{\mathrm{s}1}^{(2)}(\mathbf{r}_1, \mathbf{r}_2, \omega) = W_{xx}(\mathbf{r}_1, \mathbf{r}_2, \omega) - W_{yy}(\mathbf{r}_1, \mathbf{r}_2, \omega), \tag{4.6b}$$

$$S_{\mathrm{s}2}^{(2)}(\mathbf{r}_1, \mathbf{r}_2, \omega) = W_{xy}(\mathbf{r}_1, \mathbf{r}_2, \omega) + W_{yx}(\mathbf{r}_1, \mathbf{r}_2, \omega), \tag{4.6c}$$

$$S_{\mathrm{s}3}^{(2)}(\mathbf{r}_1, \mathbf{r}_2, \omega) = i\Big[W_{yx}(\mathbf{r}_1, \mathbf{r}_2, \omega) - W_{xy}(\mathbf{r}_1, \mathbf{r}_2, \omega)\Big]. \tag{4.6d}$$

The 2-point spectral Stokes parameters depend linearly on the elements of the cross-spectral density matrix, so they are related to the temporal 2-point Stokes parameters in Eq. (3.7) via Eqs. (4.3) and (4.4) applied elementwise to $\mathbf{W}(\mathbf{r}_1, \mathbf{r}_2, \omega)$. The 2-point parameters have similar physical interpretations as the temporal (1-point) Stokes parameters [38].

4.2 Spectral polarization matrix

The spectral polarization properties at a single point in space are presented in the *spectral polarization matrix*

$$\mathbf{\Phi}(\mathbf{r}, \omega) = \mathbf{W}(\mathbf{r}, \mathbf{r}, \omega). \tag{4.7}$$

As evident from Eq. (4.4) and the definition of the polarization matrix $\mathbf{J}(\mathbf{r})$ in Eq. (3.11), $\mathbf{J}(\mathbf{r})$ and $\mathbf{\Phi}(\mathbf{r}, \omega)$ are related via

$$\mathbf{J}(\mathbf{r}) = \int_0^\infty \mathbf{\Phi}(\mathbf{r}, \omega) \mathrm{d}\omega, \tag{4.8}$$

and the spectral polarization matrix can be calculated from the (temporal) coherence matrix using Eq. (4.3):

$$\mathbf{\Phi}(\mathbf{r}, \omega) = \frac{1}{2\pi} \int_{-\infty}^\infty \mathbf{\Gamma}(\mathbf{r}, \mathbf{r}, \tau) e^{i\omega\tau} \mathrm{d}\tau. \tag{4.9}$$

The diagonal elements $\Phi_{ii}(\mathbf{r}, \omega)$ are the *spectral densities* of the components of the field. The spectral density gives the intensity in the field component oscillating at frequency ω, i.e., the intensity related to the component i at the frequency interval $[\omega, \omega + \mathrm{d}\omega]$ is $S_i(\omega, \mathbf{r})\,\mathrm{d}\omega = \Phi_{ii}(\mathbf{r}, \omega)\,\mathrm{d}\omega$. From Eq. (4.8) it follows that integrating the spectral density of a component over all frequencies yields the (time domain) intensity of that component. The total spectral density is then $\mathrm{tr}\,\mathbf{\Phi}(\mathbf{r}, \omega) = S_x(\mathbf{r}, \omega) + S_y(\mathbf{r}, \omega) = S(\mathbf{r}, \omega)$. The off-diagonal element $\Phi_{xy}(\mathbf{r}, \omega)$ measures the correlation between the orthogonal field components at frequency ω.

Equation (4.2) shows that the spectral polarization matrix is Hermitian in the usual sense, and the non-negative definiteness (4.5) of $\mathbf{W}(\mathbf{r}_1, \mathbf{r}_2, \omega)$ implies that the spectral polarization matrix is non-negative definite:

$$\mathbf{a}^\dagger \mathbf{\Phi}(\mathbf{r}, \omega) \mathbf{a} \geq 0, \tag{4.10}$$

where $\mathbf{a}$ is an arbitrary complex vector. The non-negative definiteness signifies that the determinant of $\mathbf{\Phi}(\mathbf{r}, \omega)$ is also non-negative, and thus the absolute value of the off-diagonal element $\Phi_{xy}(\mathbf{r}, \omega)$ is bounded as $0 \leq |\Phi_{xy}(\mathbf{r}, \omega)| \leq \sqrt{\Phi_{xx}(\mathbf{r}, \omega)\Phi_{yy}(\mathbf{r}, \omega)}$. The off-diagonal term may then be normalized to give the normalized correlation coefficient

$$\mu_{xy}(\mathbf{r}, \omega) = \frac{\Phi_{xy}(\mathbf{r}, \omega)}{\sqrt{\Phi_{xx}(\mathbf{r}, \omega)\Phi_{yy}(\mathbf{r}, \omega)}}, \tag{4.11}$$

which is is bounded as $0 \leq |\mu_{xy}(\mathbf{r}, \omega)| \leq 1$. The lower bound corresponds to no correlation at frequency ω between field components, and upper bound corresponds to full correlation. The correlation coefficient $\mu_{xy}(\mathbf{r}, \omega)$ is analogous to the correlation coefficient $\gamma_{xy}(\mathbf{r})$ [Eq. (3.14)] in time domain.

The spectral coherence matrix therefore has the same mathematical properties as the (time domain) polarization matrix $\mathbf{J}(\mathbf{r})$, and this mathematical similarity will be employed in the following section.

4.3 Spectral polarization

4.3.1 Spectral degree of polarization

The polarization properties of the spectral components of a random beam may be investigated using a formalism analogous to the one presented in the previous chapter. The Hermiticity and non-negative definiteness of $\mathbf{\Phi}(\mathbf{r},\omega)$ imply that, like the polarization matrix $\mathbf{J}(\mathbf{r})$, it may always be decomposed into two parts:

$$\mathbf{\Phi}(\mathbf{r},\omega) = \mathbf{\Phi}^{(\mathrm{unpol})}(\mathbf{r},\omega) + \mathbf{\Phi}^{(\mathrm{pol})}(\mathbf{r},\omega), \tag{4.12}$$

where

$$\mathbf{\Phi}^{(\mathrm{unpol})}(\mathbf{r},\omega) = A(\mathbf{r},\omega)\begin{bmatrix}1 & 0\\ 0 & 1\end{bmatrix}, \qquad \mathbf{\Phi}^{(\mathrm{pol})}(\mathbf{r},\omega) = \begin{bmatrix}B(\mathbf{r},\omega) & D(\mathbf{r},\omega)\\ D^{*}(\mathbf{r},\omega) & C(\mathbf{r},\omega)\end{bmatrix}, \tag{4.13}$$

with $A(\mathbf{r},\omega), B(\mathbf{r},\omega), C(\mathbf{r},\omega) \geq 0$ and $\det \mathbf{\Phi}^{(\mathrm{pol})}(\mathbf{r},\omega) = B(\mathbf{r},\omega)C(\mathbf{r},\omega) - |D(\mathbf{r},\omega)|^2 = 0$. The matrix $\mathbf{\Phi}^{(\mathrm{unpol})}(\mathbf{r},\omega)$ represents a fully unpolarized spectral component, as there are no correlations between the orthogonal field components, and none will appear even if the coordinate system is subjected to an arbitrary unitary transformation.

Similarly, the *spectral degree of polarization* may be defined as the fraction of the spectral density that is in the fully polarized component, i.e.,

$$P_{\mathrm{s}}(\mathbf{r},\omega) = \frac{\mathrm{tr}\,\mathbf{\Phi}^{(\mathrm{pol})}(\mathbf{r},\omega)}{\mathrm{tr}\,\mathbf{\Phi}(\mathbf{r},\omega)} = \sqrt{1 - 4\frac{\det \mathbf{\Phi}(\mathbf{r},\omega)}{\mathrm{tr}^2\,\mathbf{\Phi}(\mathbf{r},\omega)}} = \sqrt{2\frac{\mathrm{tr}\,\mathbf{\Phi}^2(\mathbf{r},\omega)}{\mathrm{tr}^2\,\mathbf{\Phi}(\mathbf{r},\omega)} - 1}. \tag{4.14}$$

The spectral degree of polarization is bounded as $0 \leq P_{\mathrm{s}}(\mathbf{r},\omega) \leq 1$, with 0 and 1 corresponding to full unpolarization and full polarization, respectively. The time-domain degree of polarization of the beam cannot, in general, be obtained from the spectral degree of polarization. It is also apparent from Eqs. (3.11) and (4.9), by setting $\mathbf{r}_1 = \mathbf{r}_2 = \mathbf{r}$, that whereas the temporal degree of polarization does not depend on the temporal coherence properties of the field, the spectral degree of coherence does [39].

4.3.2 Spectral Stokes parameters

The polarization state of a random beam at frequency ω may be represented using the spectral Stokes parameters, which are defined analogously to their temporal counterparts

in Eq. (3.20) using the elements of the spectral coherence matrix:

$$S_{\mathrm{s}0}(\mathbf{r},\omega) = \Phi_{xx}(\mathbf{r},\omega) + \Phi_{yy}(\mathbf{r},\omega), \tag{4.15a}$$

$$S_{\mathrm{s}1}(\mathbf{r},\omega) = \Phi_{xx}(\mathbf{r},\omega) - \Phi_{yy}(\mathbf{r},\omega), \tag{4.15b}$$

$$S_{\mathrm{s}2}(\mathbf{r},\omega) = \Phi_{xy}(\mathbf{r},\omega) + \Phi_{yx}(\mathbf{r},\omega), \tag{4.15c}$$

$$S_{\mathrm{s}3}(\mathbf{r},\omega) = i\left[\Phi_{yx}(\mathbf{r},\omega) - \Phi_{xy}(\mathbf{r},\omega)\right]. \tag{4.15d}$$

The spectral Stokes parameters are the coefficients in the Pauli decomposition of $\mathbf{\Phi}(\mathbf{r},\omega)$:

$$\mathbf{\Phi}(\mathbf{r},\omega) = \frac{1}{2}\sum_{i=0}^{3} S_{\mathrm{s}i}(\mathbf{r},\omega)\boldsymbol{\sigma}_i, \tag{4.16}$$

similarly to the Pauli expansion of the time-domain polarization matrix $\mathbf{J}(\mathbf{r})$ in Eq. (3.18). According to Eq. (4.8), each spectral Stokes parameter, when integrated over all positive frequencies, yields the corresponding time domain Stokes parameter of Eqs. (3.20):

$$S_{\mathrm{t}i}(\mathbf{r}) = \int_0^\infty S_{\mathrm{s}i}(\mathbf{r},\omega)\,\mathrm{d}\omega. \tag{4.17}$$

Conversely, the spectral Stokes parameters may be obtained from the 2-point Stokes parameters in Eq. (3.7) at a single point in space via

$$S_{\mathrm{s}i}(\mathbf{r},\omega) = \frac{1}{2\pi}\int_{-\infty}^{\infty} S_{\mathrm{t}i}^{(2)}(\mathbf{r},\mathbf{r},\tau)e^{i\omega\tau}\mathrm{d}\tau. \tag{4.18}$$

In full analogy to the temporal case, the spectral degree of polarization may be expressed using the spectral Stokes parameters as

$$P_{\mathrm{s}}^2(\mathbf{r},\omega) = \frac{S_{\mathrm{s}1}^2(\mathbf{r},\omega) + S_{\mathrm{s}2}^2(\mathbf{r},\omega) + S_{\mathrm{s}3}^2(\mathbf{r},\omega)}{S_{\mathrm{s}0}^2(\mathbf{r},\omega)}. \tag{4.19}$$

The Stokes parameters may be used to define the spectral Poincaré vector [cf. Eq. (3.24)]:

$$\mathbf{S}_{\mathrm{s}}(\mathbf{r},\omega) = S_{\mathrm{s}1}(\mathbf{r},\omega)\hat{u}_1 + S_{\mathrm{s}2}(\mathbf{r},\omega)\hat{u}_2 + S_{\mathrm{s}3}(\mathbf{r},\omega)\hat{u}_3, \tag{4.20}$$

and the spectral degree of polarization may then be expressed as

$$P_{\mathrm{s}}(\mathbf{r},\omega) = \frac{|\mathbf{S}_{\mathrm{s}}(\mathbf{r},\omega)|}{S_{\mathrm{s}0}(\mathbf{r},\omega)}. \tag{4.21}$$

The spectral Stokes parameters have the same physical interpretation as the respective temporal parameters. Similarly, the Stokes parameters may be used to construct the spectral Poincaré sphere, which describes the behavior of the field component at frequency ω.

4.3.3 Differences between time and frequency domain polarization

Due to the integral relation between the spectral and temporal Stokes parameters it is not possible to derive a general connection between the degrees of polarization in the two domains, and it is not known whether any such connection exists [39, 40]

To illustrate the difference between temporal and spectral polarization, the following examples are considered [39]. The first example is a beam whose x and y components are mutually uncorrelated and of equal intensity $I(\mathbf{r})$, and thus the beam at a single point has the coherence and polarization matrices

$$\mathbf{\Gamma}(\mathbf{r}, \mathbf{r}, \tau) = \begin{bmatrix} I(\mathbf{r}) f_x(\tau) & 0 \\ 0 & I(\mathbf{r}) f_y(\tau) \end{bmatrix}, \tag{4.22}$$

$$\mathbf{J}(\mathbf{r}) = \begin{bmatrix} I(\mathbf{r}) & 0 \\ 0 & I(\mathbf{r}) \end{bmatrix}, \tag{4.23}$$

where $f_x(\tau)$ and $f_y(\tau)$ are the normalized autocorrelation functions of the x and y components of the field, respectively. The spectral polarization matrix is

$$\mathbf{\Phi}(\mathbf{r}, \omega) = \begin{bmatrix} I(\mathbf{r}) \tilde{f}_x(\omega) & 0 \\ 0 & I(\mathbf{r}) \tilde{f}_y(\omega) \end{bmatrix}, \tag{4.24}$$

where the quantities $I(\mathbf{r})\tilde{f}_x(\omega)$ and $I(\mathbf{r})\tilde{f}_y(\omega)$ are the power spectral densities of the x and y components of the field, respectively. The field is temporally unpolarized, as mentioned in Sec. 3.2, because there are no correlations between the field components and none will appear in any coordinate rotation due to the equal intensities of the components. However, the diagonal elements of the spectral coherence matrix are, in general, not equal, and thus spectrally the field is not necessarily fully unpolarized. The spectral degree of polarization is

$$P_{\mathrm{s}}(\omega) = \left| \frac{\tilde{f}_x(\omega) - \tilde{f}_y(\omega)}{\tilde{f}_x(\omega) + \tilde{f}_y(\omega)} \right|, \tag{4.25}$$

which may have any value on the interval $0 \leq P_{\mathrm{s}}(\omega) \leq 1$. The field is spectrally fully unpolarized at frequencies for which the power spectral densities in the x and y components are equal, and fully polarized at frequencies for which either of the components has zero spectral density.

Another example is a beam whose y component is a delayed copy of the x component, i.e., $E_y(\mathbf{r}, t) = E_x(\mathbf{r}, t - \tau_d)$. The coherence and polarization matrices are then

$$\mathbf{\Gamma}(\mathbf{r}, \mathbf{r}, \tau) = I(\mathbf{r}) \begin{bmatrix} \gamma(\mathbf{r}, \tau) & \gamma(\mathbf{r}, \tau - \tau_d) \\ \gamma(\mathbf{r}, \tau + \tau_d) & \gamma(\mathbf{r}, \tau) \end{bmatrix}, \tag{4.26}$$

$$\mathbf{J}(\mathbf{r}) = I(\mathbf{r}) \begin{bmatrix} 1 & \gamma(\mathbf{r}, -\tau_d) \\ \gamma(\mathbf{r}, \tau_d) & 1 \end{bmatrix}, \tag{4.27}$$

where $I(\mathbf{r}) = \langle |E_x(\mathbf{r}, t)|^2 \rangle$ is the intensity, and $\gamma(\mathbf{r}, \tau) = \langle E_x^*(\mathbf{r}, t) E_x(\mathbf{r}, t + \tau) \rangle / I(\mathbf{r})$ characterizes the coherence of the components. The spectral polarization matrix is

$$\mathbf{\Phi}(\mathbf{r}, \omega) = I(\mathbf{r}) \tilde{\gamma}(\mathbf{r}, \omega) \begin{bmatrix} 1 & e^{i\omega\tau_d} \\ e^{-i\omega\tau_d} & 1 \end{bmatrix}, \tag{4.28}$$

where again $I(\mathbf{r})\tilde{\gamma}(\mathbf{r}, \omega)$ is the spectral density. Inserting $\mathbf{\Phi}(\mathbf{r}, \omega)$ into Eq. (4.14) gives that $P_\mathrm{s}(\mathbf{r}, \omega) = 1$, i.e., the field is spectrally fully polarized at all frequencies independently of the temporal coherence of the field. The temporal polarization turns out to be $P_\mathrm{t}(\mathbf{r}) = |\gamma(\tau_d)|$. With no delay between the x and y components, the field is necessarily fully temporally polarized [since $\gamma(0) = 1$]. Also, all physically meaningful fields are incoherent for sufficient large time delays, i.e., $\gamma(\tau) = 0$ for large τ, and so for large τ_d the field is unpolarized. Therefore the described configuration leads to a field for which the temporal degree of polarization is tunable between 0 and 1, and the spectral degree of polarization is 1 for all frequencies.

An overview of the temporal and spectral polarization properties of some typical optical fields, including the examples presented above, is given in Table 4.1.

Table 4.1: Temporal and spectral polarization properties of various types of electromagnetic beams. After [41].

Beam type	Time domain	Spectral domain	Comments
Monochromatic	$P_\mathrm{t} = 1$	$P_\mathrm{s} = 1$	Idealization
Quasi-monochromatic	$0 \leq P_\mathrm{t} \leq 1$	$P_\mathrm{s}(\omega_0) = P_\mathrm{t}$	At center frequency
Uncorrelated orthogonal waves, equal intensities	$P_\mathrm{t} = 0$	$0 \leq P_\mathrm{s}(\omega) \leq 1$	P_s depends on spectra of components
Uncorrelated orthogonal waves, unequal intensities	$0 < P_\mathrm{t} < 1$	$0 \leq P_\mathrm{s}(\omega) \leq 1$	P_s depends on spectra of components
Delayed orthogonal waves	$0 \leq P_\mathrm{t} \leq 1$	$P_\mathrm{s}(\omega) = 1$	At all frequencies

Chapter 5

Pulsed beams in time domain

In this chapter the polarization formalism of stationary beams reviewed in Chap. 3 is extended to non-stationary beams. The temporal polarization and coherence matrices for a non-stationary beam are presented, and the quantities describing the polarization of the field, the degree of polarization and the Stokes parameters, are derived in terms of the polarization matrix.

5.1 Coherence matrix of non-stationary field

The second-order statistical properties of a non-stationary beam are expressed using the 2×2 coherence matrix $\mathbf{\Gamma}(\mathbf{r}_1, \mathbf{r}_2, t_1, t_2)$ [43]

$$\begin{aligned} \mathbf{\Gamma}(\mathbf{r}_1, \mathbf{r}_2, t_1, t_2) &= \langle \mathbf{E}^*(\mathbf{r}_1, t_1) \mathbf{E}^T(\mathbf{r}_2, t_2) \rangle \\ &= \begin{bmatrix} \langle E_x^*(\mathbf{r}_1, t_1) E_x(\mathbf{r}_2, t_2) \rangle & \langle E_x^*(\mathbf{r}_1, t_1) E_y(\mathbf{r}_2, t_2) \rangle \\ \langle E_y^*(\mathbf{r}_1, t_1) E_x(\mathbf{r}_2, t_2) \rangle & \langle E_y^*(\mathbf{r}_1, t_1) E_y(\mathbf{r}_2, t_2) \rangle \end{bmatrix}, \end{aligned} \tag{5.1}$$

which unlike in the stationary case depends explicitly on both t_1 and t_2, and not on their difference. The average $\langle \cdot \rangle$ is the ensemble average over many individual pulses. The coherence matrix is Hermitian and non-negative definite:

$$\mathbf{\Gamma}(\mathbf{r}_1, \mathbf{r}_2, t_1, t_2) = \mathbf{\Gamma}^\dagger(\mathbf{r}_2, \mathbf{r}_1, t_2, t_1), \tag{5.2}$$

and

$$\sum_{m,n=1,2} \mathbf{a}^\dagger(\mathbf{r}_m, t_m) \mathbf{\Gamma}(\mathbf{r}_m, \mathbf{r}_n, t_m, t_n) \mathbf{a}(\mathbf{r}_n, t_n) \geq 0, \tag{5.3}$$

where $\mathbf{a}(\mathbf{r}, t)$ is an arbitrary complex vector function. The non-negative definity can be shown by starting from $\langle|\mathbf{a}^T(\mathbf{r}_1, t_1)\mathbf{E}(\mathbf{r}_1, t_1) + \mathbf{a}^T(\mathbf{r}_2, t_2)\mathbf{E}(\mathbf{r}_2, t_2)|^2\rangle \geq 0$, from which Eq. (5.3) is obtained. The coherence matrix may be decomposed using the Pauli matrices

$$\mathbf{\Gamma}(\mathbf{r}_1, \mathbf{r}_2, t_1, t_2) = \frac{1}{2}\sum_{i=0}^{3} S_{\mathrm{t}i}^{(2)}(\mathbf{r}_1, \mathbf{r}_2, t_1, t_2)\boldsymbol{\sigma}_i, \tag{5.4}$$

where $\boldsymbol{\sigma}_i$ are the Pauli matrices given in Eq. (3.4) and the coefficients $S_{\mathrm{t}i}^{(2)}(\mathbf{r}_1, \mathbf{r}_2, t_1, t_2)$ are the *2-point, 2-time Stokes parameters*. The trace-orthonormality of $\{\boldsymbol{\sigma}_i\}$ may be used to obtain the expansion coefficients via

$$S_{\mathrm{t}i}^{(2)}(\mathbf{r}_1, \mathbf{r}_2, t_1, t_2) = \mathrm{tr}\,[\mathbf{\Gamma}(\mathbf{r}_1, \mathbf{r}_2, t_1, t_2)\boldsymbol{\sigma}_i], \tag{5.5}$$

to yield

$$S_{\mathrm{t}0}^{(2)}(\mathbf{r}_1, \mathbf{r}_2, t_1, t_2) = \Gamma_{xx}(\mathbf{r}_1, \mathbf{r}_2, t_1, t_2) + \Gamma_{yy}(\mathbf{r}_1, \mathbf{r}_2, t_1, t_2), \tag{5.6a}$$
$$S_{\mathrm{t}1}^{(2)}(\mathbf{r}_1, \mathbf{r}_2, t_1, t_2) = \Gamma_{xx}(\mathbf{r}_1, \mathbf{r}_2, t_1, t_2) - \Gamma_{yy}(\mathbf{r}_1, \mathbf{r}_2, t_1, t_2), \tag{5.6b}$$
$$S_{\mathrm{t}2}^{(2)}(\mathbf{r}_1, \mathbf{r}_2, t_1, t_2) = \Gamma_{xy}(\mathbf{r}_1, \mathbf{r}_2, t_1, t_2) + \Gamma_{yx}(\mathbf{r}_1, \mathbf{r}_2, t_1, t_2), \tag{5.6c}$$
$$S_{\mathrm{t}3}^{(2)}(\mathbf{r}_1, \mathbf{r}_2, t_1, t_2) = i\left[\Gamma_{yx}(\mathbf{r}_1, \mathbf{r}_2, t_1, t_2) - \Gamma_{xy}(\mathbf{r}_1, \mathbf{r}_2, t_1, t_2)\right]. \tag{5.6d}$$

Since $\mathbf{\Gamma}(\mathbf{r}_1, \mathbf{r}_2, t_1, t_2)$ is, in general, not purely Hermitian, the generalized Stokes parameters are complex.

5.1.1 Degree of coherence

The field's ability to interfere is measured by the degree of coherence. Quantitatively, the electromagnetic degree of coherence $\gamma_{\mathrm{EM}}(\mathbf{r}_1, \mathbf{r}_2, t_1, t_2)$ measures the mutual correlation between the fields $\mathbf{E}(\mathbf{r}_1, t_1)$ and $\mathbf{E}(\mathbf{r}_2, t_2)$ via the normalized correlation function

$$\gamma_{\mathrm{EM}}^2(\mathbf{r}_1, \mathbf{r}_2, t_1, t_2) = \frac{\mathrm{tr}\,[\mathbf{\Gamma}(\mathbf{r}_1, \mathbf{r}_2, t_1, t_2)\mathbf{\Gamma}(\mathbf{r}_2, \mathbf{r}_1, t_2, t_1)]}{\mathrm{tr}\,\mathbf{\Gamma}(\mathbf{r}_1, \mathbf{r}_1, t_1, t_1)\mathrm{tr}\,\mathbf{\Gamma}(\mathbf{r}_2, \mathbf{r}_2, t_2, t_2)} = \frac{\sum_{i,j}|\langle E_i^*(\mathbf{r}_1, t_1)E_j(\mathbf{r}_2, t_2)\rangle|^2}{I(\mathbf{r}_1, t_1)I(\mathbf{r}_2, t_2)}. \tag{5.7}$$

The coherence function is bounded as $0 \leq \gamma_{\mathrm{EM}}(\mathbf{r}_1, \mathbf{r}_2, t_1, t_2) \leq 1$, where the lower bound corresponds to no coherence and upper bound to full coherence. The traces in the denominator of Eq. (5.7) represent the intensities at points $\mathbf{r}_1, \mathbf{r}_2$ and times t_1, t_2, as explained in the next section.

5.1.2 Polarization matrix

The properties of the beam at a single point $(\mathbf{r}, t)$ in space–time are contained in the polarization matrix

$$\mathbf{J}(\mathbf{r}, t) = \mathbf{\Gamma}(\mathbf{r}, \mathbf{r}, t, t). \tag{5.8}$$

From this definition and Eqs. (5.2) and (5.3) follow that the polarization matrix is Hermitian and non-negative definite in the usual sense:

$$\mathbf{J}(\mathbf{r}, t) = \begin{bmatrix} \langle |E_x(\mathbf{r}, t)|^2 \rangle & \langle E_x^*(\mathbf{r}, t) E_y(\mathbf{r}, t) \rangle \\ \langle E_y^*(\mathbf{r}, t) E_x(\mathbf{r}, t) \rangle & \langle \left| E_y(\mathbf{r}, t) \right|^2 \rangle \end{bmatrix} = \mathbf{J}^\dagger(\mathbf{r}, t), \tag{5.9}$$

$$\mathbf{a}^\dagger \mathbf{J}(\mathbf{r}, t) \mathbf{a} \geq 0, \tag{5.10}$$

where $\mathbf{a}$ is an arbitrary complex vector. The diagonal elements of $\mathbf{J}(\mathbf{r}, t)$ are the *average* intensities $I_x(\mathbf{r}, t) = \langle |E_x(\mathbf{r}, t)|^2 \rangle$ and $I_y(\mathbf{r}, t) = \langle |E_y(\mathbf{r}, t)|^2 \rangle$, and their sum (the trace of the polarization matrix) is the total intensity $I(\mathbf{r}, t)$. The off-diagonal element $J_{xy}(\mathbf{r}, t)$ characterizes the correlation between the field components, and due to the non-negative definity of the polarization matrix [$\det \mathbf{J}(\mathbf{r}, t) \geq 0$] its absolute value is bounded by

$$|J_{xy}(\mathbf{r}, t)| \leq \sqrt{J_{xx}(\mathbf{r}, t) J_{yy}(\mathbf{r}, t)}. \tag{5.11}$$

This property can be used to define the normalized correlation coefficient

$$\gamma_{xy}(\mathbf{r}, t) = J_{xy}(\mathbf{r}, t) / \sqrt{J_{xx}(\mathbf{r}, t) J_{yy}(\mathbf{r}, t)}, \tag{5.12}$$

which is bounded $0 \leq |\gamma_{xy}(\mathbf{r}, t)| \leq 1$. The lower bound corresponds to a situation where the field components are not correlated, and upper bound corresponds to full correlation. The upper limit is obtained via Eq. (2.30) and the definition of $\mathbf{J}(\mathbf{r}, t)$.

5.2 Polarization of non-stationary fields

The statistical properties of a non-stationary field, including the intensity of the beam components and the correlation between components, change with time as the name implies. The polarization state of the beam is thus not constant, as was the case in stationary beams. The polarization formalism needs therefore to be reformulated to take into account the time-varying polarization properties.

The degree of polarization of a pulse is defined similarly to the degree of polarization in the stationary case, i.e., as the fraction of the intensity in the fully polarized component

of the pulse. The polarization matrix $\mathbf{J}(\mathbf{r}, t)$ is Hermitian and non-negative definite, so it may be decomposed into fully unpolarized and fully polarized parts similarly to the stationary polarization matrix:

$$\mathbf{J}(\mathbf{r}, t) = \mathbf{J}^{(\mathrm{unpol})}(\mathbf{r}, t) + \mathbf{J}^{(\mathrm{pol})}(\mathbf{r}, t), \tag{5.13}$$

where

$$\mathbf{J}^{(\mathrm{unpol})}(\mathbf{r}, t) = A(\mathbf{r}, t)\begin{bmatrix} 1 & 0 \\ 0 & 1 \end{bmatrix}, \qquad \mathbf{J}^{(\mathrm{pol})}(\mathbf{r}, t) = \begin{bmatrix} B(\mathbf{r}, t) & D(\mathbf{r}, t) \\ D^*(\mathbf{r}, t) & C(\mathbf{r}, t) \end{bmatrix}, \tag{5.14}$$

represent unpolarized and fully polarized components, respectively, with the conditions $A(\mathbf{r}, t), B(\mathbf{r}, t), C(\mathbf{r}, t) \geq 0$ and $B(\mathbf{r}, t)C(\mathbf{r}, t) - |D(\mathbf{r}, t)|^2 = 0$. The degree of polarization is the ratio of the intensity in the polarized component to the total intensity:

$$P_{\mathrm{t}}(\mathbf{r}, t) = \frac{\operatorname{tr} \mathbf{J}^{(\mathrm{pol})}(\mathbf{r}, t)}{\operatorname{tr} \mathbf{J}(\mathbf{r}, t)} = \sqrt{2\frac{\operatorname{tr} \mathbf{J}^2(\mathbf{r}, t)}{\operatorname{tr}^2 \mathbf{J}(\mathbf{r}, t)} - 1}. \tag{5.15}$$

Unlike in the stationary case, the degree of polarization now depends on time. Thus the degree of polarization at different points of the pulse may be different.

5.3 Stokes parameters and the Poincaré sphere for non-stationary fields

The Stokes parameters may readily be extended to non-stationary fields, for which the parameters are time dependent. The Stokes parameters are the expansion coefficients of the decomposition of the polarization matrix in terms of the identity matrix $\mathbf{I} = \boldsymbol{\sigma}_0$ and the Pauli matrices $\boldsymbol{\sigma}_1, \boldsymbol{\sigma}_2, \boldsymbol{\sigma}_3$:

$$\mathbf{J}(\mathbf{r}, t) = \frac{1}{2}\sum_{i=0}^{3} S_{\mathrm{t}i}(\mathbf{r}, t)\boldsymbol{\sigma}_i. \tag{5.16}$$

The above expansion exists and is unique for any 2×2 matrix. Explicitly, the coefficients are

$$S_{\mathrm{t}0}(\mathbf{r}, t) = J_{xx}(\mathbf{r}, t) + J_{xx}(\mathbf{r}, t) = I_x(\mathbf{r}, t) + I_y(\mathbf{r}, t), \tag{5.17a}$$

$$S_{\mathrm{t}1}(\mathbf{r}, t) = J_{xx}(\mathbf{r}, t) - J_{xx}(\mathbf{r}, t) = I_x(\mathbf{r}, t) - I_y(\mathbf{r}, t), \tag{5.17b}$$

$$S_{\mathrm{t}2}(\mathbf{r}, t) = J_{xy}(\mathbf{r}, t) + J_{yx}(\mathbf{r}, t) = I_\alpha(\mathbf{r}, t) - I_\beta(\mathbf{r}, t), \tag{5.17c}$$

$$S_{\mathrm{t}3}(\mathbf{r}, t) = i\Big[J_{yx}(\mathbf{r}, t) - J_{xy}(\mathbf{r}, t)\Big] = I_r(\mathbf{r}, t) - I_l(\mathbf{r}, t), \tag{5.17d}$$

where α, β, r, l are as in Eqs. (3.21). The time-dependent Stokes parameters above should not be confused with the instantaneous Stokes parameters used in the investigation of polarization dynamics [19]. The instantaneous Stokes parameters, which measure the instantaneous polarization state of the field, may be used to calculate the single-time Stokes parameters by averaging over all realizations in the ensemble.

In order to analyze the polarization state of the field separately from its intensity, the Stokes parameters $S_{t1}(\mathbf{r}, t), S_{t2}(\mathbf{r}, t), S_{t3}(\mathbf{r}, t)$ may be normalized using the intensity $S_{t0}(\mathbf{r}, t)$:

$$s_{ti}(\mathbf{r}, t) = \frac{S_{ti}(\mathbf{r}, t)}{S_{t0}(\mathbf{r}, t)}, \tag{5.18}$$

which have the property $s_{t1}^2(\mathbf{r}, t) + s_{t2}^2(\mathbf{r}, t) + s_{t3}^2(\mathbf{r}, t) \leq 1$.

Inserting Eq. (5.16) into Eq. (5.15) gives that the degree of polarization, expressed using the Stokes parameters, is

$$P_t^2(\mathbf{r}, t) = \frac{S_{t1}^2(\mathbf{r}, t) + S_{t2}^2(\mathbf{r}, t) + S_{t3}^2(\mathbf{r}, t)}{S_{t0}^2(\mathbf{r}, t)} = s_{t1}^2(\mathbf{r}, t) + s_{t2}^2(\mathbf{r}, t) + s_{t3}^2(\mathbf{r}, t). \tag{5.19}$$

The quantities $S_{t1}(\mathbf{r}, t), S_{t2}(\mathbf{r}, t), S_{t3}(\mathbf{r}, t)$ can be interpreted as a point in a three-dimensional vector space, where the position vector is the Poincaré vector

$$\mathbf{S}_t(\mathbf{r}, t) = S_{t1}(\mathbf{r}, t)\hat{u}_1 + S_{t2}(\mathbf{r}, t)\hat{u}_2 + S_{t3}(\mathbf{r}, t)\hat{u}_3, \tag{5.20}$$

with $\hat{u}_i$ being orthonormal vectors. The degree of polarization is compactly expressed as

$$P_t(\mathbf{r}, t) = \frac{|\mathbf{S}_t(\mathbf{r}, t)|}{S_{t0}(\mathbf{r}, t)}. \tag{5.21}$$

From this equation it is seen that the length of the normalized Poincaré vector gives the degree of polarization. The normalized Poincaré vector may be interpreted as representing a point inside or on the surface of a sphere. The surface of this Poincaré sphere corresponds to fully polarized states; the origin corresponds to unpolarized state; and the points in between correspond to partially polarized states.

The Poincaré sphere construction is analogous to the stationary case presented in Sec. 3.2.2, with the exception that the Poincaré vector is no longer constant in time. It should be noted that this time variance is not the same as the time-dependent fluctuation of the *instantaneous* Poincaré vector, which is present even in the stationary case, and is responsible for the partial polarization [19].

Chapter 6

Pulsed beams in frequency domain

This chapter presents the polarization and coherence properties of non-stationary beams in frequency domain. The spectral coherence matrix and its connection with the temporal coherence matrix given in Chap. 5 are derived, and they are used to define the spectral polarization matrix. Quantities describing the spectral polarization of a non-stationary field, the spectral degree of polarization and the spectral Stokes parameters, are put forward and their connection with the time-domain quantities is discussed. Properties of and differences between temporal and spectral polarization are illustrated using examples.

6.1 Spectral coherence matrix

The spectral coherence and polarization properties are represented with the spectral coherence matrix $\mathbf{W}(\mathbf{r}_1, \mathbf{r}_2, \omega_1, \omega_2)$, defined by

$$\mathbf{W}(\mathbf{r}_1, \mathbf{r}_2, \omega_1, \omega_2) = \langle \widetilde{\mathbf{E}}^*(\mathbf{r}_1, \omega_1) \widetilde{\mathbf{E}}^T(\mathbf{r}_2, \omega_2) \rangle. \tag{6.1}$$

Comparison to the cross-spectral density matrix of a stationary beam [Eq. (4.1)] shows that the cross-spectral density is now a function of two frequencies, instead of just one. The matrix is Hermitian and non-negative definite in the sense that

$$\mathbf{W}(\mathbf{r}_1, \mathbf{r}_2, \omega_1, \omega_2) = \mathbf{W}^\dagger(\mathbf{r}_2, \mathbf{r}_1, \omega_2, \omega_1), \tag{6.2}$$

and

$$\sum_{m,n=1,2} \mathbf{a}^\dagger(\mathbf{r}_m, \omega_m) \mathbf{W}(\mathbf{r}_m, \mathbf{r}_n, \omega_m, \omega_n) \mathbf{a}(\mathbf{r}_n, \omega_n) \geq 0, \tag{6.3}$$

where $\mathbf{a}(\mathbf{r}_i, \omega_i)$ is an arbitrary complex vector function. The (time domain) mutual coherence matrix and the cross-spectral density matrix are connected via the Fourier transform relation

$$\mathbf{W}(\mathbf{r}_1, \mathbf{r}_2, \omega_1, \omega_2) = \frac{1}{4\pi^2} \iint_{-\infty}^{\infty} \mathbf{\Gamma}(\mathbf{r}_1, \mathbf{r}_2, t_1, t_2) e^{i(-\omega_1 t_1 + \omega_2 t_2)} \mathrm{d}t_1 \mathrm{d}t_2, \tag{6.4}$$

$$\mathbf{\Gamma}(\mathbf{r}_1, \mathbf{r}_2, t_1, t_2) = \iint_{0}^{\infty} \mathbf{W}(\mathbf{r}_1, \mathbf{r}_2, \omega_1, \omega_2) e^{-i(-\omega_1 t_1 + \omega_2 t_2)} \mathrm{d}\omega_1 \mathrm{d}\omega_2. \tag{6.5}$$

Equations (6.4) and (6.5) are obtained by inserting Eq. (2.33) into Eq. (6.1) and Eq. (2.32) into Eq. (5.1), respectively.

The diagonal elements of the spectral coherence matrix, evaluated at a single point and single frequency, give the spectral densities $S_i(\mathbf{r}, \omega) = W_{ii}(\mathbf{r}, \mathbf{r}, \omega, \omega)$ of the beam components. Integrating $S_i(\mathbf{r}, \omega)$ over all frequencies ω gives, using Eq. (6.4), that

$$\begin{aligned}
\int_0^\infty S_i(\mathbf{r}, \omega)\, \mathrm{d}\omega &= \int_0^\infty \frac{1}{4\pi^2} \iint_{-\infty}^{\infty} \Gamma_{ii}(\mathbf{r}, \mathbf{r}, t_1, t_2) e^{i\omega(t_2 - t_1)} \mathrm{d}t_1 \mathrm{d}t_2 \mathrm{d}\omega \\
&= \frac{1}{2\pi} \iint_{-\infty}^{\infty} \Gamma_{ii}(\mathbf{r}, \mathbf{r}, t_1, t_2) \frac{1}{2\pi} \int_0^\infty e^{i\omega(t_2 - t_1)} \mathrm{d}\omega\, \mathrm{d}t_1 \mathrm{d}t_2 \\
&= \frac{1}{2\pi} \iint_{-\infty}^{\infty} \Gamma_{ii}(\mathbf{r}, \mathbf{r}, t_1, t_2)\, \delta(t_2 - t_1)\, \mathrm{d}t_1 \mathrm{d}t_2 \\
&= \frac{1}{2\pi} \int_{-\infty}^{\infty} I_i(\mathbf{r}, t)\, \mathrm{d}t.
\end{aligned} \tag{6.6}$$

The integration of the time-domain intensity $I_i(\mathbf{r}, t)$ over all times gives the total energy in the beam, and thus $S_i(\mathbf{r}, \omega)$ is proportional to the energy density in a frequency interval, i.e., the spectral density. The total spectral density of the beam is the sum of the spectral densities of the beam components, $S(\mathbf{r}, \omega) = S_x(\mathbf{r}, \omega) + S_y(\mathbf{r}, \omega)$.

The elements $W_{ij}(\mathbf{r}_1, \mathbf{r}_2, \omega_1, \omega_2)$ of the spectral coherence matrix can be written using the spectral densities $S_i(\mathbf{r}, \omega)$ and the correlation functions $\mu_{ij}(\mathbf{r}_1, \mathbf{r}_2, \omega_1, \omega_2)$:

$$W_{ij}(\mathbf{r}_1, \mathbf{r}_2, \omega_1, \omega_2) = \sqrt{S_i(\mathbf{r}_1, \omega_1) S_j(\mathbf{r}_2, \omega_2)}\, \mu_{ij}(\mathbf{r}_1, \mathbf{r}_2, \omega_1, \omega_2). \tag{6.7}$$

The magnitude of $\mu_{ij}(\mathbf{r}_1, \mathbf{r}_2, \omega_1, \omega_2)$ is bounded as $0 \leq |\mu_{ij}(\mathbf{r}_1, \mathbf{r}_2, \omega_1, \omega_2)| \leq 1$, which follows from the general properties of cross-correlation functions in Eq. (2.30).

Setting $t_2 = t_1 + \tau$ and assuming that the coherence matrix depends on time only via

the time difference τ, $\mathbf{\Gamma}(\mathbf{r}_1, \mathbf{r}_2, t_1, t_1 + \tau) = \mathbf{\Gamma}(\mathbf{r}_1, \mathbf{r}_2, \tau)$, gives that

$$\begin{aligned}\mathbf{W}(\mathbf{r}_1, \mathbf{r}_2, \omega_1, \omega_2) =& \frac{1}{4\pi^2} \iint_{-\infty}^{\infty} \mathbf{\Gamma}(\mathbf{r}_1, \mathbf{r}_2, t_1, t_2) e^{i(-\omega_1 t_1 + \omega_2 t_2)} \mathrm{d}t_1 \mathrm{d}t_2 \\ =& \frac{1}{2\pi} \int_{-\infty}^{\infty} \mathbf{\Gamma}(\mathbf{r}_1, \mathbf{r}_2, \tau) e^{i\omega_2 \tau} \mathrm{d}\tau \cdot \frac{1}{2\pi} \int_{-\infty}^{\infty} e^{i(\omega_2 - \omega_1) t_1} \mathrm{d}t_1 \\ =& \frac{1}{2\pi} \int_{-\infty}^{\infty} \mathbf{\Gamma}(\mathbf{r}_1, \mathbf{r}_2, \tau) e^{i\omega_2 \tau} \mathrm{d}\tau \cdot \delta(\omega_2 - \omega_1),\end{aligned} \tag{6.8}$$

which is the same as the stationary result (4.3). This result shows that the stationarity necessarily implies that the different frequency components are uncorrelated.

6.2 Spectral polarization matrix

The spectral polarization properties are encoded in the *spectral polarization matrix*

$$\mathbf{\Phi}(\mathbf{r}, \omega) = \mathbf{W}(\mathbf{r}, \mathbf{r}, \omega, \omega). \tag{6.9}$$

The matrix is Hermitian and non-negative definite in the usual sense:

$$\mathbf{\Phi}^{\dagger}(\mathbf{r}, \omega) = \mathbf{\Phi}(\mathbf{r}, \omega), \tag{6.10}$$

and

$$\mathbf{a}^{\dagger} \mathbf{\Phi}(\mathbf{r}, \omega) \mathbf{a} \geq 0, \tag{6.11}$$

which is seen by setting $\mathbf{r}_1 = \mathbf{r}_2 = \mathbf{r}$ and $\omega_1 = \omega_2 = \omega$ in Eqs. (6.2) and (6.3). Relation between the time and frequency domains is provided by

$$\mathbf{\Phi}(\mathbf{r}, \omega) = \frac{1}{4\pi^2} \iint_{-\infty}^{\infty} \mathbf{\Gamma}(\mathbf{r}, \mathbf{r}, t_1, t_2) e^{i\omega(t_2 - t_1)} \mathrm{d}t_1 \mathrm{d}t_2. \tag{6.12}$$

The spectral polarization properties are seen to depend on the temporal coherence, in analogy to the stationary case. On the other hand, the spectral polarization matrix alone cannot provide sufficient information to obtain the temporal polarization matrix:

$$\mathbf{J}(\mathbf{r}, t) = \iint_{0}^{\infty} \mathbf{W}(\mathbf{r}, \mathbf{r}, \omega_1, \omega_2) e^{-i(\omega_2 - \omega_1) t} \mathrm{d}\omega_1 \mathrm{d}\omega_2, \tag{6.13}$$

which shows that the temporal polarization properties depend also on the spectral coherence properties.

The diagonal elements $\Phi_{xx}(\mathbf{r},\omega)$ and $\Phi_{yy}(\mathbf{r},\omega)$ of the spectral polarization matrix represent the spectral densities of the orthogonal field components, as shown in Eq. (6.6), and their sum gives the spectral density $\operatorname{tr}\mathbf{\Phi}(\mathbf{r},\omega) = S_x(\mathbf{r},\omega) + S_y(\mathbf{r},\omega) = S_(\mathbf{r},\omega)$. The off-diagonal element $\Phi_{xy}(\mathbf{r},\omega)$ characterizes the correlations between the field components, and thus it will be useful to define the correlation coefficient

$$\mu_{xy}(\mathbf{r},\omega) = \frac{\Phi_{xy}(\mathbf{r},\omega)}{\sqrt{\Phi_{xx}(\mathbf{r},\omega)\Phi_{yy}(\mathbf{r},\omega)}}, \tag{6.14}$$

which is bounded as $0 \leq |\mu_{xy}(\mathbf{r},\omega)| \leq 1$, due to the non-negative definity of $\mathbf{\Phi}(\mathbf{r},\omega)$. The upper bound corresponds to fully correlated field components, and the lower to uncorrelated field components.

6.2.1 Polarization equivalence of coherence matrices

A closer examination of Eqs. (6.12) and (6.13) shows interesting polarization equivalence relations. Similar equivalence theorems have previously been presented for intensity distribution [44] and spatial coherence [45].

The integration in Eq. (6.12) is over the two variables t_1 and t_2. Prompted by the form of the argument of the exponential function, $i\omega(t_2 - t_1)$, the following coordinate transformation is made:

$$\begin{cases} \bar{t} = (t_1 + t_2)/2, \\ \tau = t_2 - t_1. \end{cases} \tag{6.15}$$

The integration limits remain at $\pm\infty$, and the differential $\mathrm{d}t_1\mathrm{d}t_2$ transforms to $\mathrm{d}\bar{t}\,\mathrm{d}\tau$, since this particular choice of $\bar{t}$ and τ ensures that the Jacobian of the transformation is unity. Equation (6.12) may be expressed as

$$\mathbf{\Phi}(\mathbf{r},\omega) = \frac{1}{2\pi}\int_{-\infty}^{\infty} \overline{\mathbf{\Gamma}}(\mathbf{r},\mathbf{r},\tau)e^{i\omega\tau}\mathrm{d}\tau, \tag{6.16}$$

where

$$\overline{\mathbf{\Gamma}}(\mathbf{r},\mathbf{r},\tau) = \frac{1}{2\pi}\int_{-\infty}^{\infty} \mathbf{\Gamma}(\mathbf{r},\mathbf{r},\bar{t}-\tau/2,\bar{t}+\tau/2)\,\mathrm{d}\bar{t}. \tag{6.17}$$

Equation (6.16) is now of the same form as the corresponding stationary equation (4.9), with the stationary coherence matrix replaced by the time-integrated non-stationary coherence matrix. It is seen that the spectral polarization matrices of two different fields are equal if their time-averaged coherence matrices [Eq. (6.17)] are equal. Since the spectral

polarization matrix and the time-averaged coherence matrix form a Fourier transform pair, for each $\mathbf{\Phi}(\mathbf{r}, \omega)$ there exists only one unique $\overline{\mathbf{\Gamma}}(\mathbf{r}, \mathbf{r}, \tau)$. Therefore the set of coherence matrices $\mathbf{\Gamma}(\mathbf{r}_1, \mathbf{r}_2, t_1, t_2)$ corresponding to the same spectral polarization matrix is exactly the set of coherence matrices corresponding to the same $\overline{\mathbf{\Gamma}}(\mathbf{r}, \mathbf{r}, \tau)$.

A similar relation holds for the correspondence of different spectral coherence matrices to a single polarization matrix $\mathbf{J}(\mathbf{r}, t)$. Starting from Eq. (6.13), the frequency variables ω_1 and ω_2 are transformed to new coordinates $\bar{\omega}$ and Ω as

$$\begin{cases} \bar{\omega} = (\omega_1 + \omega_2)/2, \\ \Omega = \omega_2 - \omega_1. \end{cases} \tag{6.18}$$

which leads to $\mathrm{d}\omega_1 \mathrm{d}\omega_2 = \mathrm{d}\bar{\omega}\,\mathrm{d}\Omega$, and integration limits in the integration with respect to $\bar{\omega}$ and Ω will be $(|\Omega|/2, \infty)$ and $(-\infty, \infty)$, respectively. The temporal polarization matrix may be written

$$\mathbf{J}(\mathbf{r}, t) = \int_{-\infty}^{\infty} \overline{\mathbf{W}}(\mathbf{r}, \mathbf{r}, \Omega) e^{-i\Omega t} \mathrm{d}\Omega, \tag{6.19}$$

where

$$\overline{\mathbf{W}}(\mathbf{r}_1, \mathbf{r}_2, \Omega) = \frac{1}{4\pi^2} \int_{|\Omega|/2}^{\infty} \mathbf{W}(\mathbf{r}_1, \mathbf{r}_2, \bar{\omega} - \Omega/2, \bar{\omega} + \Omega/2)\, \mathrm{d}\bar{\omega}, \tag{6.20}$$

is the averaged spectral coherence matrix. The polarization matrix is conveniently an inverse Fourier transform of the averaged spectral coherence matrix. This can be compared to Eq. (4.8), which states that for stationary fields the temporal polarization matrix is the integral of the spectral polarization matrix over all frequencies ω, not a Fourier transform. This is in contrast to Eqs. (4.9) and (6.16) used to obtain the spectral polarization matrix from the coherence matrix and from the integrated coherence matrix in stationary and non-stationary cases, respectively: both Eq. (4.9) and Eq. (6.16) have the same form, only the matrix in the integrand is different between the stationary and non-stationary equations.

6.3 2-point Stokes parameters

The spectral coherence matrix may be expressed as a weighted sum of the Pauli matrices (3.4),

$$\mathbf{W}(\mathbf{r}_1, \mathbf{r}_2, \omega_1, \omega_2) = \frac{1}{2} \sum_{i=0}^{3} S_{si}^{(2)}(\mathbf{r}_1, \mathbf{r}_2, \omega_1, \omega_2) \boldsymbol{\sigma}_i, \tag{6.21}$$

where the expansion coefficients $S_{si}^{(2)}(\mathbf{r}_1, \mathbf{r}_2, \omega_1, \omega_2)$ are the 2-point Stokes parameters for non-stationary fields. Explicitly, the parameters, using the correlation coefficient defined

in Eq. (6.7), are the following:

$$\begin{aligned}
S_{\mathrm{s0}}^{(2)}(\mathbf{r}_1,\mathbf{r}_2,\omega_1,\omega_2) &= W_{xx}(\mathbf{r}_1,\mathbf{r}_2,\omega_1,\omega_2) + W_{yy}(\mathbf{r}_1,\mathbf{r}_2,\omega_1,\omega_2) \\
&= \sqrt{S_x(\mathbf{r}_1,\omega_1)S_x(\mathbf{r}_2,\omega_2)}\mu_{xx}(\mathbf{r}_1,\mathbf{r}_2,\omega_1,\omega_2) \\
&+ \sqrt{S_y(\mathbf{r}_1,\omega_1)S_y(\mathbf{r}_2,\omega_2)}\mu_{yy}(\mathbf{r}_1,\mathbf{r}_2,\omega_1,\omega_2), \qquad (6.22a) \\
S_{\mathrm{s1}}^{(2)}(\mathbf{r}_1,\mathbf{r}_2,\omega_1,\omega_2) &= W_{xx}(\mathbf{r}_1,\mathbf{r}_2,\omega_1,\omega_2) - W_{yy}(\mathbf{r}_1,\mathbf{r}_2,\omega_1,\omega_2) \\
&= \sqrt{S_x(\mathbf{r}_1,\omega_1)S_x(\mathbf{r}_2,\omega_2)}\mu_{xx}(\mathbf{r}_1,\mathbf{r}_2,\omega_1,\omega_2) \\
&- \sqrt{S_y(\mathbf{r}_1,\omega_1)S_y(\mathbf{r}_2,\omega_2)}\mu_{yy}(\mathbf{r}_1,\mathbf{r}_2,\omega_1,\omega_2), \qquad (6.22b) \\
S_{\mathrm{s2}}^{(2)}(\mathbf{r}_1,\mathbf{r}_2,\omega_1,\omega_2) &= W_{yx}(\mathbf{r}_1,\mathbf{r}_2,\omega_1,\omega_2) + W_{xy}(\mathbf{r}_1,\mathbf{r}_2,\omega_1,\omega_2) \\
&= \sqrt{S_y(\mathbf{r}_1,\omega_1)S_x(\mathbf{r}_2,\omega_2)}\mu_{yx}(\mathbf{r}_1,\mathbf{r}_2,\omega_1,\omega_2) \\
&+ \sqrt{S_x(\mathbf{r}_1,\omega_1)S_y(\mathbf{r}_2,\omega_2)}\mu_{xy}(\mathbf{r}_1,\mathbf{r}_2,\omega_1,\omega_2), \qquad (6.22c) \\
S_{\mathrm{s3}}^{(2)}(\mathbf{r}_1,\mathbf{r}_2,\omega_1,\omega_2) &= i\Big[W_{yx}(\mathbf{r}_1,\mathbf{r}_2,\omega_1,\omega_2) - W_{xy}(\mathbf{r}_1,\mathbf{r}_2,\omega_1,\omega_2)\Big] \\
&= i\Big[\sqrt{S_y(\mathbf{r}_1,\omega_1)S_x(\mathbf{r}_2,\omega_2)}\mu_{yx}(\mathbf{r}_1,\mathbf{r}_2,\omega_1,\omega_2) \\
&- \sqrt{S_x(\mathbf{r}_1,\omega_1)S_y(\mathbf{r}_2,\omega_2)}\mu_{xy}(\mathbf{r}_1,\mathbf{r}_2,\omega_1,\omega_2)\Big]. \qquad (6.22d)
\end{aligned}$$

The formulation using the correlation coefficients is used to underline the physical significance of the two-point parameters. The parameter $S_{\mathrm{s0}}^{(2)}(\mathbf{r}_1,\mathbf{r}_2,\omega_1,\omega_2)$ is the sum of the correlation coefficients, weighted by the geometric means of the spectral densities in the x and y components of the beam. Parameters $S_{\mathrm{s1}}^{(2)}(\mathbf{r}_1,\mathbf{r}_2,\omega_1,\omega_2)$, $S_{\mathrm{s2}}^{(2)}(\mathbf{r}_1,\mathbf{r}_2,\omega_1,\omega_2)$, and $S_{\mathrm{s3}}^{(2)}(\mathbf{r}_1,\mathbf{r}_2,\omega_1,\omega_2)$ are the differences of the correlation functions weighted by spectral densities of the orthogonal components, expressed in different coordinate systems as detailed in conjunction with the stationary time-domain Stokes parameters in Eq. (3.21).

6.4 Spectral polarization

6.4.1 Spectral degree of polarization

The spectral polarization matrix for non-stationary fields, like its time-domain counterpart, may be decomposed into a sum of two matrices:

$$\mathbf{\Phi}(\mathbf{r},\omega) = \mathbf{\Phi}^{(\mathrm{pol})}(\mathbf{r},\omega) + \mathbf{\Phi}^{(\mathrm{unpol})}(\mathbf{r},\omega), \qquad (6.23)$$

where $\mathbf{\Phi}^{(\mathrm{pol})}(\mathbf{r},\omega)$ represents the fully spectrally polarized part and $\mathbf{\Phi}^{(\mathrm{unpol})}(\mathbf{r},\omega)$ represents the spectrally unpolarized part of the beam. The ratio of the spectral density in the fully

polarized part to the total spectral density is defined as the spectral degree of polarization,

$$P_{\mathrm{s}}(\mathbf{r},\omega) = \frac{\operatorname{tr}\boldsymbol{\Phi}^{(\mathrm{pol})}(\mathbf{r},\omega)}{\operatorname{tr}\boldsymbol{\Phi}(\mathbf{r},\omega)} = \sqrt{1-4\frac{\det\boldsymbol{\Phi}(\mathbf{r},\omega)}{\operatorname{tr}^2\boldsymbol{\Phi}(\mathbf{r},\omega)}} = \sqrt{2\frac{\operatorname{tr}\boldsymbol{\Phi}^2(\mathbf{r},\omega)}{\operatorname{tr}^2\boldsymbol{\Phi}(\mathbf{r},\omega)}-1}. \tag{6.24}$$

The expression for the spectral degree of polarization is similar to the equation in the stationary case [Eq. (4.14)].

6.4.2 Spectral Stokes parameters

Another convenient method for expressing the spectral polarization matrix as a linear combination is the Pauli decomposition

$$\boldsymbol{\Phi}(\mathbf{r},\omega) = \frac{1}{2}\sum_{i=0}^{3} S_{si}(\mathbf{r},\omega)\boldsymbol{\sigma}_i, \tag{6.25}$$

where the trace-orthonormal basis $\{\boldsymbol{\sigma}_i\}$ consists of the Pauli matrices given in Eq. (3.4). The expansion coefficients $S_{si}(\mathbf{r},\omega)$ are obtained, e.g., by setting $\mathbf{r}_1 = \mathbf{r}_2 = \mathbf{r}$ and $\omega_1 = \omega_2 = \omega$ in Eqs. (6.22), yielding the spectral Stokes parameters:

$$\begin{aligned}
S_{\mathrm{s}0}(\mathbf{r},\omega) &= \Phi_{xx}(\mathbf{r},\omega) + \Phi_{yy}(\mathbf{r},\omega) \\
&= S_x(\mathbf{r},\omega) + S_y(\mathbf{r},\omega), && \text{(6.26a)} \\
S_{\mathrm{s}1}(\mathbf{r},\omega) &= \Phi_{xx}(\mathbf{r},\omega) - \Phi_{yy}(\mathbf{r},\omega) \\
&= S_x(\mathbf{r},\omega) - S_y(\mathbf{r},\omega), && \text{(6.26b)} \\
S_{\mathrm{s}2}(\mathbf{r},\omega) &= \Phi_{yx}(\mathbf{r},\omega) + \Phi_{xy}(\mathbf{r},\omega) \\
&= \sqrt{S_x(\mathbf{r},\omega)S_y(\mathbf{r},\omega)}\left[\mu_{yx}(\mathbf{r},\mathbf{r},\omega,\omega) + \mu_{xy}(\mathbf{r},\mathbf{r},\omega,\omega)\right], && \text{(6.26c)} \\
S_{\mathrm{s}3}(\mathbf{r},\omega) &= i\left[\Phi_{yx}(\mathbf{r},\omega) - \Phi_{xy}(\mathbf{r},\omega)\right] \\
&= i\sqrt{S_x(\mathbf{r},\omega)S_y(\mathbf{r},\omega)}\left[\mu_{yx}(\mathbf{r},\mathbf{r},\omega,\omega) - \mu_{xy}(\mathbf{r},\mathbf{r},\omega,\omega)\right]. && \text{(6.26d)}
\end{aligned}$$

The first parameter is proportional to the total spectral density of the field, the second represents the excess of the spectral density in the x component over the spectral density in the y component. The third and fourth parameters give similar information on the correlation between the field components; the terms in brackets in Eqs. (6.26c) and (6.26d) are proportional to the real and imaginary parts of $\mu_{xy}(\mathbf{r},\mathbf{r},\omega,\omega)$, respectively.

Analogously to the time domain, the spectral polarization may be analyzed using the

normalized spectral Stokes parameters

$$s_{si}(\mathbf{r},\omega) = \frac{S_{si}(\mathbf{r},\omega)}{S_{s0}(\mathbf{r},\omega)}, \tag{6.27}$$

which due to their normalization obey the equation $s_{s1}^2(\mathbf{r},\omega) + s_{s2}^2(\mathbf{r},\omega) + s_{s3}^2(\mathbf{r},\omega) \leq 1$.

The spectral degree of polarization may be expressed using the Stokes parameters by substituting expression (6.25) into Eq. (6.24). This gives

$$P_s^2(\mathbf{r},\omega) = \frac{S_{s1}^2(\mathbf{r},\omega) + S_{s2}^2(\mathbf{r},\omega) + S_{s3}^2(\mathbf{r},\omega)}{S_{s0}^2(\mathbf{r},\omega)} = s_{s1}^2(\mathbf{r},\omega) + s_{s2}^2(\mathbf{r},\omega) + s_{s3}^2(\mathbf{r},\omega). \tag{6.28}$$

This result is the same as in the stationary case.

6.5 Examples of partially polarized pulses

In order to illustrate the formalism presented in this and the previous chapter, two examples are considered. The examples have been chosen to be relatively simple such that they can be analyzed analytically, and yet have enough structure to illustrate interesting phenomena in the time and frequency domains.

6.5.1 Two delayed, orthogonal Gaussian Schell-model pulses

In order to investigate specific electric fields, it is shown that a complex analytic signal of an electric field may be written as a product of a complex amplitude term, called the *complex envelope*, and a complex exponential term which oscillates at the central frequency of the field.

Starting from Eq. (2.32), the electric field may be written as

$$\mathbf{E}(\mathbf{r},t) = \int \widetilde{\mathbf{E}}(\mathbf{r},\omega) e^{-i(\omega-\omega_0)t} \mathrm{d}\omega \, e^{-i\omega_0 t} = \mathbf{A}(\mathbf{r},t) e^{-i\omega_0 t}, \tag{6.29}$$

where ω_0 is the central frequency of the field and $\mathbf{A}(\mathbf{r},t)$ is the complex envelope of the field at point $\mathbf{r}$. This representation is especially useful when all significant contributions to the field arise from frequencies close to ω_0, i.e., $\widetilde{\mathbf{E}}(\mathbf{r},\omega)$ is nonzero only for frequencies for which $|\omega - \omega_0| \ll \omega_0$, and thus $\mathbf{A}(\mathbf{r},t)$ varies slowly in time compared to the term oscillating at frequency ω_0.

The propagation of an axial pulse through a vacuum-like medium, e.g., air, can be calculated from Eq. (2.18). The expression for the parameter k is obtained from Eq. (2.11) by noting that for vacuum, the refractive index n is 1 at all frequencies, and thus $k = \omega/c$.

Inserting this into Eq. (2.18) gives

$$\begin{aligned}\mathbf{E}(\mathbf{r},t) &= \int \widetilde{\mathbf{E}}(0,\omega)e^{i[(\omega-\omega_0)z/c-(\omega-\omega_0)t]}\mathrm{d}\omega\, e^{-i\omega_0(t-z/c)} \\ &= \int \widetilde{\mathbf{E}}(0,\omega)e^{-i(\omega-\omega_0)(t-z/c)}\mathrm{d}\omega\, e^{-i\omega_0(t-z/c)},\end{aligned} \tag{6.30}$$

where the integral is identified to be the complex envelope $\mathbf{A}(t')$ evaluated at $t' = t - z/c$. After propagating over a distance z in vacuum the pulse is therefore

$$\mathbf{E}(\mathbf{r},t) = \mathbf{A}\left(t - \frac{z}{c}\right)e^{-i\omega_0(t-z/c)}. \tag{6.31}$$

It is seen that since vacuum is not dispersive, the axial pulse retains its shape and phase, and introducing a time delay into the pulse, i.e., $\mathbf{E}_2(t) = \mathbf{E}_1(t-\tau_d)$ is equivalent to propagating the pulse over the distance $z = c\tau_d$. These results holds also for scalar pulses, where the vector field and the vector complex envelope are simply replaced by a scalar field and a scalar complex envelope.

An electromagnetic pulse may be constructed by taking a pulse linearly polarized in the x direction and making a y-polarized, delayed copy of it, with the delay between the components being τ_d. Then $E_x(t) = E(t)$ and $E_y(t) = E(t-\tau_d)$, where $E(t)$ is the complex analytic signal of a scalar pulse. A conceptual arrangement to achieve this is demonstrated in Fig. 6.1. The linearly polarized pulse is passed through a 50:50 beam splitter to divide the pulse into two identical pulses. One of the pulses is directed into a delay line which introduces a time delay of τ_d with respect to the other pulse while retaining the pulse shape and phase, as shown above. The delayed pulse is also passed through a half-wave plate, denoted by $\lambda/2$, oriented such that the polarization direction of the pulse is rotated by 90°. Both pulses are finally combined using another beam splitter. The half-wave plate functions properly only for beams with all frequency components sufficiently close to the frequency for which the waveplate is designed, but the bandwidth of the pulse is assumed to be sufficiently narrow for all frequency components of the pulse to be rotated upon traversal through the plate. A frequency independent polarization rotation could be achieved, e.g., with a suitable arrangement of mirrors.

An example of a scalar pulse is a pulse with Gaussian intensity profile and Gaussian coherence function. The field of the pulse may be written as

$$E(t) = A(t)e^{-i\omega_0 t}, \tag{6.32}$$

where ω_0 is the carrier (or central) frequency of the pulse and $A(t)$ is the complex envelope

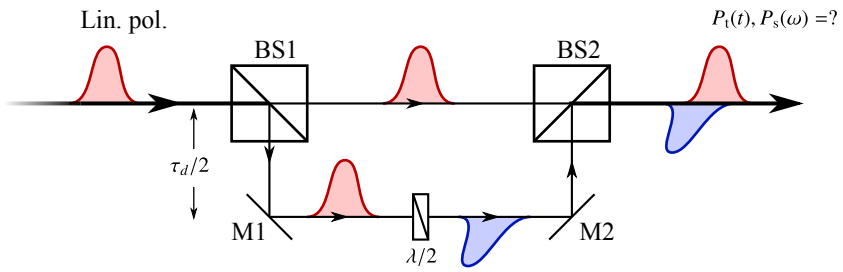

Figure 6.1: Experimental setup for producing a pulse with orthogonal Gaussian components. The incoming pulse is linearly polarized, and it is split into two identical pulses using beam splitter BS1. The mirrors M1 and M2 are used to form a delay line which introduces a delay of τ_d compared to the shorter beam path. The delay line also includes the half-wave plate $\lambda/2$ oriented so that it rotates the polarization direction of the incoming pulse by 90°. The pulses from the direct path and the delay line are combined using beam splitter BS2 to form the desired electromagnetic pulse.

of the pulse. Here $A(t)$ is a random complex function whose magnitude and phase fluctuate. The intensity of a Gaussian pulse at time t is given by

$$I(t) = \langle |E(t)|^2 \rangle = \langle |A(t)|^2 \rangle = A_0^2 e^{-t^2/T_0^2}, \tag{6.33}$$

where T_0 is the pulse width and A_0^2 is the peak intensity of the pulse. The random amplitude and phase variations may be separated from the Gaussian envelope of the pulse by defining the normalized amplitude function

$$a(t) = \frac{A(t)}{\sqrt{I(t)}} = \frac{A(t)}{A_0 e^{-t^2/2T_0^2}}. \tag{6.34}$$

The normalized coherence function

$$\gamma(t_1, t_2) = \frac{\Gamma(t_1, t_2)}{\sqrt{I(t_1) I(t_2)}}, \tag{6.35}$$

where $\Gamma(t_1, t_2) = \langle E^*(t_1) E(t_2) \rangle$, depends in the general case on both t_1 and t_2 in a nontrivial way. In this case the Schell model [18, 46] is employed: the coherence function depends only on the time difference, i.e., $\gamma(t_1, t_2) = \gamma(t_2 - t_1)$. Using the notation above, the coherence function is

$$\gamma(t_1, t_2) = \frac{\langle E^*(t_1) E(t_2) \rangle}{\sqrt{I(t_1) I(t_2)}} = \frac{\langle A^*(t_1) A(t_2) \rangle e^{-i\omega_0(t_2 - t_1)}}{\sqrt{I(t_1)}\,\sqrt{I(t_2)}} = \langle a^*(t_1) a(t_2) \rangle e^{-i\omega_0(t_2 - t_1)}. \tag{6.36}$$

In order for the Schell model to hold, the correlation function $\langle a^*(t_1) a(t_2) \rangle$ may only depend

on the difference $t_2 - t_1$. The final assumption made is that the coherence function, aside from the deterministic phase factor, is Gaussian:

$$\gamma(t_2 - t_1) = e^{-(t_2-t_1)^2/T_c^2} e^{-i\omega_0(t_2-t_1)}, \tag{6.37}$$

where T_c characterizes the coherence time of the field. This kind of pulse is the Gaussian Schell-model (GSM) pulse.

6.5.1a Time-domain polarization analysis

The coherence matrix of the described electromagnetic GSM pulse (GSMP) is

$$\begin{aligned}\mathbf{\Gamma}(t_1, t_2) &= \begin{bmatrix} \langle E_x^*(t_1)E_x(t_2)\rangle & \langle E_x^*(t_1)E_y(t_2)\rangle \\ \langle E_y^*(t_1)E_x(t_2)\rangle & \langle E_y^*(t_1)E_y(t_2)\rangle \end{bmatrix} \\ &= \begin{bmatrix} \langle E^*(t_1)E(t_2)\rangle & \langle E^*(t_1)E(t_2-\tau_d)\rangle \\ \langle E^*(t_1-\tau_d)E(t_2)\rangle & \langle E^*(t_1-\tau_d)E(t_2-\tau_d)\rangle \end{bmatrix} \\ &= \begin{bmatrix} \Gamma(t_1, t_2) & \Gamma(t_1, t_2-\tau_d) \\ \Gamma(t_1-\tau_d, t_2) & \Gamma(t_1-\tau_d, t_2-\tau_d) \end{bmatrix},\end{aligned} \tag{6.38}$$

and the polarization matrix $\mathbf{J}(t) = \mathbf{\Gamma}(t, t)$ is

$$\mathbf{J}(t) = \begin{bmatrix} I(t) & \sqrt{I(t)I(t-\tau_d)}\,\gamma(t, t-\tau_d) \\ \sqrt{I(t)I(t-\tau_d)}\,\gamma(t-\tau_d, t) & I(t-\tau_d) \end{bmatrix}. \tag{6.39}$$

Inserting the expressions for intensity and coherence functions as given by Eqs. (6.33) and (6.37), the degree of polarization is obtained:

$$P_\mathrm{t}(t) = \sqrt{\tanh^2\left(\frac{\tau_d^2 - 2t\tau_d}{2T_0^2}\right) + \operatorname{sech}^2\left(\frac{\tau_d^2 - 2t\tau_d}{2T_0^2}\right) e^{-2\tau_d^2/T_c^2}}. \tag{6.40}$$

The degree of polarization, as a function of time, is shown in Fig. 6.2 for several values of the inter-component delay τ_d and coherence time T_c. The thin blue (solid) and green (dashed) lines show the intensities of the x and y components of the field, respectively, and the turquoise (solid, top), red (dash-dotted), green (dashed) and blue (solid, bottom) curves show the value of the degree of polarization $P_\mathrm{t}(t)$ for fields with coherence time parameters T_c of $2T_0$, T_0, $0.5T_0$, and $0.33T_0$, respectively. Insight into the effect of the ratio between these parameters can be obtained by investigating the high-coherence limit $\tau_d \ll T_c$ and the low-coherence limit $\tau_d \gg T_c$. In the highly coherent case, $\tau_d \ll T_c$, the exponential term in Eq. (6.40) tends to 1 and the degree of polarization becomes equal to 1, i.e., the

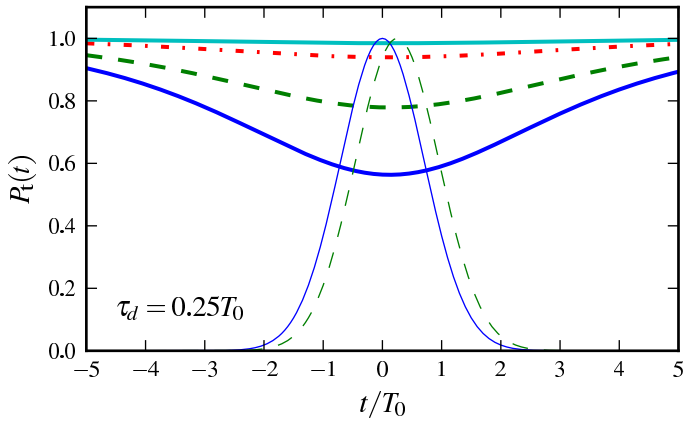

(a)

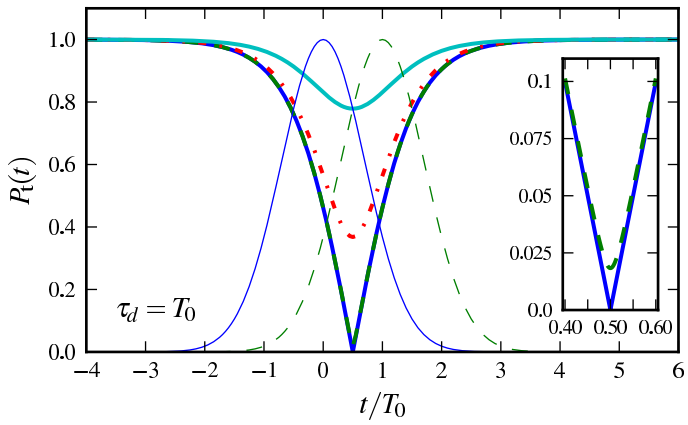

(b)

Figure 6.2: Degree of polarization for different values of the inter-component delay τ_d and coherence time T_c expressed in terms of the pulse width T_0. The thin blue (solid) and green (dashed) lines show the relative amplitude of the x and y components, respectively. The thick turquoise (solid, top), red (dash-dotted), green (dashed), and blue (solid, bottom) lines indicate degree of polarization $P_t(t)$ calculated with coherence times T_c of $2T_0$, T_0, $0.5T_0$, and $0.33T_0$, respectively. The inset in figure (b) shows how closely the degrees of polarization corresponding to coherence times $0.33T_0$ and $0.5T_0$ resemble each other.

field is fully polarized at all times. The physical background for this result is that for time delays τ_d much shorter than the coherence time T_c, the x and y components of the field are fully correlated at all times t. In the opposite case, i.e., the low-coherence limit, the exponential term is essentially equal to 0 and thus $P_t(t) = |\tanh[(\tau_d^2 - 2t\tau_d)/2T_0^2]|$. Since the coherence time is short compared to the inter-component delay, the x and y components of the field are fully uncorrelated, and the degree of polarization depends only on the intensities of the components. At the point where the intensities are equal, i.e., halfway between the intensity peaks, the field is fully unpolarized, as shown by $P_t(\tau_d/2) = 0$. Far

away from the intensity peaks the pulse is fully polarized as only one component, x or y, dominates, with $\lim_{t\to\pm\infty} P_{\mathrm{t}}(t) = 1$.

The polarization state of a pulse is described by the Stokes parameters, which for this pulse are

$$S_{\mathrm{t}0}(t) = A_0^2 e^{-t^2/T_0^2}\left[1 + e^{-(\tau_d^2 - 2t\tau_d)/T_0^2}\right], \tag{6.41a}$$

$$S_{\mathrm{t}1}(t) = A_0^2 e^{-t^2/T_0^2}\left[1 - e^{-(\tau_d^2 - 2t\tau_d)/T_0^2}\right], \tag{6.41b}$$

$$S_{\mathrm{t}2}(t) = 2A_0^2 e^{-[t^2+(t-\tau_d)^2]/2T_0^2}\cos(\omega_0\tau_d)e^{-\tau_d^2/T_c^2}, \tag{6.41c}$$

$$S_{\mathrm{t}3}(t) = 2A_0^2 e^{-[t^2+(t-\tau_d)^2]/2T_0^2}\sin(\omega_0\tau_d)e^{-\tau_d^2/T_c^2}. \tag{6.41d}$$

The normalized Stokes parameters, which are obtained from the equations above by dividing with the total intensity of the beam, are

$$s_{\mathrm{t}1}(t) = \tanh\left(\frac{\tau_d^2 - 2t\tau_d}{2T_0^2}\right), \tag{6.42a}$$

$$s_{\mathrm{t}2}(t) = \frac{\cos(\omega_0\tau_d)\exp(-\tau_d^2/T_c^2)}{\cosh\left[(\tau_d^2 - 2t\tau_d)/2T_0^2\right]}, \tag{6.42b}$$

$$s_{\mathrm{t}3}(t) = \frac{\sin(\omega_0\tau_d)\exp(-\tau_d^2/T_c^2)}{\cosh\left[(\tau_d^2 - 2t\tau_d)/2T_0^2\right]}. \tag{6.42c}$$

For large negative values of t, the value of the argument of the hyperbolic functions is a large positive number, which leads to $s_{\mathrm{t}1}(t) \approx 1$, $s_{\mathrm{t}2}(t) \approx 0$, and $s_{\mathrm{t}3}(t) \approx 0$, i.e., the pulse is fully x-polarized. The field is dominated by the leading edge of the x-component, and the contribution of the y component to the total field is negligible. When t increases, the y component of the field begins to influence the polarization state as well, with $s_{\mathrm{t}1}(t)$ and the denominators of $s_{\mathrm{t}2}(t)$ and $s_{\mathrm{t}3}(t)$ decreasing in value. If the x and y components are correlated (τ_d not significantly larger than T_c), $s_{\mathrm{t}2}(t)$ and $s_{\mathrm{t}3}(t)$ may become non-zero and the field's polarization state will change from the original x-polarized state. The polarization state depends also on the central frequency ω_0 of the pulse and the time delay τ_d. If the product $\omega_0\tau_d$ is such that $s_{\mathrm{t}3}(t)$ is non-zero, the ellipticity of the polarization ellipse will change with time as the polarization state evolves from linear x-polarized to elliptically polarized and further to linear y-polarized state.

At the midpoint $t = \tau_d/2$ between the peak intensities of the x and y components, the intensity of the x and y components are equal and thus $s_{\mathrm{t}1}(t) = 0$. The polarization state is determined by the correlations and relative phase of the x and y components, with $s_{\mathrm{t}2}(t) = \cos(\omega_0\tau_d)\exp(-\tau_d^2/T_c^2)$ and $s_{\mathrm{t}3}(t) = \sin(\omega_0\tau_d)\exp(-\tau_d^2/T_c^2)$. The degree of polarization is $P_{\mathrm{t}}(t) = [s_{\mathrm{t}2}^2(t) + s_{\mathrm{t}3}^2(t)]^{1/2} = \exp(-\tau_d^2/T_c^2)$, i.e., the degree of polarization

depends only on the coherence time and time delay, not on the relative phase of the components.

Further insight into the behavior of the polarization state is obtained by determining the polarization matrix of the fully polarized parts of the beam and investigating the behavior of its normalized Stokes parameters $s_{ti}^{(\mathrm{pol})}(t) = S_{ti}^{(\mathrm{pol})}(t)/S_{t0}^{(\mathrm{pol})}(t)$. The results obtained are

$$s_{t1}^{(\mathrm{pol})}(t) = \frac{\sinh\left[-(t\tau_d - \tau_d^2/2)/T_0^2\right]}{\sqrt{\sinh^2\left[-(t\tau_d - \tau_d^2/2)/T_0^2\right] + e^{-2\tau_d^2/T_c^2}}}, \tag{6.43a}$$

$$s_{t2}^{(\mathrm{pol})}(t) = \frac{\cos(\omega_0\tau_d)e^{-\tau_d^2/T_c^2}}{\sqrt{\sinh^2\left[-(t\tau_d - \tau_d^2/2)/T_0^2\right] + e^{-2\tau_d^2/T_c^2}}}, \tag{6.43b}$$

$$s_{t3}^{(\mathrm{pol})}(t) = \frac{\sin(\omega_0\tau_d)e^{-\tau_d^2/T_c^2}}{\sqrt{\sinh^2\left[-(t\tau_d - \tau_d^2/2)/T_0^2\right] + e^{-2\tau_d^2/T_c^2}}}. \tag{6.43c}$$

For $\tau_d \ll T_c$ these equations reduce to (6.42), which is in line with the observation that for pulses with long coherence time compared to the inter-component delay, the electromagnetic pulse is fully polarized. For pulses with $\tau_d \gg T_c$ the expressions simplify to $s_{t1}^{(\mathrm{pol})}(t) = \mathrm{sgn}[-(t\tau_d - \tau_d^2/2)/T_0^2]$, $s_{t2}^{(\mathrm{pol})}(t) = 0$, and $s_{t3}^{(\mathrm{pol})}(t) = 0$, where $\mathrm{sgn}(x) = -1$ for $x < 0$, $\mathrm{sgn}(0) = 0$, and $\mathrm{sgn}(x) = 1$ for $x > 0$. At $t = \tau_d/2$ the expressions do not have a physical meaning, since the incoherent beam is unpolarized at $\tau_d/2$.

For a partially coherent beam, i.e., τ_d comparable to T_c, the behavior of the polarized part of the beam is similar to the whole beam at the limits $t \to \pm\infty$, with $\lim_{t\to\pm\infty} s_{t1}^{(\mathrm{pol})}(t) = \mp 1$, i.e., the leading edge of the beam is fully x-polarized and the tail is fully y-polarized. When t increases from $-\infty$, the value of $s_{t1}^{(\mathrm{pol})}(t)$ starts to decrease and $s_{t2}^{(\mathrm{pol})}(t)$, $s_{t3}^{(\mathrm{pol})}(t)$ increase correspondingly such that $[s_{t1}^{(\mathrm{pol})}(t)]^2 + [s_{t2}^{(\mathrm{pol})}(t)]^2 + [s_{t3}^{(\mathrm{pol})}(t)]^2 = 1$. At the midpoint $t = \tau_d/2$, $s_{t1}^{(\mathrm{pol})}(t) = 0$, $s_{t2}^{(\mathrm{pol})}(t) = \cos(\omega_0\tau_d)$, and $s_{t3}^{(\mathrm{pol})}(t) = \sin(\omega_0\tau_d)$, indicating that the polarized part of the beam is elliptically polarized with the polarization ellipse's axes lying at 45° angles to the x and y axes. When t increases further, $s_{t1}^{(\mathrm{pol})}(t) < 0$ and decreases with increasing t, and the magnitudes of $s_{t2}^{(\mathrm{pol})}(t)$ and $s_{t3}^{(\mathrm{pol})}(t)$ decrease. At very large t, $s_{t1}^{(\mathrm{pol})}(t) = -1$, $s_{t2}(t) = 0$, and $s_{t3}(t) = 0$, indicating that the polarized part is fully linearly polarized in the y direction.

6.5.1b Frequency-domain polarization analysis

In the frequency domain, the polarization and coherence properties are given by the spectral coherence matrix $\mathbf{W}(\omega_1, \omega_2)$, which is obtained from the temporal coherence matrix by using Eq. (6.4). Applying Eq. (6.4) to the coherence matrix $\mathbf{\Gamma}(t_1, t_2)$, the following

expression is obtained:

$$\mathbf{W}(\omega_1,\omega_2) = W(\omega_1,\omega_2)\begin{bmatrix} 1 & e^{i\omega_2\tau_d} \\ e^{-i\omega_1\tau_d} & e^{i(\omega_2-\omega_1)\tau_d} \end{bmatrix}. \tag{6.44}$$

The quantity $W(\omega_1,\omega_2)$ is the spectral coherence function of the field $E(t)$,

$$W(\omega_1,\omega_2) = \sqrt{S(\omega_1)S(\omega_2)}\exp\left[-\frac{(\omega_2-\omega_1)^2}{\Omega_c^2}\right], \tag{6.45}$$

where Ω_c is the spectral coherence width of the pulse, $\Omega_c = [(T_c^2 + 4T_0^2)/T_0^4]^{1/2}$,

$$S(\omega) = \frac{A_0^2 T_0}{4\pi\delta}\exp\left[-\frac{1}{4\delta^2}(\omega-\omega_0)^2\right], \tag{6.46}$$

is the spectral density, and $\delta = [(2T_0)^{-2} + T_c^{-2}]^{1/2}$ is the bandwidth of the pulse. From Eqs. (6.45) and (6.46) it is seen that the spectral coherence properties of the Gaussian Schell-model pulse are also Gaussian and obey the Schell model in the sense that the spectral density and the normalized coherence function are both Gaussian, and the spectral coherence function depends on frequency only via the frequency difference $\omega_2 - \omega_1$. The spectral polarization matrix is

$$\mathbf{\Phi}(\omega) = \mathbf{W}(\omega,\omega) = S(\omega)\begin{bmatrix} 1 & e^{i\omega\tau_d} \\ e^{-i\omega\tau_d} & 1 \end{bmatrix}, \tag{6.47}$$

and the spectral degree of polarization

$$P_s(\omega) = \sqrt{1 - 4\frac{\det\mathbf{\Phi}(\omega)}{\mathrm{tr}^2\mathbf{\Phi}(\omega)}} = 1, \tag{6.48}$$

i.e., the field is spectrally fully polarized at all frequencies. This result is similar to the stationary case as presented in Chap. 4.

The normalized Stokes parameters, defined in Eq. (6.27), are

$$s_{s1}(\omega) = 0, \tag{6.49a}$$

$$s_{s2}(\omega) = \cos(\omega\tau_d), \tag{6.49b}$$

$$s_{s3}(\omega) = \sin(\omega\tau_d). \tag{6.49c}$$

This result is not specific for the Gaussian pulse, but rather holds for all beams which are constructed by taking a linearly polarized pulse, making a delayed copy, and using

the copy as the orthogonal polarization component. From the first equation it is seen that the spectral densities of the x and y components are equal at all frequencies. The reason behind this is that the time-domain delay between the components corresponds to a phase shift in the frequency domain. The spectral density depends only on the magnitude of the frequency component, and since x and y components differ only in phase, their spectral densities are equal.

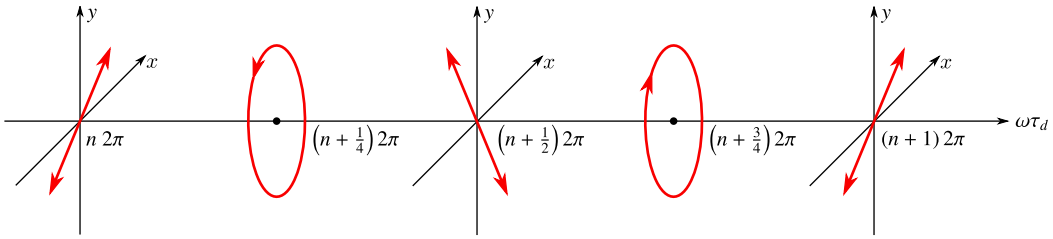

Figure 6.3: Variation of the spectral Stokes parameters with the product of the frequency ω and the time delay τ_d. The polarization state changes from linearly polarized (45° angle to the x axis) state to elliptically polarized (major axis at 45°, right-handed rotation), right-hand circular polarization, right-hand elliptical polarization (major axis at 135°, orthogonal linear polarization 135°, left-hand elliptical polarization (major axis at 135°), left-hand circular polarization, left-hand elliptical polarization (major axis at 45°), and finally back to the linear polarization at 45° angle to the x axis.

Equations (6.49b) and (6.49c) indicate that the field is elliptically polarized with the major axes of the polarization ellipse lying at angles 45° and 135° with respect to the x axis. The polarization state varies sinusoidally between the linearly polarized and circularly polarized states as ω changes. The period of the variation is given by the time delay τ_d. The change of the polarization state with frequency is shown in Fig. 6.3. At a frequency where $\omega\tau_d$ is an integer multiple of 2π, the field is linearly polarized with the angle between the polarization direction and x axis being 45°. As the frequency increases, the polarization state becomes right-handed elliptical polarization with the major axis at 45° angle to the x axis. The frequency component with $\omega\tau_d = (n + 1/4)2\pi$ is right-handed circularly polarized, and when frequency increases the field becomes, again, right-hand elliptically polarized, with the major axis at 135° angle to the x axis. At $\omega\tau_d = (n + 1/2)2\pi$ the field is linearly polarized at 135° to the x axis, i.e., orthogonal to the polarization state at frequency with $\omega\tau_d = n2\pi$. With further increase in frequency the field passes through left-handed elliptical polarization (major axis at 135°), left-hand circular polarization at $\omega\tau_d = (n + 3/4)2\pi$, left-hand elliptical polarization (major axis at 45°), and back to the linear polarization at 45° angle to the x axis.

6.5.1c Polarization equivalence analysis

The temporal coherence matrix of the field may be analyzed using the method introduced in Sec. 6.2.1 to reveal which temporal coherence matrices correspond to the same spectral polarization matrix and thus the same spectral polarization properties and spectral density.

The time-averaged coherence matrix $\overline{\mathbf{\Gamma}}(\mathbf{r}, \mathbf{r}, \tau)$ is obtained using Eq. (6.17),

$$\overline{\mathbf{\Gamma}}(\mathbf{r}, \mathbf{r}, \tau) = \frac{1}{2\sqrt{\pi}} T_0 A_0^2 e^{-i\omega_0\tau} \begin{bmatrix} e^{-\delta^2\tau^2} & e^{-\delta^2(\tau-\tau_d)^2} e^{i\omega_0\tau_d} \\ e^{-\delta^2(\tau+\tau_d)^2} e^{-i\omega_0\tau_d} & e^{-\delta^2\tau^2} \end{bmatrix}. \tag{6.50}$$

From this equation it is seen that in order for two different fields to have the same averaged correlation matrix at all values of τ (and thus the same spectral polarization matrix), the fields must have the same bandwith δ, central frequency ω_0, time delay τ_d, and the product of intensity and pulse length $T_0 A_0^2$. The last quantity is proportional to the total energy of the pulse. So if the coherence time T_c is changed, the spectral polarization properties remain the same if the pulse width is adjusted to preserve the bandwidth δ and the peak amplitude is adjusted to preserve the pulse energy.

6.5.2 Two orthogonal, linearly polarized uncorrelated pulses

A simple yet illustrative example is the superposition of two linearly polarized, uncorrelated pulses such that the polarization directions of the pulses are perpendicular to each other. Assuming that one pulse is polarized in the x direction and the other in the y direction, the coherence matrix in time domain is

$$\begin{aligned} \mathbf{\Gamma}(t_1, t_2) &= \begin{bmatrix} \Gamma_{xx}(t_1, t_2) & 0 \\ 0 & \Gamma_{yy}(t_1, t_2) \end{bmatrix} \\ &= \begin{bmatrix} \sqrt{I_x(t_1) I_x(t_2)}\, \gamma_x(t_1, t_2) & 0 \\ 0 & \sqrt{I_y(t_1) I_y(t_2)}\, \gamma_y(t_1, t_2) \end{bmatrix}, \end{aligned} \tag{6.51}$$

from which follow the polarization matrix

$$\mathbf{J}(t) = \mathbf{\Gamma}(t, t) = \begin{bmatrix} I_x(t) & 0 \\ 0 & I_y(t) \end{bmatrix}, \tag{6.52}$$

the spectral coherence matrix, obtained with Eq. (4.3),

$$\mathbf{W}(\omega_1, \omega_2) = \begin{bmatrix} W_{xx}(\omega_1, \omega_2) & 0 \\ 0 & W_{yy}(\omega_1, \omega_2) \end{bmatrix}, \tag{6.53}$$

and the spectral polarization matrix

$$\mathbf{\Phi}(\omega) = \begin{bmatrix} S_x(\omega) & 0 \\ 0 & S_y(\omega) \end{bmatrix}. \tag{6.54}$$

The time-domain degree of polarization of the pulsed field is then

$$P_{\mathrm{t}}(t) = \left| \frac{I_x(t) - I_y(t)}{I_x(t) + I_y(t)} \right|, \tag{6.55}$$

and the spectral degree of polarization is

$$P_{\mathrm{s}}(\omega) = \left| \frac{S_x(\omega) - S_y(\omega)}{S_x(\omega) + S_y(\omega)} \right|. \tag{6.56}$$

The degrees of polarization in time and frequency domains have similar expressions. From the time-domain degree of polarization it is seen that the field is fully polarized only when either orthogonal component of the field is zero; the field is unpolarized when the intensities of the components are equal; and the field is partially polarized when the intensities of the components are unequal and both nonzero.

Likewise, the field is spectrally unpolarized at frequencies where the spectral densities of x and y components are equal, $S_x(\omega) = S_y(\omega)$, and spectrally fully polarized when the spectral density of either component is zero. Intermediate cases with $S_x(\omega) \neq S_y(\omega) \neq 0$ correspond to partial spectral polarization. A special case is a beam in which the spectra of the x and y components do not overlap at all, in which case the beam is fully polarized at all frequencies, even though in time domain it may very well be partially polarized or unpolarized.

The spectral polarization matrix $\mathbf{\Phi}(\omega)$ in Eq. (6.54) depends on the time behavior of both the intensity and the coherence function of the field. However, the correspondence between the spectral polarization matrix and the temporal coherence matrix is not one-to-one, as seen from Eq. (6.12), and thus many different time-domain coherence matrices imply the same spectral polarization matrix as detailed in Sec. 6.2.1.

Chapter 7

Polarization of temporally imaged pulses

The manipulation of the time-dependent behavior of a beam of light is possible using cascades of suitable active or passive optical elements which modulate the beam's phase as a function of time or frequency [47]. This chapter details how a temporal imaging system, consisting of dispersive optical fibers and a time-dependent phase modulator, modifies the polarization of a partially polarized pulse traversing through the device depending on the choice of the fibers' dispersive properties.

7.1 Light propagation in dispersive media

Practically all material media in which light may propagate are dispersive, that is, different frequency components travel at different velocities. This is expressed mathematically by noting that the propagation constant β, introduced in Eq. (2.19), depends on frequency: $\beta(\omega) = \omega n(\omega)/c$. The dispersion properties may be characterized by approximating the propagation constant with its Taylor expansion around the central frequency ω_0:

$$\beta(\omega) \approx \beta_0 + \beta_1(\omega - \omega_0) + \frac{\beta_2}{2}(\omega - \omega_0)^2, \tag{7.1}$$

where $\beta_0 = \beta(\omega_0)$ is the propagation constant evaluated at the central frequency ω_0, and β_1 and β_2 are the first and second derivatives of $\beta(\omega)$ with respect to ω, evaluated at ω_0. A propagation medium for which the second-order Taylor expansion is sufficient is called a linearly dispersive medium. Media for which the second-order approximation for the propagation constant is not sufficiently accurate over the bandwidth of interest are beyond the scope of this work.

The group delay β_1 gives the group velocity $v_g = 1/\beta_1$, the propagation velocity of the envelope of the pulse. If β_2 and higher Taylor expansion terms are negligibly small over the bandwidth of the pulse, the envelope of the pulse is not changed during propagation. However, short pulses necessarily have a considerable bandwidth, and thus for, e.g., optical fibers the dispersion effects become important, i.e., low-frequency components of the pulse arrive with significantly different propagation delay compared to the high-frequency components. This separation of the frequency components with propagation is known as chirping. The difference $\delta\tau$ between the propagation delays of components separated by $\delta\omega$ is given by

$$\delta\tau = \beta_2 z \delta\omega = \Phi\delta\omega, \tag{7.2}$$

where $\Phi = \beta_2 z$ is the group delay dispersion (GDD) parameter. It is seen that when $\beta_2 > 0$, the propagation delay over distance z is larger for higher frequency components, i.e., the low-frequency components of the pulse arrive first, and the pulse has become up-chirped. The propagation medium is said to exhibit normal dispersion. For $\beta_2 < 0$, the converse holds, and the pulse becomes down-chirped; the medium exhibits anomalous dispersion.

Inserting Eq. (7.1) into Eq. (2.19) and examining the propagation a single polarization component $E(z,t)$ gives

$$E(z,t) = \int \widetilde{E}(0,\omega) e^{i\{[\beta_0 + (\omega-\omega_0)\beta_1 + (\omega-\omega_0)^2\beta_2/2]z - \omega t\}} \mathrm{d}\omega. \tag{7.3}$$

It is convenient to investigate the behavior of the complex envelope $A(z,t)$, introduced for vector fields in Sec. 6.5.1, instead of the complex analytic signal $E(t)$. The Fourier components $\widetilde{A}(z,\Omega)$ of the complex envelope are related to the Fourier components of the complex-analytic signal via $\widetilde{E}(z,\omega_0+\Omega) = \widetilde{A}(z,\Omega)$. The complex envelope after propagation through the distance z is given by

$$A(z,t) = e^{i\beta_0 z} \int \widetilde{A}(0,\Omega) e^{i(\beta_1\Omega + \beta_2\Omega^2/2)z} e^{-i\Omega t} \mathrm{d}\Omega. \tag{7.4}$$

Expanding the Fourier components $\widetilde{A}(0,\Omega)$, changing the order of integration of the resulting two integrals, and integrating gives that the envelope after propagation through the dispersive medium is

$$A(z,t) = \int A(0,t') K_f(t,t';z)\, \mathrm{d}t', \tag{7.5}$$

where the kernel $K_f(t, t'; z)$ is

$$K_f(t, t'; z) = e^{i\beta_0 z} \sqrt{\frac{i}{2\pi\beta_2 z}} \exp\{-i[(t' - t) + \beta_1 z]^2 / 2\beta_2 z\}. \tag{7.6}$$

The subscript f refers to "fiber", as this chapter will deal with a system which involves dispersive optical fibers. The phase factor $\exp(i\beta_0 z)$ will be ignored, as it is common to all frequencies and does not affect the shape of the pulse or relative phases of the components.

In order to increase clarity, the time t at which the envelope is investigated is replaced with the reduced time $t_r = t - \beta_1 z = t - z/v_g$. The reduced time therefore gives the time relative to the center of the pulse, which propagates at the group velocity v_g. Noting that the kernel only depends on time via the time difference $t' - t_r$, the expression for the kernel can be written as

$$K_f(\tau) = \sqrt{\frac{i}{2\pi\Phi}} \exp(-i\tau^2 / 2\Phi). \tag{7.7}$$

Equation (7.4) becomes

$$A(t_r) = \int A(0, t') K_f(t_r - t') \, \mathrm{d}t', \tag{7.8}$$

which is immediately recognized as a convolution. From the properties of Fourier transforms it is evident that Fourier representation of the envelope after the propagation is obtained as the product of the Fourier representation of the input envelope and the Fourier transform of the kernel $K_f(\tau)$, known as the transfer function. This shows that in frequency space, propagation through a linearly dispersive (second-order) medium introduces relative phase differences between the frequency components, but the spectra of polarization components i, given by $\langle|\widetilde{E}_i(z, \omega)|^2\rangle$, remain unchanged.

The phase of a field may be altered using so-called phase filters, which, as the name suggests, leave the amplitude of the field untouched and manipulate the phase. An interesting class of phase filters are the quadratic phase modulators (QPM). The phase change imparted on the field by the QPM depends quadratically on time, hence the name:

$$E^{(\mathrm{out})}(t) = E^{(\mathrm{in})}(t) e^{it^2/2\gamma}, \tag{7.9}$$

or, equivalently,

$$A^{(\mathrm{out})}(t) = A^{(\mathrm{in})}(t) e^{it^2/2\gamma}. \tag{7.10}$$

The QPM may be realized using, e.g., electrical modulation of an electro-optic medium or self phase modulation in a nonlinear medium [48]. The parameter γ characterizes the

strength of the modulation. Since the QPM only affects the phase of the pulse, the intensity profile of the pulse remains unchanged. In the frequency space, the convolution theorem states that the output spectrum is proportional to the absolute square of the convolution of the Fourier components of the pulse with the Fourier transform of the exponential phase modulation term. The spectrum therefore may be changed significantly by the temporal phase modulation.

7.2 Space–time analogy of diffraction and dispersion

When the mathematical form of second-order dispersion on a time-domain signal is compared to the formula for Fresnel diffraction, it is immediately seen that dispersion and propagation in free space are analogous, with (retarded) time t_r corresponding to the transverse coordinate ρ, ω corresponds to spatial frequency k_x, and $-2\pi\beta_2$ corresponds to wavelength λ. The analogy extends also to the QPM, whose counterpart is the thin lens, with the quantity $-\gamma/\beta_2$ corresponding the focal length f of the lens [49,50]. A fundamental difference between spatial and temporal optics is that wavelength λ is always a positive quantity, however its counterpart $-2\pi\beta_2$ may be either positive (anomalous dispersion) or negative (normal dispersion). The consequence of the necessarily positive wavelength in spatial optics is that the components with high spatial frequency always diffract more strongly, a fact which, e.g., necessarily limits the resolution of any conventional optical imaging system. Another difference between spatial and temporal optics is that time-domain signals need to be causal, whereas no such notion exists in space.

7.3 Temporal imaging of electromagnetic beams

The space–time analogy points to an intriguing use of two dispersive propagation media and a QPM. The simplest conventional optical imaging system consists of an illuminated object, a thin lens with positive focal length, and a screen. If the system is assumed to be infinite in the directions perpendicular to the optical axis of the lens, the intensity distribution of light at the object plane is perfectly imaged on the image plane if the distance between the object plane and the lens, z_o, the distance between the lens and the image plane, z_i, and the focal length fulfill Newton's lens law:

$$1/f = 1/z_o + 1/z_i. \tag{7.11}$$

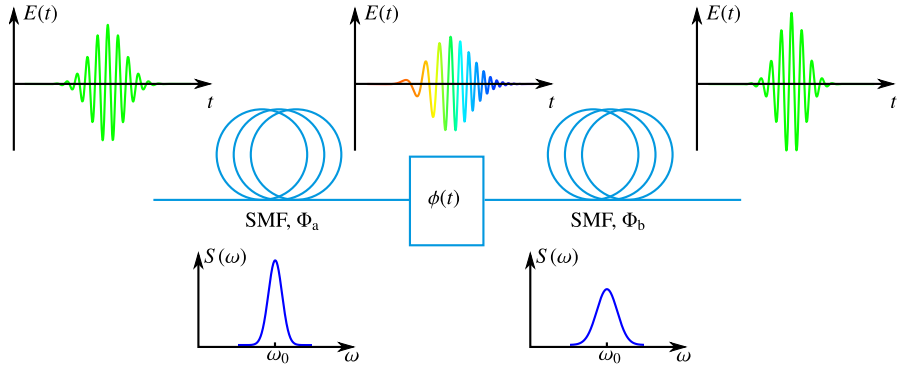

Figure 7.1: Schematic of a time lens. The first single-mode fiber (SMF) with group dispersion delay (GDD) parameter Φ_a acts as a spectral phase filter for the originally unchirped pulse, introducing phase differences between different spectral components, thus broadening the temporal profile of the pulse and introducing chirp while retaining the spectrum of the pulse. The temporal quadratic phase modulator (QPM) leaves the temporal profile of the pulse unchanged, but changes the phase by different amounts at different instants of the pulse, broadening the frequency spectrum of the pulse. The second SMF, with GDD parameter Φ_b, retains the broadened spectral profile but changes the relative phases of different frequency components of the pulse, changing the temporal profile. If the GDD parameters and the QPM are suitably chosen with respect to each other, the chirp introduced by propagation through the first fiber is cancelled by the second fiber. The temporal profile of the pulse is changed, in the case shown, compressed.

This lens law can be derived by calculating the propagation of the field from the object to the lens using the Fresnel diffraction integral, applying the phase change imparted by the lens, and using the Fresnel diffraction integral again to propagate the field from the lens to the image plane. The resulting double integral involves a quadratic complex-exponential term which can be eliminated by mandating that Eq. (7.11) holds. The result obtained is that the field distribution at the image plane is a magnified or demagnified copy of the field distribution at the object plane, plus a residual quadratic phase term which does not affect the intensity distribution.

Applying the analogy between second-order dispersion and free-space propagation and that between a QPM and a thin lens, the arrangement shown in Fig. 7.1 is considered. The system consists of a dispersive single-mode fiber (SMF, fiber a), a QPM, i.e., the 'time lens', and another single-mode fiber (b). The fibers are assumed to be polarization-maintaining fibers, so that energy exchange between polarization modes does not occur during propagation. Therefore the propagation of two orthogonally polarized fields may be calculated independently, treating each component $i = x, y$ as a scalar quantity. The GDDs and the temporal focal parameter γ are not necessarily the same for both components of the field, so the GDDs of fibers a and b are denoted with Φ_{ai} and Φ_{bi}, respectively, and the

effective temporal focal parameters γ_i.

An input pulse with the envelope $A_i^{(\mathrm{in})}(t)$ will lead to the envelopes $A_i^{(\mathrm{a})}(t_a)$, $A_i^{(\mathrm{l})}(t_a)$, and $A_i^{(\mathrm{out})}(t_b)$ after passing through fiber a, the QPM, and fiber b, respectively:

$$A_i^{(\mathrm{a})}(t_a) = e^{i\beta_0 z_a} \int_{-\infty}^{\infty} \sqrt{\frac{i}{2\pi\Phi_{\mathrm{a}i}}} A_i^{(\mathrm{in})}(t') \exp\left[-i\frac{(t'-t_a)^2}{2\Phi_{\mathrm{a}i}}\right] \mathrm{d}t', \tag{7.12a}$$

$$A_i^{(\mathrm{l})}(t_a) = A_i^{(\mathrm{a})}(t_a) \exp\left(i\frac{t_a^2}{2\gamma_i}\right), \tag{7.12b}$$

$$A_i^{(\mathrm{out})}(t_b) = e^{i\beta_0 z_b} \int_{-\infty}^{\infty} \sqrt{\frac{i}{2\pi\Phi_{\mathrm{b}i}}} A_i^{(\mathrm{l})}(t') \exp\left[-i\frac{(t'-t_b)^2}{2\Phi_{\mathrm{b}i}}\right] \mathrm{d}t', \tag{7.12c}$$

For a sufficiently narrow spectral bandwidth these expressions can be shown to be causal in time [50]. When Eqs. (7.12a)–(7.12c) are combined to get a single equation relating $A_i^{(\mathrm{in})}(t)$ and $A_i^{(\mathrm{out})}(t_b)$, the following integral expression is obtained:

$$A_i^{(\mathrm{out})}(t_b) = \int_{-\infty}^{\infty} A_i^{(\mathrm{in})}(t') K_i(t_b, t')\, \mathrm{d}t'. \tag{7.13}$$

The kernel $K(t_b, t')$ is

$$K_i(t_b, t') = e^{i\phi(t_b,t')} \sqrt{\frac{i}{2\pi\Phi_{\mathrm{a}i}}} \sqrt{\frac{i}{2\pi\Phi_{\mathrm{b}i}}} \int_{-\infty}^{\infty} \exp\left[-\frac{i}{2}Lt''^2 + i\left(\frac{t'}{\Phi_{\mathrm{a}i}} + \frac{t_b}{\Phi_{\mathrm{b}i}}\right)t''\right] \mathrm{d}t'', \tag{7.14}$$

where $\phi(t_b, t') = \beta_{0\mathrm{a}} z_\mathrm{a} + \beta_{0\mathrm{b}} z_\mathrm{b} - (t'^2/\Phi_{\mathrm{a}i} + t_b^2/\Phi_{\mathrm{b}i})/2$. The quantity $L = 1/\Phi_{\mathrm{b}i} + 1/\Phi_{\mathrm{a}i} - 1/\gamma_i$ bears resemblance to the lens law. If the temporal focal parameter γ_i and the GDD parameters $\Phi_{\mathrm{a}i}$ and $\Phi_{\mathrm{b}i}$ are chosen such that $L = 0$, i.e.,

$$\frac{1}{\gamma_i} = \frac{1}{\Phi_{\mathrm{a}i}} + \frac{1}{\Phi_{\mathrm{b}i}}, \tag{7.15}$$

the quadratic term in Eq. (7.14) vanishes. The integral may be evaluated to yield the kernel

$$K_i(t', t_b) = e^{i\phi(t',t_b)} \sqrt{\frac{i}{\Phi_{\mathrm{a}i}}} \sqrt{\frac{i}{\Phi_{\mathrm{b}i}}} |\Phi_{\mathrm{a}i}|\, \delta\left(t' + \frac{\Phi_{\mathrm{a}i}}{\Phi_{\mathrm{b}i}} t_b\right). \tag{7.16}$$

Using this kernel, the complex envelope at the output of the system is

$$A_i^{(\mathrm{out})}(t_b) = e^{i[\beta_{0\mathrm{a}} z_\mathrm{a} + \beta_{0\mathrm{b}} z_\mathrm{b} + (M-1)t_b^2/2\Phi_{\mathrm{b}i}]} \sqrt{\frac{i}{\Phi_{\mathrm{a}i}}} \sqrt{\frac{i}{\Phi_{\mathrm{b}i}}} |\Phi_{\mathrm{a}i}|\, A_i^{(\mathrm{in})}\left(Mt_b\right), \tag{7.17}$$

where the temporal magnification M has been defined as $M = -\Phi_{\mathrm{a}i}/\Phi_{\mathrm{b}i}$. It is evident that if the system parameters obey the temporal lens equation, Eq. (7.15), the output envelope

is a scaled and magnified or demagnified copy of the input envelope, with the temporal magnification given by the ratio of the fiber GDD parameters. If both fibers are operated in the same dispersion regime (normal or anomalous), the pulse is also reversed, since the M will be negative.

The arrangement of two dispersive elements and a quadratic phase modulator thus acts as a temporal imaging system if the dispersion parameters and the strength of the phase modulation are chosen properly. This kind of a system may be exploited, e.g., to decompress a pulse to keep its peak intensity within the limits of an optical component while retaining pulse shape and energy, or to better resolve the temporal shape of the pulse.

7.4 Time lens and temporal coherence

Since the temporal shape and phase of a pulse passing through a temporal imaging system are altered, its coherence and polarization properties will also undergo some changes. In order to explore them, the coherence matrix of the output pulse is calculated as a function of the input coherence matrix.

The relationship between input and output of the temporal imaging system has been formulated above using the complex envelope of the pulse instead of its complex analytic signal. The coherence of the pulse may also be characterized using the envelope coherence matrix $\mathbf{\Gamma}^{(\mathrm{e})}(t_1, t_2)$ with the elements

$$\Gamma_{ij}^{(\mathrm{e})}(t_1, t_2) = \langle A_i^*(t_1) A_j(t_2) \rangle = \langle E_i^*(t_1) e^{-i\omega_0 t_1} E_j(t_2) e^{i\omega_0 t_2} \rangle = \Gamma_{ij}(t_1, t_2) e^{i\omega_0 (t_2 - t_1)}. \tag{7.18}$$

When a pulse traverses a temporal imaging system, the coherence matrix $\mathbf{\Gamma}_0^{(\mathrm{e})}(t_1', t_2')$ at the input of the system is transformed upon propagation into $\mathbf{\Gamma}^{(\mathrm{e})}(t_1, t_2)$ at the output. The primed time variables serve to remind that the origin of time is different at input and output, as discussed in the previous section, with $t_k = t_k' - z_\mathrm{a}/v_{g\mathrm{a}} - z_\mathrm{b}/v_{g\mathrm{b}}$, where z_a and z_b are the lengths and $v_{g\mathrm{a}}$ and $v_{g\mathrm{b}}$ are the group velocities in fibers a and b, respectively. The group velocities for both x and y components are assumed to be the same. Dissimilar group velocities for orthogonal polarizations could be incorporated in the calculations, but this would complicate the analysis of the results unnecessarily and is thus relegated for further study.

The envelope coherence matrix at the output, in general, will be

$$\Gamma_{ij}^{(\mathrm{e})}(t_1, t_2) = \iint \Gamma_{0ij}^{(\mathrm{e})}(t_1', t_2') K_{ij}(t_1, t_2; t_1', t_2') \, \mathrm{d}t_1' \mathrm{d}t_2', \tag{7.19}$$

where the propagation kernel of the coherence matrix, $K_{ij}(t_1, t_2; t_1', t_2')$ is obtained from the

kernel in Eq. (7.14) via

$$K_{ij}(t_1, t_2; t_1', t_2') = K_i^*(t_1, t_1') K_j(t_2, t_2'). \tag{7.20}$$

If the imaging condition (7.15) holds for both x and y components, the coherence matrix will be, explicitly,

$$\Gamma_{ij}^{(\mathrm{e})}(t_1, t_2) = \sqrt{|M_i M_j|}\, e^{i\phi_{ij}(t_1,t_2)}\, \Gamma_{0ij}^{(\mathrm{e})}(M_i t_1, M_j t_2), \tag{7.21}$$

where

$$\phi_{ij}(t_1, t_2) = \frac{\pi}{4}[\mathrm{sgn}(\Phi_{aj}) + \mathrm{sgn}(\Phi_{bj}) - \mathrm{sgn}(\Phi_{\mathrm{a}i}) - \mathrm{sgn}(\Phi_{\mathrm{b}i})] - \frac{(M_i - 1)}{2\Phi_{\mathrm{b}i}} t_1^2 + \frac{(M_j - 1)}{2\Phi_{\mathrm{b}j}} t_2^2 \tag{7.22}$$

is a quadratic phase, and $\mathrm{sgn}(\Phi) = \Phi/|\Phi|$ is the signum function. The corresponding expression for the coherence matrix is

$$\Gamma_{ij}(t_1, t_2) = \sqrt{|M_i M_j|}\, e^{i\phi_{ij}(t_1,t_2)}\, \Gamma_{0ij}(M_i t_1, M_j t_2)\, e^{-i\omega_0[(1-M_i)t_2 - (1-M_j)t_1]}. \tag{7.23}$$

The temporal coherence properties of the field are clearly altered on propagation through the temporal imaging system if at least one of the magnifications M_i differs from value 1. The coherence time and length of the pulse thus change.

The polarization properties after propagation through the system are seen, as usual, from the polarization matrix $\mathbf{J}(t) = \mathbf{\Gamma}(t, t)$:

$$J_{ij}(t) = \sqrt{|M_i M_j|}\, e^{i\phi_{ij}(t)}\, \Gamma_{0ij}(M_i t, M_j t) e^{-i\omega_0(M_i - M_j)t}, \tag{7.24}$$

with the quadratic phase

$$\phi_{ij}(t) = \frac{\pi}{4}[\mathrm{sgn}(\Phi_{\mathrm{a}j}) + \mathrm{sgn}(\Phi_{\mathrm{b}j}) - \mathrm{sgn}(\Phi_{\mathrm{a}i}) - \mathrm{sgn}(\Phi_{\mathrm{b}i})] + \left(\frac{M_j - 1}{2\Phi_{\mathrm{b}j}} - \frac{M_i - 1}{2\Phi_{\mathrm{b}i}}\right) t^2. \tag{7.25}$$

The intensities $I_i(t) = J_{ii}(t)$ at the output are

$$I_i(t) = |M_i|\, J_{0ii}(M_i t), \tag{7.26}$$

which shows that the intensity at the output of the temporal imaging system is a scaled copy of the input intensity.

The time lens may also be analyzed in the frequency domain. Starting from Eq. (7.17) and the relationship between complex analytic signal and complex envelope, polarization

component i of the pulse in frequency domain is

$$\widetilde{E}_i(\omega) = \widetilde{\Psi}_i \int_{-\infty}^{\infty} \widetilde{E}_{0i}\left(\omega_0 + \frac{\omega' - \omega_0}{M_i}\right) \exp\left[-i\frac{\Phi_{\mathrm{b}i}}{2(M_i - 1)}(\omega - \omega')^2\right] \mathrm{d}\omega', \tag{7.27}$$

where

$$\widetilde{\Psi}_i = \sqrt{\frac{i\Phi_{\mathrm{b}i}}{2\pi\,|M_i|\,(M_i - 1)}}\, e^{i\tilde{\phi}_i} \tag{7.28}$$

and $\tilde{\phi}_i = [\mathrm{sgn}(\Phi_{\mathrm{b}i}) + \mathrm{sgn}(\Phi_{\mathrm{a}i})]\pi/4$. Using Eq. (4.1), the spectral coherence matrix $\mathbf{W}(\omega_1, \omega_2)$ at the output of the system is obtained as a function of the spectral coherence matrix $\mathbf{W}_0(\omega_1, \omega_2)$ at the input:

$$\begin{aligned} W_{ij}(\omega_1, \omega_2) = \widetilde{\Psi}_i^* \widetilde{\Psi}_j \iint_{-\infty}^{\infty} W_{0ij}\left(\omega_0 + \frac{\omega_1' - \omega_0}{M_i}, \omega_0 + \frac{\omega_2' - \omega_0}{M_j}\right) \\ \times \exp\left[i\frac{\Phi_{\mathrm{b}i}}{2(M_i - 1)}(\omega_1 - \omega_1')^2 - i\frac{\Phi_{\mathrm{b}j}}{2(M_j - 1)}(\omega_2 - \omega_2')^2\right] \mathrm{d}\omega_1' \mathrm{d}\omega_2'. \end{aligned} \tag{7.29}$$

The somewhat complicated form for the coherence matrix is mainly due to the quadratic phase term in Eq. (7.17). If the functional form of $W_{0ij}(\omega_1, \omega_2)$ is not known, the analysis can not be carried any further. However, some qualitative arguments may be used to ascertain the behavior of the frequency-domain coherence. The exponential term in the integral will oscillate very rapidly for values of ω_1' and ω_2' which are not sufficiently close to ω_1 and ω_2, respectively. If this oscillation with changing ω_1' and ω_2' is sufficiently swift compared to how fast the value of W_{0ij} changes with ω_1'/M_i and ω_2'/M_j, the contribution to the integral will be washed out by the oscillation. The values of $W_{0ij}(\omega_1, \omega_2)$ that contribute to the spectral coherence matrix after the output will be those which are within $(\omega_1' - \omega_0)/M_i$ and $(\omega_2' - \omega_0)/M_j$ off the central frequency ω_0. Changing the magnifications M_i and M_j will clearly affect the width of the spectral coherence function.

7.5 Temporally imaged Gaussian Schell-model pulses

The effect of temporal imaging is futher explored using the delayed Gaussian-correlated pulses, which were introduced and investigated in Chap. 6. Applying Eq. (7.24) to the coherence and polarization matrices in Eqs. (6.38) and (6.39) gives

$$\begin{aligned} &J_{xx}(t) = I_x(t) = |M_x|\, I(M_x t), \quad J_{yy}(t) = I_y(t) = |M_y|\, I(M_y t - \tau_d), \\ &J_{xy}(t) = \sqrt{I_x(t) I_y(t)}\, \exp\left\{i[\phi_{xy}(t) + \omega_0 \tau_d] - \Delta^2(t)/T_c^2\right\}, \end{aligned} \tag{7.30}$$

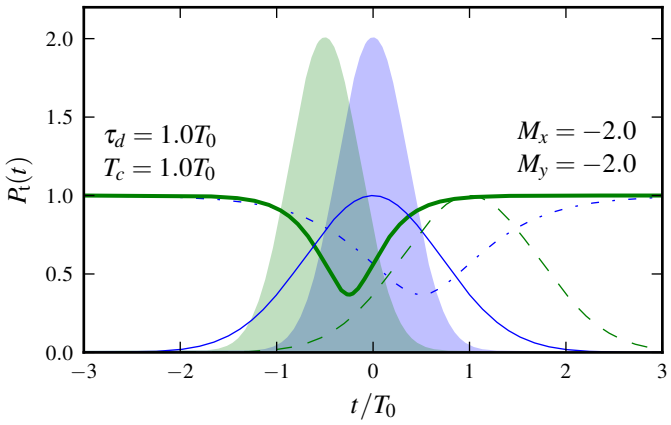

Figure 7.2: Component intensities and degrees of polarization of a GSM pulse before and after temporal magnification. The thin solid, dashed, and dash-dotted curves show the intensities of the x and y components and the degree of polarization, respectively, before the pulse is temporally imaged. The shaded blue and green curves show the intensities of the x and y components of the imaged pulse, and the thick green curve shows the degree of polarization of the imaged pulse. The intensities are normalized to the same scale with the intensities before imaging, so it is seen that the peak intensity has doubled during the imaging, and the order of the components has been reversed (y component precedes the x component after the imaging). Both the intensities of the pulse components and the degree of polarization have been compressed in time with factor 2, but otherwise the shape of the degree of polarization curve, including the minimum value of $P_t(t)$, has been preserved.

where $\Delta(t) = (M_y - M_x)t - \tau_d$, and $I(t)$ is the Gaussian intensity function defined in Eq. (6.33). The Stokes parameters $S_i(t)$ and the normalized Stokes parameters $s_i(t)$ are obtained using Eqs. (5.17) and (5.18). The label t in the subscripts has been dropped, since all of the analysis in this section is done only in time domain. Although the departure from the original example of a GSM pulse is relatively small, there is a wealth of new phenomena to be observed.

The simplest case is equal magnification for both orthogonal components, $M_x = M_y = M$. In that case, the quadratic phase term $\phi_{xy}(t) = 0$ and $\Delta(t) = \tau_d$ for all t. This leads to $\mathbf{J}(t) = \mathbf{J}_0(Mt)$, i.e., the polarization matrix after the imaging is simply a compressed copy of the original polarization matrix. The polarization and coherence properties are conserved. This is illustrated in Fig. 7.2 with $M = -2$. The pulses have been compressed in time, the order of the x and y components has been reversed (y component comes first, and only then comes the x component), and the maximum intensity has doubled to conserve pulse energy. Similar compression can be observed in the degree of polarization. The position of the maximum intensity of the y component has been shifted closer to $t = 0$. Whereas the peak intensities of the orthogonal polarization components have doubled with

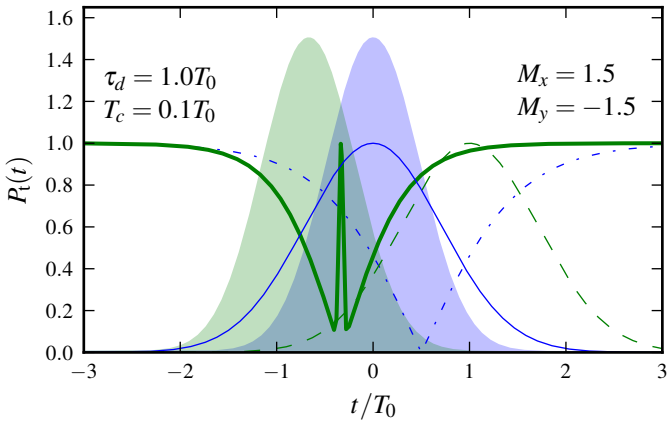

Figure 7.3: Component intensities and the degree of polarization before and after temporal imaging with opposite magnifications for x and y components. The thin lines show the intensities of the x and y components (blue solid and green dashed, respectively) and the degree of polarization (blue dash-dotted) before temporal imaging, shaded blue and green curves show the intensities of the x and y components, respectively, after the temporal imaging, and the thick green curve shows the degree of polarization after imaging. Intensities before and after imaging are represented on the same scale to show the temporal compression-induced change in peak intensity. The main difference to the case $M_x = M_y$ in Fig. 7.2 is the short period of full polarization midway between the intensity peaks.

the temporal imaging, the minimum value of the degree of polarization has been preserved.

A more intriguing case is when the temporal magnifications applied to the orthogonal components are different. Again, in order to keep the example as simple as reasonable, the GDD parameters are assumed to be chosen such that the time-dependent part of the phase term $\phi_{xy}(t)$ vanishes. If the magnifications are equal in magnitude (but still not equal in value), then $M_x = -M_y$. The constant part in $\phi_{xy}(t)$ will be either $\pi/2$ ($M_y < 0$, $\Phi_{ay} > 0$ or $M_x < 0$, $\Phi_{ax} < 0$) or $-\pi/2$ (other possible combinations). The degree of polarization is plotted in Fig. 7.3, and mostly the features resemble the equal magnification case presented in the previous paragraph. However, especially at short coherence times a striking difference is seen: at midway between the intensity peaks, where one would expect the minimum of the degree of polarization, there is a sudden peak, the sharper the smaller the coherence time is compared to the inter-component delay. The presence of this peak may be shown analytically: at times when $I_x(t) = I_y(t)$, the degree of polarization is given by $P_t(t) = |\gamma_{xy}(t)|$, and for a temporally imaged GSM pulse

$$|\gamma_{xy}(t)| = \frac{|J_{xy}(t)|}{\sqrt{I_x(t)I_y(t)}} = \exp\left[-\frac{\Delta^2(t)}{T_c^2}\right] = \exp\left[-\frac{(2M_y t - \tau_d)^2}{T_c^2}\right]. \tag{7.31}$$

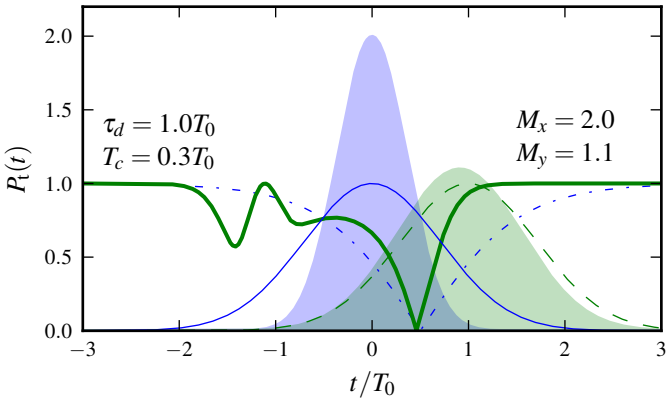

Figure 7.4: Component intensities and the degree of polarization before and after temporal imaging with unequal component magnifications. The thin lines show the intensities of the x and y components (blue solid and green dashed, respectively) and the degree of polarization (blue dash-dotted) before temporal imaging, shaded blue and green curves show the intensities of the x and y components, respectively, after the temporal imaging, and the thick green curve shows the degree of polarization after imaging. Intensities before and after imaging are represented on the same scale to show the temporal compression-induced change in peak intensity.

The zero of the numerator in the rightmost exponential expression is at $t = \tau_d/2M_y$, which can be verified to be the midpoint between the intensity peaks, irrespective of the value of M_y and τ_d. Physically, there is a simple explanation for the short period of full polarization preceded and followed by relatively unpolarized field. A brief calculation shows that the midpoint between the intensity peaks, where the sudden peak in the degree of polarization is located, corresponds to the same instant of time in the original linearly polarized beam from which the electromagnetic beam is derived: at time t the envelope of the x component is equal, up to a scalar multiplier, to the envelope of the original pulse at $t_{0x} = M_x t$, and the envelope of the y component is proportional to the envelope of the original pulse at $t_{0y} = M_y t - \tau_d$. Setting $t_{0x} = t_{0y}$ yields that $t = \tau_d/(M_y - M_x)$. The width of the polarization peak may be tuned by adjusting the coherence time, and the polarization state by adjusting the time delay τ_d with respect to the carrier frequency ω_0.

Other interesting results are obtained when the temporal magnifications of the x and y components have different absolute values, as demonstrated in Figs. 7.4 and 7.5 with $M_x = 1.1$ and $M_y = 2.0$. For $t \ll 0$, the field is fully linearly polarized in the y direction, by the virtue of the y component decaying more slowly than the x component because of the smaller absolute value of the magnification. This is the first clear difference from the non-imaged case analysed in the previous chapter. As t increases, the intensities of both

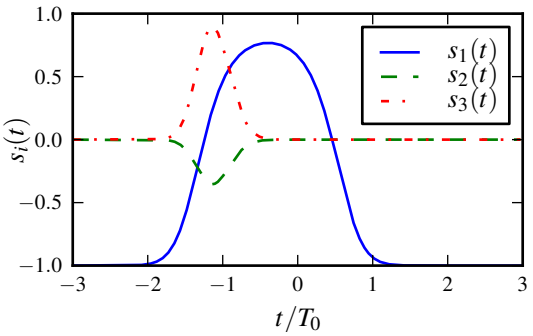

(a) Normalized Stokes parameters of a temporally imaged pulse with unequal magnifications for the orthogonally polarized components. Most striking difference is the behavior of $s_1(t)$, which indicates that the field is y polarized for both large negative and large positive values of t.

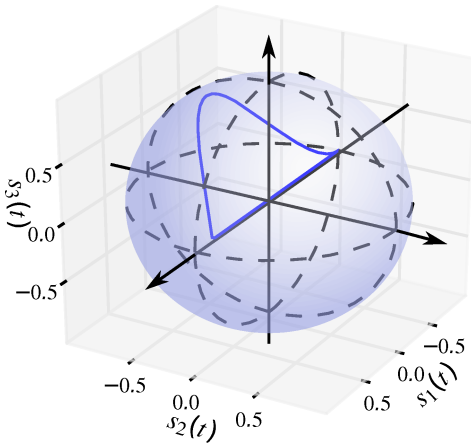

(b) Polarization state represented using a Poincaré sphere, solid curve, and the intersections of the planes $s_1(t) = 0$, $s_2(t) = 0$, and $s_3(t) = 0$ with the surface of the Poincaré sphere, dashed circles. The locus of the points representing the polarization states of the beam at different instants of time forms a closed curve.

Figure 7.5: Behavior of polarization states in a pulse which has been temporally imaged with different magnifications M_x and M_y for the orthogonal polarization components.

polarization components increase. Due to the disparity in the temporal magnifications, the intensity of the x component increases more rapidly. At the first equal-intensity point, the field is partially polarized due to the partial correlation between the x and y components. As can be seen in Fig. 7.5(a), the increasing correlation between the x and y components causes the Stokes parameters $s_2(t)$ and $s_3(t)$ to depart from value 0. At the time $t = \tau_d/(M_y - M_x) \approx -1.1T_0$ the components are fully correlated due to both components having originated at the same point in the original, linearly polarized pulse, and the resultant temporally imaged pulse is fully polarized. The polarization state may be tuned by adjusting the product $\omega_0\tau_d$. When t increases further, the correlations between the x and y components die out, and the degree of polarization is essentially dictated by $|s_1(t)|$, with the degree of polarization after the peak at $t = -1.1T_0$ first decreasing rapidly, then increasing slightly, and then decreasing until the pulse becomes fully unpolarized as the intensities of the x and y component become equal at $t \approx 0.5T_0$. For larger values of t, the field becomes again dominated by the less rapidly decreasing y component. The behavior of the polarization state of the field is illustrated using a Poincaré sphere in Fig. 7.5(b). The locus of the points representing polarization states forms a closed curve.

The final example to be considered is, at a first glance, very similar to the first example, with $M_x = M_y = 1.5$. The degree of polarization, shown in Fig. 7.6(a), behaves very

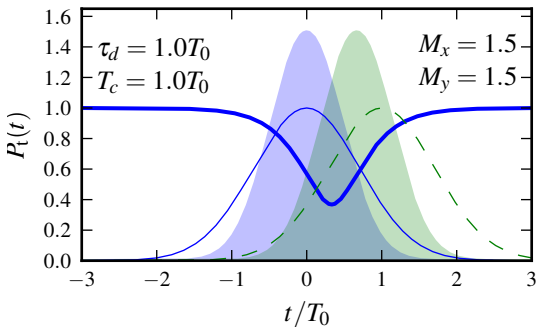

(a) Intensities of x (blue) and y (green) components before (thin solid and dashed lines) and after (shaded curves) the temporal imaging, and the degree of polarization after temporal imaging (thick solid curve).

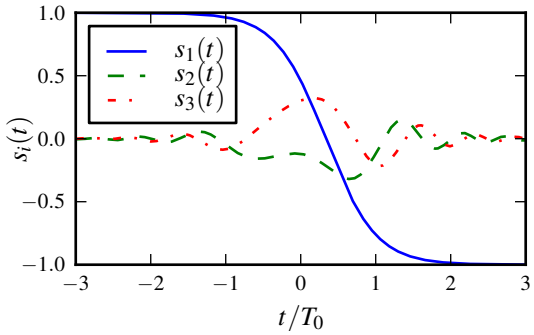

(b) Normalized Stokes parameters. The qualitative behavior of $s_1(t)$ does not change on imaging, but the quadratic phase change causes $s_2(t)$ and $s_3(t)$ to oscillate in time.

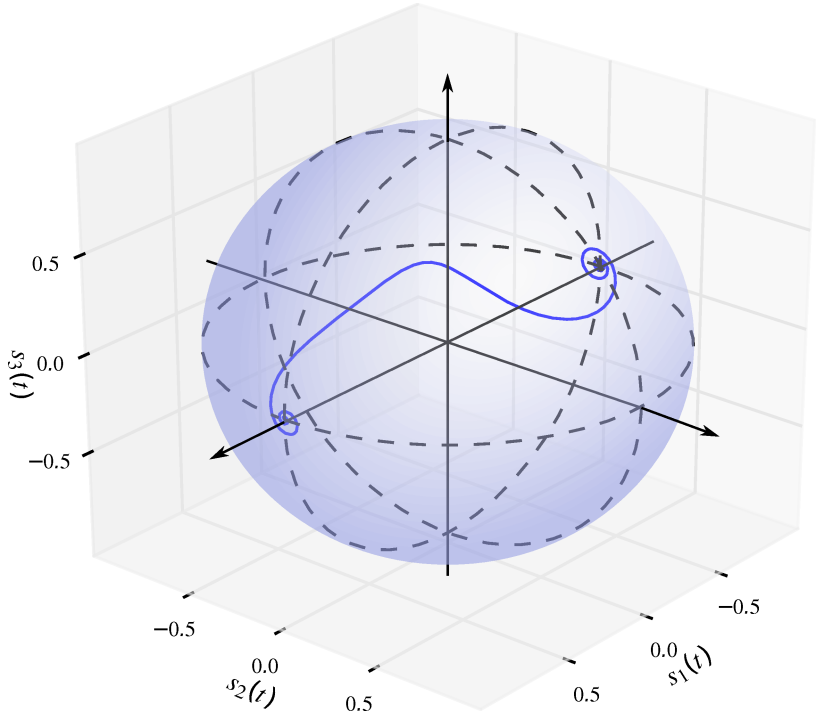

(c) Evolution of the polarization state represented in the Poincaré sphere, shown with the solid curve. The dashed circles show the intesection of the $s_1(t) = 0$, $s_2(t) = 0$, and $s_3(t) = 0$ planes with the surface of the Poincaré sphere.

Figure 7.6: Polarization characteristics of a temporally imaged pulse with non-compensated quadratic phase term.

similarly to the non-magnified case. However, there is a crucial difference to the first example: the GDD parameters are no longer assumed to be such that the phase term $\phi_{ij}(t)$ is actually independent of time t. The parameters have been chosen to be $\Phi_{\mathrm{a}x} = 0.15T_0^2$, $\Phi_{\mathrm{b}x} = -0.10T_0^2$, $\Phi_{\mathrm{a}y} = 1.5T_0^2$, and $\Phi_{\mathrm{b}x} = -1.0T_0^2$. These values have not been picked entirely arbitrarily, although the values are conveniently of the order of 1. The pulse is assumed to propagate in a fused silica fiber, the most common telecommunication fiber material, and correspondingly the carrier frequency of the pulse is assumed to correspond to the region of the lowest loss in fused silica at 1550 nm. In a single-mode fiber the total dispersion is approximately $D_\lambda = 10\ \mathrm{ps/nm \cdot km}$, which corresponds to $\beta_2 \approx -10^{-26}\ \mathrm{s/Hz \cdot m}$ [50]. For a fiber 100 m long, this translates to a GDD parameter value $-10^{-24}\ \mathrm{s/Hz}$. Assuming a pulse length of $T_0 = 1$ ps, the calculated GDD is $\Phi \approx -T_0^2$.

With the chosen parameters, the quadratic term in the phase factor $\phi_{ij}(t)$ becomes $2.25(t/T_0)^2$. Its is visible on the Stokes parameter and Poincaré sphere plots in Figs. 7.6(b) and 7.6(c), respectively. The difference between x and y linearly polarized components, given by $s_1(t)$, behaves in the same way as in beams where the quadratic term was compensated. The polarization state fluctuates between elliptically polarized and linearly polarized states, ending up as linearly y polarized. The locus of the points representing the polarization state of the pulse forms the curve shown in Fig. 7.6(c), which displays the rather eccentric behavior of the polarization state. This serves to demonstrate that starting from a relatively simple, linearly polarized pulse, and using two relatively simple processes to modify the pulse, a wealth of different polarization effects have been obtained.

Chapter 8

Summary and conclusions

This thesis presented the theory of partial polarization of non-stationary fields both in time domain and in frequency domain. Chapter 2 recalled the principles of electromagnetic random beams, and Chaps. 3 and 4 reviewed the formalism used to describe partial polarization of stationary beams in time and frequency domains, respectively. Chapters 5 and 6 introduced the formalism for characterizing partial polarization of non-stationary beams in time and frequency domains, respectively, and the connection between temporal and spectral polarization, and illustrated both temporal and spectral polarization with examples. In Chap. 7 a temporal imaging system was introduced, and the polarization changes induced by traversal through such a system were analyzed.

The main result of this work is construction of a thorough, consistent formalism for partial polarization in non-stationary electromagnetic beams. In time domain, the degree of polarization and polarization state become time-dependent quantities, e.g., a pulse may be fully or partially polarized at its leading edge and entirely differently polarized at the trailing edge. The spectral polarization of a non-stationary beam behaves similarly to that of a stationary beam, and the differences between stationary and non-stationary beams become apparent only when the correlations between different frequency components of the beam are analyzed. The connections between the polarization and coherence properties in time and frequency domains were derived, and the results show that polarization properties in time domain depend on spectral coherence properties, and spectral polarization depends on temporal coherence properties. A polarization equivalence theorem was derived as a consequence of the connection between temporal and spectral polarization properties, and it sets out the criteria for beams with different temporal coherence to have identical spectral polarization properties. The theory was illustrated by analyzing two examples of electromagnetic pulses. The first example was a beam constructed by using two mutually

delayed copies of the same linearly polarized, Gaussian Schell-model (GSM) pulse as the orthogonal polarization components of an electromagnetic pulse. The analysis showed that for such a pulse the degree and state of polarization are time-dependent quantities, and they can be varied by altering the delay between the orthogonal components of the pulse and the coherence time of the original linearly polarized pulse. The spectral degree of polarization was shown to be unity at all frequencies, indicating full spectral polarization, and the spectral Stokes parameters indicated that the polarization state varied sinusoidally as a function of frequency.

The developed polarization formalism was also applied to the study of the polarization changes induced by passing a pulse through a temporal imaging system constructed out of two dispersive optical fibers and a temporal quadratic phase modulator (QPM) which behaves as a time lens. It was shown that if the temporal imaging system acted isotropically on the pulse, propagation through the system compresses or expands the envelope of the pulse in time, and if the temporal magnification is negative, i.e., the group dispersion delays of the two fibers have the same sign, the envelope is also reversed in time on traversing the system. The same compression or expansion and possible reversal in time take place in the polarization properties of the pulse. The imaging system may be made anisotropic such that the orthogonal polarization components of the input pulse undergo imaging with different magnifications. Among the demonstrated effects was a situation where a very narrow time window of full polarization appeared within an otherwise weakly polarized pulse. This peak was located at the midpoint between the intensity maxima of the polarization components. Even if the fiber dispersion parameters were chosen such that the temporal magnifications acting on the orthogonal polarization components were equal, the state of polarization at the output could differ from the input polarization due to the quadratic relative phase difference imparted between the components by traversal through the system. The analysis was limited to time domain, and expanding the investigation into frequency domain would, without a doubt, be a revealing research topic in itself.

Other interesting subjects for future research in this field include a more thorough and deeper analysis of the connection between polarization in time and frequency domains, the role of unitary transformations in frequency domain in altering the polarization in time domain, spatial and propagation properties of polarization quantities, and polarization changes in optical fibers. Pulses with tailored polarization and intensity profiles have a variety of applications, e.g., in materials processing, light–matter interactions, and in classical and quantum nanophotonics. Controlled polarization dynamics can be used in information coding and for high bit rate information transfer. Polarization of electromagnetic beams is also closely related to fundamental physics as is evidenced by the Pancharatnam–Berry (geometric) phase and the emergence of polarization entanglement [51].

References

[1] Ch. Brosseau, "Polarization and Coherence Optics: Historical Perspective, Status, and Future Directions," in *Progress in Optics*, ed. E. Wolf, vol. 54 (Elsevier, 2010), p. 149.

[2] E. Bartholinus, "Experimenta crystalli islandici disdiaclastici quibus mira & insolita refractio detegitur," Copenhagen (1669).

[3] T. Young, "An account of some cases of the production of colours, not hitherto described," Phil. Trans. Roy. Soc. (London) **92**, 387 (1802).

[4] T. Young, "The Bakerian lecture: Experiments and calculations relative to physical optics," Phil. Trans. Roy. Soc. (London) **94**, 1 (1804).

[5] J. C. Maxwell, "A dynamical theory of the electromagnetic field," Proc. Roy. Soc. (London) **13**, 531 (1864).

[6] Ch. Brosseau, *Fundamentals of Polarized Light* (Wiley, 1998).

[7] Ch. Brosseau and A. Dogariu, "Symmetry properties and polarization descriptors for an arbitrary electromagnetic wavefield," in *Progress in Optics*, ed. E. Wolf, vol. 49 (Elsevier, 2006), p. 315

[8] L. Novotny and B. Hecht, *Principles of Nano-Optics* (Cambridge University Press, 2006).

[9] Y. B. Band, *Light and Matter* (Wiley, 2006).

[10] E. Wolf, "Optics in terms of observable quantities," Nuovo Cimento **12**, 884 (1954).

[11] E. Wolf, "A macroscopic theory of interference and diffraction of light from finite sources. I. Fields with a narrow spectral range," Proc. Roy. Soc. A **225**, 96 (1954).

[12] E. Wolf, "Coherence properties of partially polarized electromagnetic radiation," Nuovo Cimento **13**, 1165 (1959).

[13] R. Barakat, "*n*-fold polarization measures and associated thermodynamic entropy of *N* partially coherent pencils of radiation," Optica Acta **30**, 1171 (1983).

[14] D. F. V. James, "Polarization of light radiated by black-body sources," Opt. Commun. **109**, 209 (1994).

[15] J. Peřina, *Coherence of Light*, 2nd ed. (Kluwer, 1985).

[16] J. W. Goodman, *Statistical Optics* (Wiley, 1985).

[17] M. J. Beran and G. B. Parrent, *Theory of Partial Coherence*, 2nd ed. (SPIE, 1974).

[18] L. Mandel and E. Wolf, *Optical Coherence and Quantum Optics* (Cambridge University Press, 1995).

[19] T. Setälä, A. Shevchenko, M. Kaivola, and A. T. Friberg, "Polarization time and length for random optical beams," Phys. Rev. A **78**, 033817 (2008).

[20] A. Shevchenko, T. Setälä, M. Kaivola, and A. T. Friberg, "Characterization of polarization fluctuations in random electromagnetic beams," New J. Phys. **11**, 073004 (2009).

[21] T. Voipio, T. Setälä, A. Shevchenko, and A. T. Friberg, "Polarization dynamics and polarization time of random three-dimensional electromagnetic fields," Phys. Rev. A **82**, 063807 (2010).

[22] T. Voipio, T. Setälä, A. Shevchenko, and A. T. Friberg, "Polarization dynamics of random 3D fields," in *9th Euro-American Workshop on Information Optics, WIO'10,* (Helsinki, Finland, 2010). IEEE Xplore doi: 10.1109/WIO.2010.5582490.

[23] G. D. VanWiggeren and R. Roy, "Communication with dynamically fluctuating states of light polarization," Phys. Rev. Lett. **88**, 097903 (2002).

[24] M. Bertolotti, A. Ferrari, and L. Sereda, "Coherence properties of nonstationary light sources," J. Opt. Soc. Am. B **12**, 341 (1995).

[25] P. Pääkkönen, J. Turunen, P. Vahimaa, A. T. Friberg, and F. Wyrowski, "Partially coherent Gaussian pulses," Opt. Commun. **204**, 53 (2002).

[26] C. Ding, L. Pan, and B. Lü, "Characterization of stochastic spatially and spectrally partially coherent electromagnetic pulsed beams," New J. Phys. **11**, 083001 (2009).

[27] J. D. Jackson, *Classical Electrodynamics*, 3rd ed. (Wiley, 1997).

[28] J. Ellis and A. Dogariu, "Complex degree of mutual polarization," Opt. Lett. **29**, 536 (2004).

[29] T. Setälä, J. Tervo, and A. T. Friberg, "Contrasts of Stokes parameters in Young's interference experiment and electromagnetic degree of coherence," Opt. Lett. **31**, 2669 (2006).

[30] J. Tervo, T. Setälä, and A. T. Friberg, "Degree of coherence for electromagnetic fields," Opt. Express **11**, 1137 (2003).

[31] T. Setälä, J. Tervo, and A. T. Friberg, "Theorems on complete electromagnetic coherence in the space-time domain," Opt. Commun. **238**, 229 (2004).

[32] E. Wolf, "Can a light beam be considered to be the sum of a completely polarized and a completely unpolarized beam?" Opt. Lett. **33**, 642 (2008).

[33] J. Tervo and J. Turunen, "Comment on 'Can a light beam be considered to be the sum of a completely polarized and a completely unpolarized beam?'," Opt. Lett. **34**, 1001 (2009).

[34] E. Wolf, "Reply to Comment on 'Can a light beam be considered to be the sum of a completely polarized and a completely unpolarized beam?'," Opt. Lett. **34**, 1002 (2009).

[35] J. J. Gil, "Polarimetric characterization of light and media," Eur. Phys. J. Appl. Phys. **40**, 1 (2007).

[36] J. Tervo, T. Setälä, and A. T. Fribarg, "Theory of partially coherent electromagnetic fields in the space–frequency domain," J. Opt. Soc. Am. A **21**, 2205 (2004).

[37] O. Korotkova and E. Wolf, "Generalized Stokes parameters of random electromagnetic beams," Opt. Lett. **30**, 198 (2005).

[38] J. Tervo, T. Setälä, A. Roueff, Ph. Refrégiér, and A. T. Friberg, "Two-point Stokes parameters: interpretation and properties," Opt. Lett. **24**, 3074 (2009).

[39] T. Setälä, F. Nunziata, and A. T. Friberg, "Differences between partial polarizations in the space–time and space–frequency domains," Opt. Lett. **34**, 2924 (2009).

[40] Ph. Refrégiér, T. Setälä, and A. T. Friberg, "Temporal and spectral degrees of polarization of light," Proc. SPIE **8171**, 817102 (2011).

[41] T. Setälä, F. Nunziata, and A. T. Friberg, "Partial polarization of optical beams: temporal and spectral descriptions," in *Information Optics and Photonics: Algorithms, Systems, and Applications*, ed. T. Fournel and B. Javidi (Springer, 2010), p. 207.

[42] M. Born and E. Wolf, *Principles of Optics*, 7th ed. (Cambridge University Press, 2001).

[43] T. Voipio, T. Setälä, and A. T. Friberg, "Partial polarization of pulsed light beams," Proc. SPIE **8306**, 83061C (2011).

[44] E. Collett and E. Wolf, "Is complete spatial coherence necessary for the generation of highly directional light beams?" Opt. Lett. **2**, 27 (1978).

[45] H. C. Kandpal and E. Wolf, "Partially coherent sources which generate far fields with the same spatial coherence properties," Opt. Commun. **110**, 255 (1994).

[46] A. C. Schell, "A technique for the determination of the radiation pattern of a partially coherent aperture," IEEE Trans. Antennas Propag. **AP-15**, 187 (1967).

[47] I. A. Walmsley and C. Dorrer, "Characterization of ultrashort electromagnetic pulses," Adv. Opt. Photon. **1**, 308 (2009).

[48] B. Kolner and M. Nazarathy, "Temporal imaging with a time lens," Opt. Lett. **14**, 630 (1989).

[49] B. Kolner, "Space–time duality and the theory of temporal imaging," IEEE J. Quantum Elec. **30**, 1951 (1994).

[50] B. E. A. Saleh and M. C. Teich, *Fundamentals of Photonics*, 2nd ed. (Wiley, 2007).

[51] X.-F. Qian and J. H. Eberly, "Entanglement and classical polarization states," Opt. Lett. **36**, 4110 (2011).